IAEA-TECDOC-667

Coolant technology of water cooled reactors

Volume 2:
Corrosion in the primary coolant systems of water cooled reactors

INTERNATIONAL ATOMIC ENERGY AGENCY IAEA

The IAEA does not normally maintain stocks of reports in this series. However, microfiche copies of these reports can be obtained from

INIS Clearinghouse
International Atomic Energy Agency
Wagramerstrasse 5
P.O. Box 100
A-1400 Vienna, Austria

Orders should be accompanied by prepayment of Austrian Schillings 100,– in the form of a cheque or in the form of IAEA microfiche service coupons which may be ordered separately from the INIS Clearinghouse.

COOLANT TECHNOLOGY OF WATER COOLED REACTORS
VOLUME 2: CORROSION IN THE PRIMARY COOLANT SYSTEMS
OF WATER COOLED REACTORS
IAEA, VIENNA, 1992
IAEA-TECDOC-667
ISSN 1011-4289

Printed by the IAEA in Austria
September 1992

FOREWORD

More than 95% of the nuclear power in the world is derived from water cooled reactors. In nuclear power plants water is used in primary circuits, secondary circuits (PWRs and PHWRs) and in a number of auxiliary systems. Water is an aggressive medium at high temperature when in contact with structural materials. This means that the reliability of many nuclear power plant systems (fuel, steam generators, etc.) is dependent on the water chemistry during normal operations, startups, shutdowns and abnormal operations. Reliable water chemistry specifications have been developed for the existing water cooled reactors; however, there is still room for improvement. Water cooled power reactor experience shows that even under normal operating conditions some undesirable effects can occur: corrosion, erosion or deposition of corrosion products on heat transfer surfaces.

Moreover, beyond the adverse effect of corrosion on the mechanical properties of components and of corrosion product deposits on heat transfer, the migration and transfer of activated corrosion products lead to the formation of highly radioactive deposits on some out-of-core surfaces of the primary circuit. This is the main cause of radiation exposure during repair and maintenance, and could require decontamination of some equipment or of the primary circuit as a whole. This is of particular importance when the level of the maximum average permissible dose is under discussion and will probably be decreased to 20 mSv over a year.

The need to decrease radiation levels is now supported by greater management interest, and efforts are being made to improve, for instance, the understanding of fundamental processes and to develop the on-line monitoring technique. Understanding the chemistry is now a major task in the improvement of the operating performance especially with the increase in burnup levels, higher coolant temperatures and with the possibility of nucleate boiling in PWRs.

This report is a summary of the work performed within the framework of the Co-ordinated Research Programme on Investigations on Water Chemistry Control and Coolant Interaction with Fuel and Primary Circuit Materials in Water Cooled Power Reactors (WACOLIN) organized by the IAEA and carried out from 1987 to 1991. It is the continuation of a programme entitled Reactor Water Chemistry Relevant to Coolant-Cladding Interaction (IAEA-TECDOC-429), which ran from 1981 to 1986. Subsequent meetings resulted in the title of the programme being changed to Coolant Technology of Water Cooled Reactors.

The results of this Co-ordinated Research Programme are published in four volumes with an overview in the Technical Reports Series.

The titles of the four volumes are as follows:

Volume 1: Chemistry of Primary Coolant in Water Cooled Reactors

Volume 2: Corrosion in the Primary Coolant Systems of Water Cooled Reactors

Volume 3: Activity Transport Mechanisms in Water Cooled Reactors

Volume 4: Decontamination of Water Cooled Reactors.

These publications should be of interest to experts in water chemistry at nuclear power plants, experts in engineering, fuel designers, R&D institutes active in the field and to consultants to these organizations.

EDITORIAL NOTE

This text was compiled before the recent changes in the former Union of Soviet Socialist Republics.

CONTENTS

OVERVIEW

NATIONAL CONTRIBUTIONS

Czechoslovakia

Finland

Germany

India

Japan

Union of Soviet Socialist Republics

OVERVIEW

CORROSION IN PRIMARY COOLANT SYSTEMS

D.H. LISTER
System Chemistry and Corrosion Branch,
Chalk River Nuclear Laboratories,
Atomic Energy of Canada Limited,
Chalk River, Ontario,
Canada

Abstract

Corrosion aspects of three areas of reactor coolant circuits are highlighted - zirconium alloy corrosion and hydriding in-core, primary water stress corrosion cracking in steam generators, and general oxide film formation on circuit piping steels. Some recent investigations in each area are described briefly and their results are summarized.

INTRODUCTION

The overview of this WACOLIN project[1] describes the coolant systems of the major types of water reactor and discusses the corrosion issues that are currently of concern to the industry.

Such issues are continually under review in the international nuclear community. Thus, general water reactor chemistry and corrosion are the subject of regular conferences (see, for example, Refs. [1-3]), while specialists' topics such as Irradiation-Assisted Stress Corrosion Cracking (IASCC, Ref. [4]), or fuel performance - including coolant-clad interaction (Ref. [5]), are discussed at conferences, workshops, etc., from time to time. Here, in the Corrosion Section of the WACOLIN documents, a range of topics dealing with corrosion both in-core and out-core is considered. This introductory paper presents several highlights and recent findings of programs investigating several aspects of corrosion in reactor coolant systems.

ZIRCONIUM ALLOY CORROSION

The increasing pressure on utilities to guarantee service from reactor components and to extend plant lifetimes is putting renewal emphasis on the prediction of materials behaviour in-core [Ref. 6].

In reactor cores, the zirconium alloys used for fuel cladding and structural components are subjected to the rigorous conditions of temperature, pressure, and coolant chemistry along with the constraints of radiation. Predicting the behaviour of these alloys in their operating environment is consequently a complicated undertaking. The fact that there are many models describing zirconium alloy corrosion in-core is an indication of the complexity of the problem.

Comprehensive explanations of in-reactor corrosion of zirconium alloys consider the microstructure of the metal, the chemistry of the environment, and the barrier between them (i.e., the oxide film). Thus, for fuel cladding made of Zircaloy-2 or Zircaloy-4, constituent elements Fe, Cr and Ni form precipitates or intermetallic phases in the alloy that are important for sustaining the electrochemical processes of corrosion. These intermetallics have structures such as $Zr(Cr,Fe)_2$ or $Zr_2(Ni,Fe)$, and their distribution in the alloy affects the resistance to nodular corrosion. During in-reactor exposure, neutron irradiation alters the disposition of the intermetallics, dissolving Fe from $Zr(Cr,Fe)_2$ and Fe and Ni from $Zr_2(Ni,Fe)$ into the alloy matrix [Ref. 7]. Thus, Zircaloy fuel cladding shows increased resistance to nodular corrosion with neutron irradiation - an increase that can be removed by annealing.

Such microstructure effects can be accounted for in modelling the corrosion behaviour of fuel cladding. Thus, the distribution of intermetallic particles in Zircaloy fuel cladding depends on the thermal treatment of the alloy, and can be modelled in terms of particle nucleation and growth [Ref. 8], which is a more detailed approach than the use of an empirical "annealing parameter" [Ref. 9]. By combining such microstructure models, which reflect the thermal treatment of the alloy, with corrosion models that describe the in-core oxidation of specific metallurgical conditions of the alloy [Ref. 10], the cladding oxidation can be predicted.

Within such models, the effects of the environment can be difficult to describe. Thus, while we expect BWR fuel cladding to undergo less general oxidation than PWR fuel (because of its lower temperature), the effect of the oxidizing nature of BWR coolant is to promote more oxidation - specifically, in the form of localized or nodular corrosion. The radiolysis of the coolant is clearly important here; it is affected by the boiling process at the cladding surface, for the nucleation and detachment of bubbles determine the local concentrations of oxidizing species. Impurities in the coolant also play a major rôle in determining cladding behaviour. Crud deposits on fuel surfaces can lead to excessively high cladding temperatures and promote fuel failures. Copper in BWRs has been particularly bad in this respect; it can not only reduce the heat transfer properties of thick fuel deposits in-core but also promote nodular corrosion [Ref. 11].

In PWR cores, the effect of dissolved lithium in the coolant on Zircaloy corrosion is assuming important dimensions as radiation field considerations lead reactor operators to employ higher alkalinity levels. That high lithium concentrations increase the corrosion of zirconium alloys is undisputed, and is a major reason why many utilities keep [Li] at a maximum of ca. 3.5 ppm at the start of the operating cycle until a high temperature pH of 7.4 is reached as the boron concentration decreases. Even then, the modelling approach described in Reference 9 purports to differentiate between the greater oxidation of Zircaloy-4 fuel in a PWR operated with elevated Li chemistry ([Li] of 3.5 ppm max.) and the oxidation in a PWR operated with normal Li chemistry ([Li] of 2.2 ppm max.) [Ref. 12].

The details of the mechanism by which Li increases the corrosion of zirconium alloys are not known with any certainty. Injection of Li atoms into the metal surface by recoil from the fast neutron reaction with B has recently been postulated to have an important influence on corrosion [Ref. 13], but no explanation of the mechanism of the corrosion increase was offered.

---

[1] *The overview of the WACOLIN programme is to be published in the IAEA Technical Reports Series.*

The tradition concept of the lithium effect is that Li is incorporated in solid solution in the ZrO_2 and alters the vacancy concentration and distribution in the oxide film. Since zirconium alloy corrosion proceeds by oxygen diffusion through the film, the increased number of vacancies should increase the diffusion and therefore the corrosion rate.

Observed changes in corrosion rate, however, seem to be inconsistent with Li incorporation and vacancy concentrations in the oxide, while alloy exposure to high concentrations of Li generates more porous oxide and retains Li within the oxide as an acid-soluble component [Ref. 14]. The postulate is, therefore, that the undissociated LiOH in concentrated solution (i.e., above 0.1 M) within the oxide pores interacts with the forming oxide at the metal-oxide interface to give surface groups of -OLi. Such groups modify the growth of the oxide to form a high density of fine crystallites, thereby providing many diffusion paths for the anion and leading to accelerated corrosion. The surface groups are readily dissolvable to promote the oxide porosity and to maintain the concentrated Li solution within the oxide film. Detailed surface analysis, using SEM and SIMS, has provided some evidence for this mechanism [Ref. 14].

However true this explanation of the Li effect may be, the importance of the oxide porosity in the corrosion mechanism is clear. In fact, for zirconium alloys with thick oxide films, in-core acceleration of corrosion may well be due to the radiolytic effects on coolant trapped within the pores, producing localized aggressive conditions divorced from the bulk coolant conditions because of the intervening diffusion barriers [Ref. 15].

Insights into the mechanisms of corrosion of zirconium alloys are also being provided by studies of the behaviour of pressure tubes in CANDU reactors. The first CANDU units were tubed with Zircaloy-2, but because of the possibility of precipitation of brittle hydrides within the alloy and the resulting susceptibility to cracking, later units switched to Zr-2.5Nb.

The in-reactor behaviour of the two materials can be contrasted by examining pressure tube data from operating reactors. Zircaloy-2 pressure tubes in the Hanford N-Reactor, as well as those in early CANDUs, developed oxide films in contact with the primary coolant in-core with near cubic kinetics up to a film thickness of ca. 20 µm (attained after ca. 7 years). A transition period during which the rate accelerated and became approximately linear followed (see Fig. 1).

In-reactor, Zr-2.5Nb corrodes more slowly than Zircaloy-2. Samples of pressure tubes from three operating CANDUs have indicated that oxide thicknesses on Zr-2.5Nb have not exceeded 25 µm during exposures of up to 16 years. Furthermore, there appears to be no evidence of a transition to faster corrosion kinetics, though we cannot yet completely rule out the possibility that some critical oxide thickness might be attained at longer exposures (see Fig. 1).

For both alloys, the deuterium pickup reflects the corrosion, with Zircaloy-2 exhibiting a transition beyond which rates of ingress increased and became linear and with Zr-2.5Nb continuing with generally low values. The ratio of corrosion between the two alloys is less than the ratio of deuterium ingress, reflecting the lower proportional (or "percent") pickup of corrosion-generated deuterium for Zr-2.5Nb than for Zircaloy-2 (see Fig. 2). The unusually high deuterium level measured for one Zr-2.5Nb pressure tube after ca. 15 year exposure in-reactor (see Fig. 2) is believed to have been caused by an anomalous

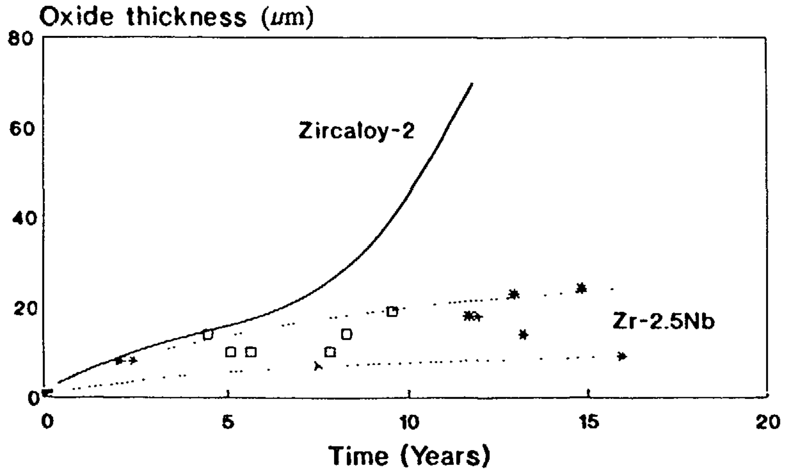

Figure 1: In-Reactor Oxidation of Zirconium Alloy Pressure Tubes.

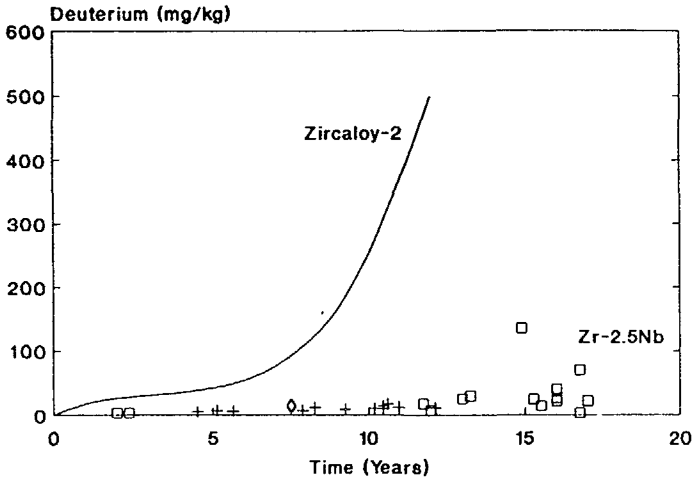

Figure 2: In-Reactor Ingress of Deuterium into Zirconium Alloy Pressure Tubes.

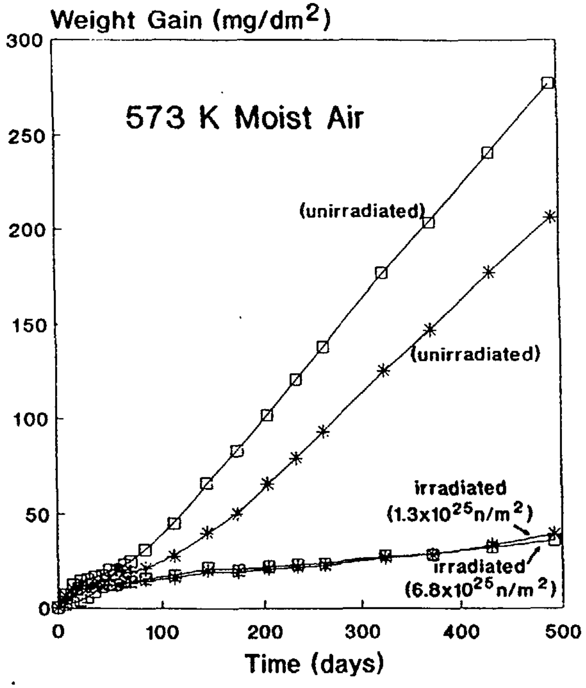

Figure 3: Effects of Reactor Radiation on Corrosion of Zr-2.5Nb Pressure Tubing.

pickup from the outside of the tube, which is in contact with an "annulus gas" of CO_2 containing traces of D_2O and D_2.

In contrast with in-reactor-exposed material, unirradiated Zr-2.5Nb corrodes faster than Zircaloy-2. The effect of irradiation on Zr-2.5Nb corrosion is illustrated by the results of an oxidation experiment reproduced in Fig. 3. Two sets of pressure tube material (archived off-cuts of Zr-2.5Nb) were exposed in a furnace for up to 500 d to moist air at 300°C. A transition behaviour, with final linear kinetics, is observed. The difference in out-reactor corrosion rate between the two samples, which were from different batches of pressure tubes, probably reflects slight differences in manufacturing of the original tubes.

Also shown in Fig. 3 are data from the two actual pressure tubes corresponding to the archived off-cuts. These were exposed in a reactor for about two and ten years to give fluences of 1.3×10^{25} $n.m^{-2}$ and 6.8×10^{25} $n.m^{-2}$, respectively, before being removed and cut for exposure in the furnace to the 300°C moist air. The data indicate that the irradiation has suppressed the corrosion rate and nullified the corrosion difference between the two tubes.

This corrosion and hydriding behaviour of pressure-tube material apparently depends upon the oxide characteristics and the alloy microstructure. For the transitional corrosion kinetics of Zircaloy-2, for example, the mechanism is postulated to be the development of porosity in the oxide as a critical thickness is achieved and as oxide recrystallization and grain growth occur [Refs. 16 and 17]. Such porosity is thought to extend to the metal-oxide interface. In-reactor, chemistry conditions within the pores may be more aggressive than in the bulk of the coolant because of local radiolytic effects, and may be responsible for accelerated corrosion below thick, post-transition oxides [Ref. 15].

For Zr-2.5Nb, an impervious "barrier" layer of oxide may exist at the metal-oxide interface; this barrier apparently persists, with an overlying layer of porous oxide, even at very high weight gains. The transport of oxygen or electrons or both through the barrier then controls the oxidation, and changes in the barrier layer thickness change the oxidation rate [Ref. 18].

The change in corrosion resistance of Zr-2.5Nb with neutron irradiation is probably related to the microstructure of the alloy. Pressure tubes for CANDU reactors are extruded at 820-850°C, cold worked 20-30%, then stress relieved in steam at 400°C for 24 h. At the extrusion temperature, the microstructure is ca. 80% beta zirconium phase and ca. 20% alpha zirconium. The air cooling after extrusion allows transformation of the beta phase to the alpha phase, with growth of the elongated alpha grains which were produced during extrusion; the grain-boundary network of the beta phase thus becomes progressively enriched in niobium. Cold working elongates the alpha grains further, and introduces a high dislocation density which is subsequently reduced by the stress relief. The alpha phase, in the as-manufactured pressure tube, is supersaturated in niobium and is more susceptible to corrosion than the "equilibrium" phase composition. During reactor irradiation, small precipitates form within the alpha grains [Ref. 19]. This in-reactor ageing effect reduces the niobium in the alpha phase by precipitating niobium-rich particles, so that the resulting near-equilibrium composition of the alpha grains exhibits considerable corrosion resistance. Since the effect is the transformation towards equilibrium of a metastable condition, we would expect the in-reactor ageing effect to persist when the radiation is removed (as is, in fact, observed - see Fig. 3).

STRESS CORROSION CRACKING OF STEAM GENERATOR TUBING

A major cause of steam generator tube plugging in PWRs has been intergranular stress corrosion cracking (IGSCC) originating from the primary side (hence, Primary Water Stress Corrosion Cracking, or PWSCC). All of the tubes plugged because of PWSCC have been made of Alloy 600, the material used for most of the steam generators world-wide; to date, only one such failure has occurred in a CANDU reactor (at the Bruce station, where the only operating CANDUs with Alloy 600 steam generator tubes are situated).

For nickel-based alloys, such as Alloy 600, a wide range of environments is known to cause SCC. In particular, caustic, chloride and sulphur compounds, occasionally with impurities such as lead or carbonate, have had severe effects on the secondary side of Alloy-600-tubed steam generators. On the primary side, SCC can occur in high temperature pure water [Ref. 20], in water containing hydrogen [Ref. 21] and in water containing oxygen and sulphate [Ref. 22]. In particular, there seems to be a synergistic effect of oxygen and sulphate on the

SCC behaviour of Alloy 600. The metallurgical factors necessary for SCC are high stress and a susceptible microstructure, with a low-temperature mill anneal (≤950°C) producing a particularly susceptible material. Subsequent thermal treatment, optimally 700°C for about 10 h, improves the resistance to SCC substantially [Ref. 23].

Even with non-susceptible heats of Alloy 600, however, there has been uncertainty about the resistance to SCC in primary coolant containing small amounts of oxygen (such as might arise from in-core boiling in some CANDUs, for example). A similar uncertainty existed for Alloy 800, though this material has generally exhibited excellent resistance to SCC.

Accordingly, a program of testing of steam generator alloys under severe CANDU primary coolant conditions was undertaken [Ref. 24]. The aim was to compare the susceptibility to cracking of alloys used in CANDU reactors with that of other well-characterized alloys.

Two types of highly-stressed sample were used: reverse U-bends (RUBs) and Constant Extension Rate Testing (CERT) samples. RUBs were prepared by slitting tubes axially along the mid-plane and then bending them backwards into a "U" and securing them with a nut and bolt without letting them relax back; this configuration leads to the tube outside wall's becoming the inner surface of the RUB U-bend. In CERT testing, a sample machined from tubing is strained to rupture, as in tensile testing, in the specific environment inside an autoclave. For these tests, a strain rate of 9.6 x $10^{-7}s^{-1}$ was used.

The materials tested were as follows:

Alloy 600 - archived tubing from a CANDU reactor (high-temperature mill-annealed, followed by a 5-8 h thermal treatment at 550-600°C);

- EPRI Lot 1A (with a similar heat treatment to that of the CANDU alloy, viz. high-temperature mill annealed followed by a 10 h thermal treatment at 600°C - see Ref. 25);

- simulated CANDU tubing (high-temperature mill-annealed followed by by a 5-8 h thermal treatment at 610-630°C);

- EPRI Lot 2, known to be susceptible to IGSCC (low-temperature mill-annealed - see Ref. 25)

Alloy 800 - Sandvik tubing, similar to that installed in CANDU reactors (mill-annealed);

- Mannesmann tubing (mill-annealed);

Alloy 690 - as-received Sandvik tubing.

The test conditions were as follows (note that a higher temperature and wider range of dissolved gases than those employed in operating reactor coolants were chosen to give a series of severe tests):

$pH_{25°C}(Li)$ = 10.4
temperature = 360°C
dissolved O_2 = 20-250 μg.kg^{-1}
dissolved H_2 = 3-40 cm^3.kg^{-1}

The results of the CERT tests are presented in the following table:

SUMMARY OF CERT DATA FOR STEAM GENERATOR TUBE MATERIALS

Alloy	Source	Dissolved Gas		Time to Failure (h)*	Comment
		O_2(μg.kg^{-1})	H_2(cm^3.kg^{-1})		
600	EPRI Lot-2	200	3	121	100% i.g.**
		250	40	109	100% i.g.
		20	20	120	60% i.g.
		20	40	81	90% i.g.
600	EPRI Lot 1A	200	3	202	ductile failure
		250	40	219	ductile failure
		20	20	166	ductile failure
		20	40	197	ductile failure
600	CANDU archive	200	3	200	ductile failure
		250	40	187	ductile failure
		20	20	190	ductile failure
		20	40	172	ductile failure
600	CANDU simulation	200	3	177	ductile failure
		250	40	166	ductile failure
		20	20	145	ductile failure
		20	40	183	ductile failure
800	Sanicro 30 (CANDU)	200	3	135	ductile failure
		250	40	123	ductile failure
		20	20	127	ductile failure
		20	40	133	ductile failure
690	Sanicro 68	200	3	156	ductile failure
		250	40	136	ductile failure
		20	20	130	ductile failure
		20	40	145	ductile failure

* average of three or four measurements, agreement within a few percent

** i.g. ≡ intergranular; measurement is percent of fracture area

As the table indicates, only the susceptible specimens of Alloy 600 (viz. EPRI Lot 2) failed intergranularly during CERT testing; these specimens also exhibited the shortest times to failure. The results suggest that, for the susceptible material, high hydrogen may have caused somewhat shorter failure times than those registered in low hydrogen.

The RUB specimens of all the alloys showed similar behaviour, in that only the susceptible material (EPRI Lot 2) cracked in exposures lasting up to one year, with high hydrogen concentrations (40 cm^3.kg^{-1}) promoting IGSCC. As was the case with the CERT tests, adequately heat treated Alloy 600 and Alloys 690 and 800 exhibited no susceptibility to PWSCC, even under the most extreme chemistry conditions that could be envisaged when in-core boiling occurs.

GENERAL CIRCUIT CORROSION

Besides the localized corrosion of major components in reactor primary coolants (such as those in-core or in the steam generators), the behaviour of general circuit materials is also of interest. For example, a great deal of effort has been spent in investigating the stress corrosion cracking behaviour of sensitized stainless steel in BWR piping, while the growth of oxide films on the stainless steel surfaces of PWR steam generator heads has been studied with a view to reducing radiation fields and, therefore, operator doses.

In all these corrosion-related phenomena, dissolved oxygen (or oxidizing species such as radiolytically-produced transients) can play an important rôle. In CANDU reactors, for example, in-core boiling in some units is apparently leading to oxidizing conditions in the primary coolant [Ref. 26]. Evidence that oxidizing conditions are generated in the core is the observation that shield plugs, made of ferritic steel and positioned in the outlet ends of channels, have been coated with red to orange oxides, while inlet plugs have been black. This suggests that reducing conditions generated the black magnetite coating at the inlet, while oxidizing conditions produced ferric species such as red haematite at the outlet. Crud samples collected from the PHTS have also varied in colour from black to orange, though the majority have been brown, and fuel bundles from single channels have shown a gradation in colour from black to brown from channel inlet to outlet [Ref. 27]. The observation that core conditions are particularly affected by the phenomenon is also supported by the fact that radiation fields due to Co-60 measured close to the reactor face are rising 2-3 times faster at the Bruce B reactors (Units 5-8), which have boiled since start up, than at the Bruce A reactors (Units 1-4) which were only uprated to full power after ca. 1200 EFPD.

To investigate the development of corrosion films on carbon steel and stainless steel under various coolant oxidizing conditions, a series of experiments in an out-reactor loop operating with simulated CANDU coolant was conducted. The intention was to correlate the characteristics of the oxides on the steels with the chemistry of the coolant; this would provide insight into how Co-60 is picked up by the different oxide phases. The transformations between haematite and magnetite under oxidizing and reducing conditions were also studied.

The nominal coolant conditions in the loop were $pH_{25^\circ C}$ 10.6 (Li) and 300°C, with several experimental phases employing different oxidizing conditions. The two phases reported here had "normal" CANDU reducing conditions (nominal dissolved H_2 = 17 $cm^3.kg^{-1}$, dissolved O_2 = 0) and oxidizing conditions in which the dissolved hydrogen was replaced with a mixture of helium and oxygen (average dissolved He = 1.3 $cm^3.kg^{-1}$, average dissolved O_2 = 66 $\mu g.kg^{-1}$).

In each phase, which lasted four weeks, coupons of type 304 SS and carbon steel were exposed to the coolant in an autoclave, while sintered pellets of magnetite and haematite (ca. 1 mm diameter) were exposed in separate beds. Samples were removed from the autoclave and beds after 144 h, 288 h, 432 h and 576 h, and examined by surface analysis techniques and Mössbauer spectroscopy.

The results indicated that during exposure to reducing chemistry the α-Fe_2O_3 occurring both in the haematite beads and as impurity in the magnetite beads is reduced slowly - viz. 10% conversion in 130-300 h. By contrast, during exposure to oxidizing coolant, the Fe_3O_4 in both types of sample diminishes more rapidly - viz. 50% conversion in ca. 50 h [Ref. 26]. Diffusion of oxygen in the beads seems to be the controlling parameter.

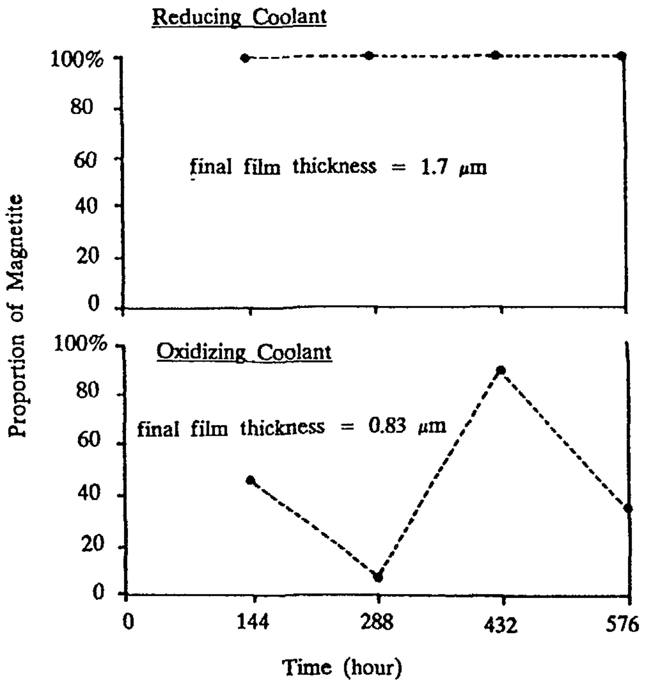

Figure 4: Iron Oxide Phases on Carbon Steel During Exposure to Reducing and Oxidizing Coolant.

The preliminary results from the carbon steel coupons are presented in Fig. 4. The total oxide film thickness (as measured by Auger Electron Spectroscopy) is clearly greater under reducing conditions than under oxidizing conditions - by a factor of ca. 2. As expected, the oxide phase (as estimated by Mössbauer spectroscopy) under reducing conditions is almost 100% magnetite throughout the experiment. By contrast, under oxidizing conditions, a large variability (from 10% to 90%) is seen in the proportion of magnetite in the oxide on the coupons examined after the four exposure periods. This would indicate that transformations within the oxide films are more rapid than in the sintered oxide beads (perhaps because of greater porosity), or that the variation from coupon to coupon is large, or both. In any case, it is clear that the reduced iron oxide phase - magnetite - is deposited in corrosion films on carbon steel, even under oxidizing conditions which normally tend to convert magnetite to an oxidized phase such as haematite.

As the preliminary results in Fig. 5 indicate, the iron oxide behaviour in films on type 403 stainless steel is different from that on carbon steel. First of

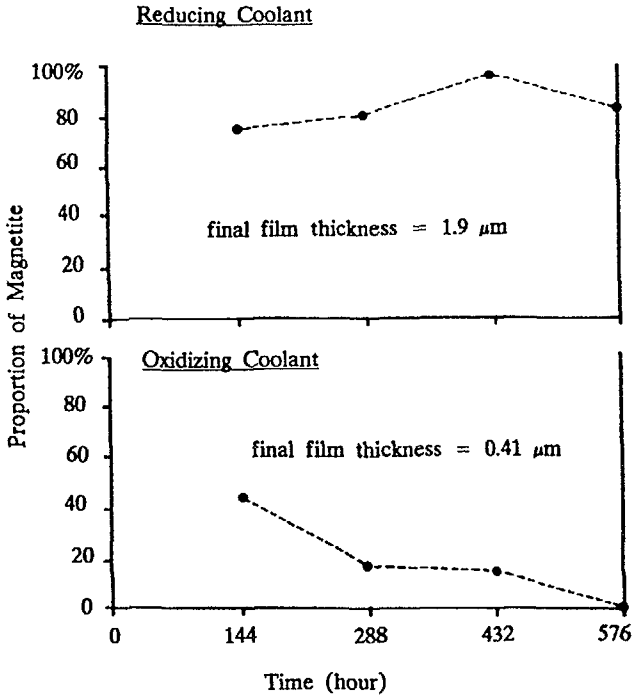

Figure 5: Iron Oxide Phases on Type 403 Stainless Steel During Exposure to Reducing and Oxidizing Coolant.

all, under reducing conditions, not all the iron is in a magnetite-type oxide - the results indicate only 75%-97%. Second, under oxidizing conditions (which produced an oxide film about a quarter as thick as that under reducing conditions), the proportion of magnetite in the oxide film diminishes from ca. 45% after the first exposure period to roughly zero after the full exposure of 576 h. As with the carbon steel, it is clear that magnetite can deposit on stainless steel even under oxidizing conditions; however, conversion to haematite after 576 h is essentially complete, suggesting that at that time the magnetite oxidation is faster than the total oxide film growth (presumably, as the material is passivated). Since cobalt incorporation within the oxides is associated with the reduced (i.e. the magnetite) portion of the films, such variable oxidation behaviour of carbon steel and stainless steel should reflect variable contamination of these materials by Co-60.

CONCLUSIONS

In-core, the microstructure of zirconium alloys is a key parameter determining the corrosion and hydriding behaviour of components such as fuel cladding and pressure tubes. Thus, the disposition of intermetallic phases within the Zircaloys and the way in which that disposition changes with radiation can affect the corrosion resistance of fuel cladding. Similarly, the radiation-induced precipitation of beta phase particles in Zr-2.5Nb provides a greater resistance to corrosion and hydriding of pressure tubes in-core than out-core.

Similarly, in steam generators, the metallurgical condition of the tubing is important in determining the resistance to primary water stress corrosion cracking. While poorly heat-treated Alloy 600 is susceptible to PWSCC, even a modest heat treatment will impart resistance under a range of oxidizing conditions. Both Alloy 800 and Alloy 690 seem immune to PWSCC.

Small concentrations of oxygen can have a profound effect on the balance of magnetite and haematite in the oxide films that develop on carbon steel and type 403 stainless steel in lithiated coolant. Such a balance affects the contamination of primary circuit materials with Co-60.

ACKNOWLEDGEMENT

Many people throughout the world contribute to our understanding of corrosion processes within nuclear reactor systems; this WACOLIN document testifies to the cooperative efforts of many countries in this important area of research. I would like to thank all participants for useful discussions during the project, and for their contributions to the report.

I should also like to thank H.A. Allsop, R.L. Tapping and V.F. Urbanic at Chalk River Laboratories for supplying results of their recent research, and the CANDU Owner's Group for allowing the release of the information.

Finally, I would like to acknowledge the efforts of M. Nöe and P. Chantoin of the IAEA in ensuring the success of the whole WACOLIN project.

REFERENCES

1. Proc. Third Internl. Symp. Environmental Degradation Matls. in Nuclear Power Systems - Water Reactors, Traverse City, Mich., U.S.A. (1987 Aug. 31-Sept. 3) National Ass. Corrosn. Engrs..
2. "Water Chemistry of Nuclear Reactor System 5", Proc. Fifth Internl. BNES Conf. on Water Chemistry of Nuclear Reactor Systems, Bournemouth, U.K. (1989 Oct. 23-27). British Nuclear Energy Soc..
3. "Water Chemistry '91", Proc. Second Internl. JAIF Conf. on Water Chemistry in Nuclear Power Plants, Fukui City, Japan (1991 Apr. 22-29), Jap. Atomic Industrial Forum.
4. IASCC Workshop, OECD Halden Project, Halden, Norway (1990 Sept. 27-28).
5. "Fuel for the 90's", Proc. Internl. Topical Meeting for LWR Fuel Performance, Avignon, France, (1991 April 21-24), American Nuclear Soc. European Nuclear Soc..

6. B. Cox, K. Ishigure, A.B. Johnson, Jr., C. Lemaignan, A.F. Nechaev, N.G. Petrik, E.A. Rezmchenko, "Mechanistic Understanding of Irradiation Corrosion of Zirconium Alloys in Nuclear Power Plants: Stimuli, Status and Outlook", Proc. Internl. Conf. on Radiation and Materials Sci., Alushka, Crimea, (1990 May 22-25), IAEA, Vienna, Austria.

7. Y. Etoh, K. Kikuchi, T. Yasuda, S. Koizumi and M. Oishi, "Neutron Irradiation Effects on the Nodular Corrosion of Zircaloy-2", Proc., Internl. Topical Meeting on LWR Fuel Performance, Avignon, France (1991 April 21-24) ANS-ENS Conference, "Fuel for the 90's", Vol 2, p 691.

8. A.R. Massih and P. Rudling, "Corrosion Behaviour of Zircaloy-2 and Zircaloy-4 Claddings in Pressurized Water Reactors", Ibid. p. 716.

9. L.F.P. Van Swam and S.H. Shann, "The Corrosion of Zircaloy-4 Fuel Cladding in PWR's", Proc. 9th Internl. Conf. on Zirconium in the Nuclear Industry, Kobe, Japan (1990 Nov. 5-8). To be published in ASTM-STP Series.

10. "MATPRO: Version 10. A Handbook of Materials Properties for Use in the Analysis of Light Water Reactor Fuel Rod Behaviour", TREE-NUREG-1180, 1978.

11. K.N. Woods, R.A. Busch, R.A. Perkins, G.M. Bain, R.L. Goodman and J.H. Schemel, "Corrosion of Zircaloy-2 Cladding in CILC BWRs", Proc. Internl. Topical Meeting on LWR Fuel Performance, Avignon, France (1991 April 21-24) ANS-ENS Conference, "Fuel for the 90's, Vol. 2, p 701.

12. S.H. Shann, L.F. Van Swam and L.A. Martin, "Effects of Coolant Li Concentration on PWR Cladding Waterside Corrosion", Ibid., p 742.

13. P. Billot, P. Beslu and J.C. Robin, "Consequences of Lithium Incorporation in Oxide Films Due to Irradiation Effect, Ibid., p. 757.

14. N. Ramasubramanian, N. Precoanin and V.C. Ling, "Lithium Uptake and the Accelerated Corrosion of Zirconium Alloys", Proc. 8th Internl. Conf. on Zirconium in the Nuclear Industry, San Diego, CA, U.S.A. (1988 June 19-23), ASTM-STP 1023, 1989.

15. A.B. Johnson, Jr., "Zirconium Alloy Oxidation and Hydriding Under Irradiation: Review of Pacific Northwest Laboratories' Test Program Results", EPRI Report NP-5132, 1987 April.

16. B. Cox, "Processes Occurring During the Breakdown of Oxide Film on Zirconium Alloys", J. Nucl. Matls., 29, 50, 1969.

17. B. Cox, "Some Effects of Pressure on the Oxidation of Zircaloy-2 in Steam and Oxygen", J. Less-Common Metals, 5, 325, 1963.

18. B. Cox, "Pore Structure in Oxide Films on Irradiated and Unirradiated Zirconium Alloys", J. Nucl. Matls., 148, 332, 1987.

19. V.F. Urbanic, B.D. Warr, A. Manolescu, C.K. Chow and M.V. Shanahan, "Oxidation and Deuterium Uptake of Zr-2.5Nb Pressure Tubes in CANDU-PHW Reactors", Proc. 8th Internl. Conf. on Zirconium in the Nuclear Industry, San Diego, CA, U.S.A. (1988 June 19-23) ASTM-STP 1023, 1989.

20. H. Coriou, L. Grall, Y. LeGall and S. Vettier, "Corrosion Fissurante Sous Contrainte de l'Inconel dans l'Eau a Haute Temperature", Troisieme Colloque de Metallurgie et Corrosion, Centre d'Etudes Nucleaires de Saclay, France, p.161 (North-Holland, Amsterdam, 1959).

21. R.S. Pathania and A.R. McIlree, "A Review of the Effect of Hydrogen on Stress Corrosion Cracking of Alloy 600 in 360°C Water", Proc. 3rd Internl. Symp. on Environmental Degradation of Matls. in Nuclear Power Systems - Water Reactors, The Metallurgical Soc., p.55 (1988).

22. L.G. Ljungberg, D. Cubicciotti and M. Trolle, "The Effect of Sulphate on Environmental Cracking in BWRs Under Constant Load or Fatigue", Paper 617, Corrosion '89, New Orleans, (1989 April).

23. G.P. Airey, "Optimization of Metallurgical Variables to Improve Corrosion Resistance of Inconel 600", EPRI Report NP-3051 (1983 July).

24. R.L. Tapping, E.G. McVey and F. Peca, "Scoping Tests to Determine the Primary Water Stress Corrosion Cracking of CANDU Steam Generator Tubing", Proc. CNS Internl. Conf. on Steam Generators and Heat Exchangers, Toronto, (1990 April).

25. Electric Power Research Institute Report, "Specialty Prepared Alloy 600 Tubing", EPRI NP-5072 (1987, Feb.).

26. D.H. Lister and P. Spekkens, "Developments in the Chemistry and Materials of CANDU Coolants", Water Chemistry '91, Proc. Second Internl. JAIF Conf. on Water Chemistry in Nuclear Power Plants, Fukui City, Japan, (1991 April 22-25).

27. G.P. Kozak, private communication from Bruce NGS "B" (1988 Nov.).

NATIONAL CONTRIBUTIONS

CORROSION OF PRESSURE VESSELS

J. KYSELA
Nuclear Research Institute,
Řež, Czechoslovakia

Abstract

This document presents a literature review of experiments performed on corrosion fatigue. The complex nature of the corrosion fatigue process makes difficult the comparison of these experiments.However this kind of corrosion seems to be influenced by irradiation,the water chemistry,more specifically the oxygen level,sulfur species,halide and pH/potential of the system.

Experiments show also that chemistry in the cracks may be different from the bulk,both for unirradiated and irradiated materials.The chemistry in such systems and its influence on crack behaviour is not yet fully understood.

Introduction

Safety concerns, extension of the operation life of nuclear power plant and to prevent corrosion related degradation it is important to establish and maintain appropriate water chemistry conditions. Corrosion phenomena, particularly stress corrosion cracking and corrosion fatigue, are caused by the interaction of environment, materials and stress. To understand the corrosion phenomena it is important for successful water chemistry control. Water chemistry control requires monitoring parameters as dissolved oxygen content, pH conductivity and impurity contents.

Pressure vessels for PWRs and BWRs are coated on the inside with stainless steel overlay weld cladding which normally prevents access of the coolant to the underlying ferritic steel. Interest in corrosion fatique of pressure vessel steels arose from overlay clad failures in pressure vessels. Stress corrosion cracks of cladding penetrate also into the base metal.

Pressure vessels steels can show enhanced crack growth rates relative to those observed in air when tested at low cyclic frequencies in high temperature water, simulating PWR or BWR operating conditions. Such enhancement was initially reported by Kondo /22/ , and later confirmed by Bamford /23/.

In recent years extensive corrosion fatigue experiments have been performed at various establishments throught the world and some of these data have been reviewed by Cullen /5/.

Upper limits must be determined for the fatigue crack growth rate in nuclear pressure vessels to assure that a small flow cannot grow to a critical size in service.

Background

The crack growth rate in pressure vessel steels tested in simulated reactor environments in sensitive to a wide range of environmental, material and testing variables /24, 25/.
The complex nature of the corrosion fatigue process and subtle interactions between the testing variables often make it difficult to compare tests performed under apparently similar conditions. Variables include the material chemistry, the initial ΔK level, the R-ratio and the solution chemistry of the crack tip. On constant ΔK tests the rapid crack growth rates seem to be associated with high sulphur levels, high oxygen levels and high R-ratios. The environment that is apparently least susceptible to the rapid fracture mechanism is the simulated PWR environment, with its low oxygen content (< 10 ppb) and the additions of boric acid and lithium hydroxide.

The importance of metallurgical variables of steels is now clear, based on the laboratory test results. The sulphur content and, especially, the MnS inclusion size, shape and distribution of the steel seem to be responsible for material-to-material and heat-to-heat variability. Large elongated MnS inclusions generally contribute to rapid crack growth rates, whereas materials containing small spherical MnS inclusions are less susceptible. The adverse influence of sulphur is thought to result from the dissolution of uncovered MnS inclusions inside the crack, which creates an aggressive local crack tip environment. The sulphur species produced (H_2S, HS^- etc.) are known both to change hydrogen absorption and to increase anodic dissolution of the steel /1, 2/.

The mechanistic study of corrosion fatigue of pressure vessel steels has covered, e.g., fractography, stress corrosion cracking, hydrogen embrittlement, crevice chemistry and electrochemistry, repassivation studies, and surface science, but it is still the general conclusion that the two relevant crack growth mechanisms-film rupture/slip dissolution and hydrogen-induced cracking-are not easily distinguished since they both depend on the same crack growth rate limiting processes: transport of species in solution, oxide film rupture and repassivation /3/. Ford and Emigh /4/ have advanced the anodic dissolution model for the stage where they can calculate the maximum environmental enhancement of crack growth quantitatively. The model still has many unproven assumptions and it cannot explain the fracture morphology. The hydrogen-induced cracking model awaits an improved understanding of the factors that control the amount of crack growth per cycle. The mechanistic understanding has recently been reviewed by, e.g., Cullen et al /5/.

The influence of environment

The results of the interlaboratory activity have shown that there are several variables acting separately or synergistically interactively to control the extent of environmental cracking in either corrosion fatigue or slow strain rate tests on pressure vessel steels /6/. These are (i) steel sulphur content, (ii) water flowrate, (iii) water chemistry, especially oxygen and sulphur anion concentration. Combinations producing the worst environmental effects observed to date for corrosion fatigue crack growth rates at low cyclic frequencies are shown in Fig. 1 /7/. These results form the basis of the current ASME flaw evaluation procedure /8/. They were obtained from experiments on pressure vessel steels with high sulphur levels by modern standards (i.e. > 0.010%) tested in simulated PWR primary water containing less than the maximum allowed 100 ppb oxygen under laminar flow conditions. Conversely, other investigators have shown negligible environmental effects of fatigue crack growth, particularly in low sulphur steels or with turbulent, high quality simulated PWR primary water of unmeasurable oxygen content (< 2 ppb) /9/. It is now known that if sufficient oxygen (~30 ppb) is present to move the corrosion potential to that characterostic of an oxygen redox electrode then, under laminar flow conditions, high environmental cracking rates will be observed in corrosion fatigue tests. Slow strain rate stress corrosion tests reveal the same trend and increasing linear flowrate reduces the adverse environmental effect /10, 11/. A similar story emerges for steel sulphur effects, even in the absence of oxygen in the aqueous environment, although there is thought to be a strong synergistic interaction between these two variables. The adverse influence of sulphur is thought to arise from the dissolution of manganase sulphide inclusions which creates an aggressive local crack tip environment. The build-up of this environment can be ameliorated or prevented by choosing low sulphur steels and increasing the external water flowrate. Nevertheless, the precise optimum low sulphur level and caveats on its morphology and distribution are not well characterised at present. It is, however, no surprise that if sulphur anions (~1 ppm) are added to the bulk environment, substantial environmental cracking rates can be observed /9/.

The variation of cracking susceptibility correlates with the electrochemical potential, and cracking occurs for this temperature range if the rest potential is greater than about -0.2 V (SHE). It was confirmed that the oxygen in the water acts as a chemical potentiostat, which drives the steel into or out of the cracking range, by showing that cracking could be prevented in 45 ppm O_2 water at 288°C by applying cathodic polarization. Cracking could also be induced in < 5 ppb O_2 content water by applying anodic potentials. Large IR drops occurred in the potentiostatically controlled tests and it is probable that the potential need only be moved slightly from the cracking potential to induce a significant reduction in the susceptibility to cracking. The cracking potential correlates well with the Fe_3O_4-Fe_2O_3 boundary for high temperature potential - pH data. It is probable that the mechanism of stress corrosion cracking requires that both Fe_2O_3 and Fe_3O_4 can form in the crack enclave. By replotting the potential - pH data in the form of the required oxygen for a given potential against temperature, it is shown that the oxygen content for inducing cracking agrees closely with the Fe_3O_4-Fe_2O_3 boundary at temperatures from 150°C to 288°C and that in this temperature range cracking is more likely to be associated with an anodic dissolution mechanism than by hydrogen-assisted cracking /12/.

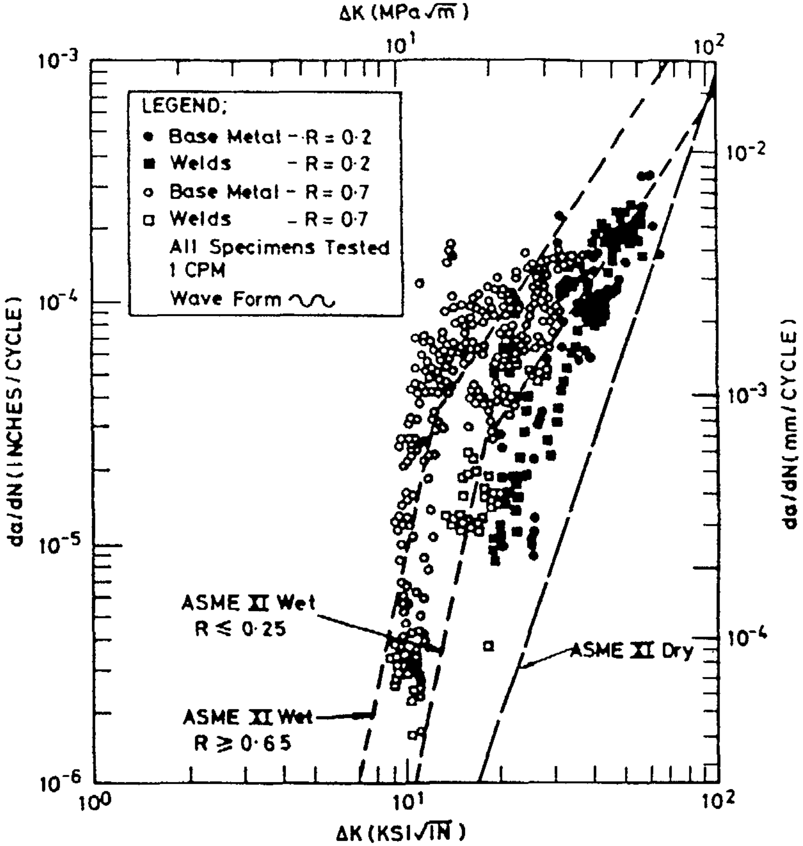

FIG. 1. Corrosion fatigue data for A533-B-1 and A508-2 steels and weldments in PWR primary water.

Radiation - corrosion synergisms

Exposure to primary water environments causes an increase in the rate of fatigue crack propagation in pressure vessel steels. This enhancement in the fatigue crack growth rate may result from anodic dissolution at the crack tip of hydrogen embrittlement near the crack tip. In either case, a wide range of material and environmental variables can affect the crack propagation rate. Irradiation may be expected to provide and additional source of variability in the corrosion fatigue crack growth rates.

However, there are apparently many other effects of equal magnitude and the net effect on the upper limit curves used in ASME Section XI is expected to be minimal. The general approach of using upper limit curves appears to be adequate to account for the effects or irradiation /13/.

Radiation embrittlement in pressure vessel steels has been attributed to the formation of a fine dispersion of copper rich precipitates which cause a hardening of the steel. These precipitates do not form in the unirradiated steel due to the low diffusion rate of copper in steel at 288°C. However, the creation of excess vacancies by irradiation can increase the mobility of the copper atoms resulting in precipitate formation in the irradiated steel. Although the physical property changes in the pressure vessel steels are significant, the microstructural changes are small in scale and subtle. Gross effects, such as large scale phase changes, decrease in grain size or alteration of the MnS inclusion distribution, which might be expected to affect the corrosion fatigue crack growth rate, are not observed in these relatively low fluence irradiations.

Due to the complexity of the experiment and the large size requirements for the test specimens, there is a limited amount of data on crack growth rates in irradiated materials.

In many cases, the corrosion fatigue crack growth rate measured in the irradiated specimens was higher than the crack growth rates measured under similar conditions in the unirradiated specimens. The most notable difference between the irradiated and unirradiated specimens was the frequency dependence of the crack growth rates measured in the irradiated specimens that was not observed in the unirradiated specimens. There was an apparent enhancement in the crack growth rates measured at 0.1 Hz in the irradiated specimens.

Depletion of solute atoms would primarily affect the anodic dissolution rate, while hydrogen trapping is important to the process of hydrogen assisted cracking. The relative importance of hydrogen assisted cracking versus anodic dissolution in determining the fatigue crack growth rate in pressure vessel steels has not been determined. Therefore, it is difficult to predict the influence of these potential radiation effects on the fatigue crack growth rate. However there are a number of potential mechanisms for enhancing the fatigue crack growth rate that are consistent with the damage level in the specimen:

1. The radiation induced increase in yield stress may alter the plastic zone size or promote fracture initiation at inclusions.
2. Radiation induced segregation to grain boundaries may promote intergranular fracture.
3. Radiation induced segregation and precipitation may cause a depletion of solute atoms that are key elements in determining the anodic dissolution rate or the formation rate of an oxide coating.
4. Trapping of hydrogen at radiation induced defects may influence the hydrogen permeability of the steel.
5. The radiation produced by decay in the specimen may alter the crevice chemistry.

There are a number of radiation-induced processes that may affect the stress-corrosion cracking behavior of materials. Radiation can alter the water chemistry by radiolysis, the passive film by atomic displacements or electronic damage, or the microstructure and microchemistry of the alloy by atomic displacements.

Radiation may also alter the corrosion behavior of materials by causing chemical changes in the environment, alterating the protective properties of the passive film, or chemical or phase changes in the alloy. Radiation-induced chemical changes in the environment occur by excitation and ionization of the atoms and molecules in the environment. Changes in chemical composition produce a change in chemical activity of the environment or the kinetics of the cathodic or anodic electrochemical processes. Radiolytic effects occur primarily from the interaction of gamma rays and beta particles from the activated structure or from radionuclides in the coolant. In a water-cooled system, the dominant radionuclide is expected to be ^{16}N formed by (n, p) reactions, which decays into 6.1 MeV gamma rays and 10.4 MeV and 4.3 MeV beta particles.

Most corrosion-resistant materials form a protective film on their surface when exposed to aqueous environments. This film is generally about 100 A thick and is thought to be a hydrated oxide that reduces cation and anion diffusion sufficiently to decrease the corrosion rate by several orders of magnitude. Radiation can degrade the protective properties of a passive film by atomic displacements that increase the cation or anion diffusivity through the film or by a photo-radiation effect that alters the semiconduction properties of the film.

Byalobzhesky /15/ reviewed the radiolytic, damage, and photoconductive effects of irradiation on corrosion; for most materials, an increase of only 1.5 to 3 times was noted. For some selected cases, however, the increase was several orders of magnitude.

In reviewing the effects of radiation on corrosion of carbon steels, Van Konynenberg and McCright /16/ concluded that in temperature and pH regimes in which a passive film is stable, radiation assists in film formation and reduces the corrosion rate. Under conditions in which radiation increased the corrosion rate, the increase was only about a factor of 2, although one study reported an increase of 12.7 for electron irradiation.

Nelson, Westerman, and Gerber /17/ recently reported corrosion tests conducted on several ferritic steels and titanium alloys in a cobalt-60 facility. While the materials, water chemistries, and gamma spectra and fluxes are not directly applicable to LWRs, it is encouraging to not that Nelson, Westerman, and Gerber observed at most a factor of 2 increase in the corrosion rate of ferritic steels.

It is very likely, therefore, that radiolytic effects are a small factor in stress corrosion of passive film-forming materials. Data by Fujita et al. /18/ support this conclusion. They evaluated the stress corrosion cracking behavior of Type 304 SS in high-temperature (250°C) water during a gamma-ray radiation of 4.5×10^4 rad/hr. They found that the fracture strain at strain rates of 5×10^{-7} to 5×10^{-6} s^{-1} was unaffected in water with less than 20 ppb oxygen but was decreased about 50% in water with 8 ppm oxygen. Fujita et al. suggested that the increased hydrogen concentration in the water from radiolysis caused the breakdown of the passive film and thereby caused intergranular stress corrosion cracking (IGSCC) of sensitized material.

It was concluded that radiation-enhanced corrosion was expected to have a small effect on the crack growth rate because the corrosion rates are only enhanced by a factor of two to three by gamma radiation. In some circumstances gamma radiation decreases the corrosion rate; hence, the crack growth rate also would be expected to decrease under those circumstances.

An evaluation of the effect of radiation-enhanced corrosion, creep, and segregation on IASCC has been conducted and supports the conclusion that RES is probably the dominant process in IASCC while radiation-enhanced creep could increase the crack nucleation rate and growth rate of short cracks in components at low stresses. Radiation-enhanced corrosion may increase the crack growth rate by a factor of two to three, but is not expected to be a major contributor to IASCC. These conclusions were based on an assessment utilizing a combination of experimental data and crack growth rate models.

In order to clarify the corrosion mechanism of structural materials used in BWR primary systems, the effects of irradiation on corrosion in high temperature boiling water have been studied experimentally. The effects of irradiation on corrosion were examined by using the gamma ray irradiation facility, GILL, which is equipped with a 10.000 Ci cobalt-60 source.
The corrosion conditions of high temperature water (~ 280°C) caused by irradiation were evaluated by using an approximation model of water radiolysis. It was found that gamma rays enhanced the electrochemical potential of stainless steel in aqueous solution at romm temperature. This was caused by the accumulation of hydrogen peroxide in the solution due to water radiolysis.
The average concentrations of hydrogen and oxygen in the water of the BWR recirculation line were calculated by the approximation model. These results suggested that hydrogen injected into they primary coolant could scavenge the decomposition products of hydrogen peroxide, which caused the suppression of oxygen concentration in the water and moderated the corrosion condition /19/.

Corrosion in an interaction between materials and a solution at their thin boundary. Irradiation can indirectly enhance the interaction through several processes. The factors listed in Table 1 are considered to play important roles in this regard.

The photo effect on the oxide film and the effects of short lived radiolytic radicals should cause rapid changes in the dose rate. The change in electrochemical potential just after irradiation was stopped was very small (less than 5%) which showed that these two effect could be neglected. Accumulation of oxygen

Table 1 Major factors which determine corrosion occurrence

	factor	estimated effects	justification for the estimations
structural materials	thickness of oxide film	corrosion suppression	serve as barriers between materials and solution
	conductivity of oxide film	very rapid effect	analogaus to irradiation effects on semiconductors
aqueous solution	concentration of O_2	negligible effect	saturated concentration
	concentrations of short lived radicals	very rapid effect	short lives (less than 1 ms)
	concentration of H_2O_2	significent effect	constant at room temperature

in the solution could not be expected during the irradiation because the solution was already saturated, so there is no oxygen effect on corrosion occurrence. On the other hand, hydrogen peroxide has a sufficiently long lifetime at room temperature (several days) and it would be expected to accumulate in the solution during irradiation.

If oxygen plays an important role as an oxidising agent in the intergranular stress corrosion cracking, the other chemical species produced by radiolysis of water such as H_2O_2, HO_2, O_2- and OH may also affect the IGSCC /20/. Hence, the constant elongation rate test (CERT) experiment was conducted to examine the effect of radiation on the IGSCC of 304 type stainless steel. It was found that radiation accelerates the IGSCC at higher oxygen concentration but rather retard the IGSCC at lower oxygen level.

It was found that radiation has significant effect on the release of corrosion products from stainless steel and carbon steel in high temperature water; gamma-irradiation enhances the release of crud or insoluble oxide particulates, while it has no appreciable effect on the release of soluble ions. This effect was explained by the hypothesis that ferrous ion released as a result of the corrosion is oxidised by water radiolysis products to ferric ion leading to hematite (α-Fe_2O_3) through the hydrolysis reactions.
One remarkable characteristic of cracks in the core region is that the concentration of oxidizing species (due to radiolysis) in the stagnant crack solution is perhaps higher than in solution external to the crack. Residence time of these species is high a there is more time to react with the material.

Water chemistry monitoring

Environmental control to prevent corrosion was reviewed by Aaltonen /21/.

In power plants extensive instrumentation and laboratory analysis programmes are applied to provide rapid and reliable diagnosis of water chemistry. However, at present chemical monitoring is applied mainly in low temperature, low pressure conditions or by using grab samples. More relevant information concerning the chemical environment could be obtained by using high temperature, high pressure measurements at least for pH, conductivity and electrochemical potentials, which indicate the presence of oxidizing elements in the water.

The major area of interest in systems monitoring material-water reactions for high temperature, high pressure environments is that of corrosion reactions. Most metals are unstable with respect to water and their utilization in water containing environments depends on the kinetics of their corrosion reactions. In many cases the reaction rates are so small that they permit practical application of the materials. However, corrosion reactions are dominating when the long term stability and integrity of energy and process plants are considered. In order to extend the life of components and to obtain higher reliability of materials the real service conditions should be known.

The IGSCC initiation and crack growth rate can be affected by the water chemistry. Under low corrosion potential conditions, which can be obtained through low oxygen content in the water, crack initiation can be avoided. The low conductivity, i.e. high purity, of the water decreases the crack growth rate to a tolerable level. However, transients in the environment which produce high potentials together with high conductivity make fast crack growth rates possible.

Uncertainties concerning the application of electrochemical techniques to environmental monitoring have diminished in recent years. At present the measurement of electrochemical potentials, conductivity and pH in high temperature, high pressure environments in used in many laboratories and also in some power plants. The ability to measure these important parameters at elevated temperatures has opened up a whole new area of solution chemistry, since real operation conditions can now be studied more accurately.

Conclusions

In recent years extensive corrosion fatigue experiments hove been performed at various establishments throught the world. The complex nature of the corrosion fatigue process make it difficult to compare the results of these experiments. Regarding the water chemistry influence corrosion is connected with oxygen level, sulphur species, halides and pH/potential of the system.

The influence of low rate to crack propagation shows that chemistry in the crack may differ from the bulk. This is valid also for irradiated system. The cravice chemistry in such systems and its influence on crack behaviour is not known.

Recommendations

Regarding the safety concerns of the degradation of low-alloy pressure vessel steels we think it is necessary to improve understanding of corrosion mechanisms in these fields:

- The influence of oxygen and trace impurities (sulphur species, halides).
- The influence of pH and potential of the system.
- The degree of radiolysis in cravice/cracks that create agressive species attacking metal surface.

After that it will be possibly to recommend the better chemistry control, water specifications and water chemistry guidelines.

In the field of water chemistry monitoring, it is very useful to continue in development and application of electrochemical high pressure measuring techniques-such as pH, conductivity and electrochemical potentials. Relevant information concerning chemical environment and materials behaviour could be obtained.

References

/ 1/ Hänninen, H., Törrönen, K., Kemppainen, M. and Salonen, S.: On the mechanisms of environment sensitive cyclic crack growth of nuclear reactor pressure vessel steels. Corrosion Sci., 23 (6((1983), pp. 663-79.

/ 2/ Cullen, W.H., Kemppainen, M., Hänninen, H. and Törrönen,K.: The effects of sulfur chemistry and flow rate on fatigue crack growth rates in LWR environments. NUREG/CR-4121 MEA-2053, 1985, 41 pp.

/ 3/ Ford, F.P.: Mechanisms of environmental cracking in systems peculiar to the power generation industry. EPRI NP-2589, Final Report, Palo Alto, CA, 1982.

/ 4/ Ford, F.P. and Emigh, P.W.: Prediction of the maximum corrosion fatigue crack propagation rate in the low alloy steel/deoxygenated water system at 288°C. Corrosion Sci., 25 (8/9) (1985), pp. 673-92.

/ 5/ Cullen, W.H., Gabetta, G. and Hänninen, H.: A review of the models and mechanisms for environmentally-assisted crack growth of pressure vessel and piping steels in PWR environments. NUREG/CR-4422 MEA-2078, 1985. 106 pp.

/ 6/ Scott, P.M.: A review of environment sensitive fracture in water reactor materials. Corrosion Sci., 25 (8/9) (1985), pp. 583-606.

/ 7/ Bamford, W.H.: ASME J.of Pressure Vessel Technology 102, p. 433 (1980).

/ 8/ ASME Boiler and Pressure Vessel Code, Section XI Appendix A (1980).

/ 9/ Jones, R.L.: Paper 170, Proceedings Corrosion '84, April 2-6 1984, New Orleans.

/10/ Hurst, P., Appleton, D.A., Banks, P. and Raffel, A.S.: "Slow strain rate stress corrosion tests on A508-III and A533-B steel in deionised water and PWR water at 290°C". This conference.

/11/ Choi, H., Beck, F.H., Szklarska-Smialowska, Z. and MacDonald, D.D.: Corrosin 38, p. 76 (1982).

/12/ Congleton, J., Shoji, T. and Parkins, R.N.: Corrosion Science, Vol. 25, No.8/9 (1985.

/13/ Lott, R.G. and Mager, T.R.: Corrosion fatigue of irradiated pressure vessel steels.

/14/ Jones, R.H.: Some radiation damage-corrosion synergisms in austenitic stainless steel. Proc. 2nd Int.Symp. on Environmental Degradation of Materials in Nuclear Power Systems - Water Reactors, Monterey, CA 9-12 September 1985, pp. 173-80.

/15/ BYALOBZHESKY, A.V.: General Regularities of Corrosion of Metals Under Radioactive Irradiation, 3rd International Congress on Metallic Corrosion, Swets and Zeitlinger, Amsterdam, 287 (1966).

/16/ Van Konynenburg, R.A., McCright, R.D., UCRL-52892, Lawrenc Livemore Lab., California (1980).

/17/ Nelson, J.L., Westermann, R.E.: Paper presented at Mater. Res.Society Symp.Boston (1983).

/18/ Fujita, N., Akiyama M., Tamura, T.: Corrosion, 36, p.335 (1981).

/19/ Uchida, S., Ibe, E. and Katsura, R.: Radiat.Phys.Chem. Vol. 22, No 3-5, pp. 515 (1983).

/20/ Ishigure, K.: Radiat.Phys.Chem., Vol. 22, No. 1/2, pp. 119-129 (1983).

/21/ Aaltonen, P., Aho-Mantila, I.: Water chemistry monitoring in prevention of ageing related corrosion phenomena, IAEA Conference SM-295/11, Vienna 1987.

/22/ Kondo, T., Kikuyama, T., Nakajima, H. and Shindo, M.: Heavy Section Steel Technology Programme, 6th Annual Information Meeting. Paper No.6, Oag Ridge National Laboratory, Oak Ridge, TN37830, April (1972).

/23/ Bamford, W.H.: I.Mech.E.Conf.Publication, No.4, p.51 (1977).

/24/ Jones, R.L., Overview of international studies on corrosion fatigue of pressure vessel steels. Corrosion 84, NACE, Houston, TX, 1984, Paper Number 170.

/25/ Scott, P.M.: A review of environment sensitive fracture in water reactor materials. Corrosion Sci. 25 (1985) 8/9, pp. 583-606.

AUSTENITIC STEEL CORROSION OUTSIDE THE CORE IN VVERs

J. KYSELA, K. ŠPLÍCHAL, K. JINDŘICH
Nuclear Research Institute,
Řež, Czechoslovakia

Abstract

Corrosion examination of WWER power plants components and of laboratory samples are presented. The in-reactor corrosion experience of steam generator tubes in Czechoslovakian power plants is reviewed.Results of laboratory tests on corrosion rate measurement in different coolant chemistry,steam generator tubes fatigue tests and on the influence of surface treatment are given.

1. Introduction

Results of plant experience and laboratory tests in austenitic steel corrosion outside the active core in VVERs are presented. Material is prepared to the WACOLIN program of the IAEA. The in-plant corrosion experience of steam generator tubes in Czechoslovakian power plants is reviewed. Results of laboratory tests - corrosion rate measurement in different coolant chemistry, steam generator tubes fatigue tests, the influence of surface treatment - are described.

2. In plant corrosion experience of steam generator tubes

2.1 Characteristic of reactor system

Parameters and material characteristics of primary systems and steam generators is given in Table 1 and 2. Both 440 and 1000 MW reactors use stainless steel for steam generators. Steam generators are horizontal type. Primary water specifications are given in Table 3. VVER type reactor use KOH and NH_3 to alkalize the primary coolant. Concentration of hydrogen which is necessary for oxygen supression is formed by the radiolytic decomposition of ammonia.

2.2 Results of examination

Defective SG tubes were cut out from steam generators and were examined in laboratory. The oxide layers were characterized by SEM and X-Ray diffraction. The results of examination are summarized in Table 4. Time of exploitation, corrosion layer description and types of corrosion attack are showed /1/.

Table 1
Characteristics and Parameters of Reactor Systems

PARAMETER	Unit	VVER-440	VVER-1000
Thermal capacity	MW	1375	3000
Electrical capacity	MW	440	1000
Number of loops		6	4
Pressure	MPa	12.25	15.7
Inlet/outlet temperature	°C	264/299	289/322
Flow rate	$m^3.h^{-1}$	39 000	76 000
Fuel element linear heat flux	$kW.m^{-1}$	13.1	17.6
Number of fuel assemblies		349	151

Table 2
Material Characteristics of Primary Systems of VVER-440 MW

SURFACE	MATERIAL	SURFACE /m²/
Fuel Cladding	Zr-Nb	4007
Steam generator, piping	stainless steel 08CH18N10T	15000
In-core structures	stainless steel 08CH19N10G	140

Table 3
Reactor Water Quality Specifications for VVER Reactors Types

PARAMETER	Unit	VVER-440	VVER-1000
H_3BO_3	$g.kg^{-1}$	0 - 6	0 - 13.5
pH (25°C)	6	6	6
KOH	$mg.kg^{-1}$	2.5 - 16	2.5 - 30
NH_3	$mg.kg^{-1}$	5	5
H_2	$mg.kg^{-1}$	30 - 60	30 - 60
O_2	$mg.kg^{-1}$	0.01	0.01
Cl^-	$mg.kg^{-1}$	0.1	-
$Cl^- + F^-$	$mg.kg^{-1}$	-	0.1
Fe	$mg.kg^{-1}$	0.2	0.2
Cu	$mg.kg^{-1}$	-	0.02

Table 4 Summary of in-plant corrosion experience of SG tubes - primary side

Plant	Time of exp.	Corrosion layer charact.	Corr.attack
VVER-440, Bohunice 8 tubes	7000 h	Fe_3O_4 (2-3% Cr, 1-3% Ni), 4-10 µm thick single crystals 1-6 µm	No
VVER-440, Bohunice 1 tube	10530 h	Fe_3O_4 (Cr, Ni) 15-17 µm thick single crystals 4-5 µm	No
VVER-440, Bohunice 1 tube	14100 h	$Fe_{2.72}Ni_{0.28}O_4$ 0.4-16 µm thick single crystals 0.4-16 µm	No
VVER-440, Nord 1 tube	61300 h	Fe_3O_4 (Cr, Ni) single crystals 5-30 µm	Etching surf. by DEKO

3. Laboratory tests

3.1 Coolant chemistry influence on corrosion of stainless steel and activity build-up

Coolant chemistry has been recognized as the major factor which influences radiation fields around primary systems. We suppose that there are two possibilities to modify the primary coolant chemistry at the VVER reactors: hifher pH and hydrazine water chemistry. The results of plant tests were recently published and the experience achieved was the base for decision to start experimental program. We joined our efforts with GDR (German Democratic Republic) institute ZfK Rosendorf and KKW Rheinsberg NPP. The experiments of pressurized water loops were decided as a first step in the pro-*gram before the implementation on* Rheinsberg power plant and then on reactors VVER 440 /2/.

The main objective was to compare three loops experiments with different coolant chemistry: standard water chemistry, high pH and hydrazine. Data and measurements were collected during and after each experiment and were divided into: coolant analysis, corrosion and activity measurements on metal samples, dose measurements. Before each of experiments the RVS-3 loop was decontamined and thus the same initial conditions were maintained. The decontamination procedure has two steps and was developed in the KKW Rheinsberg /3/.

The conditions of experimental runs and results of corrosion rates measurements are summarized in Tables 5, 6, 7 and in Fig. 1. The corrosion rate measurement from metal samples shows no differences between the experiments (Table 7). Corrosion rates from decontamination of the loop internal surfaces increase as follows: hydrazine < standard water *chemistry < high pH. The first decontamination of the loop* was not fully succesfull so the procedure had to be repeated (see Table 8). Possible explanation of this fact is the oxide layer formed at high pH chemistry is more resistant to de - contamination.

Table 5. Thermohydraulic parameters in the loop during activity build-up experiments

	Main Circuit	Heater	Samples		
			Active channel	Measuring Circuit	Comparative channel
Temperature °C	274-294	274-294	290	270-285	294
Pressure MPa	12	12	12	12	12
Flow Rate $t.h^{-1}$	2.5	2.5	2.5	0.14	2.5
Linear Velocity $m.s^{-1}$	0.97	0.025	4.6	0.25	4.6
Reynolds Number	274 000	22 200	189 000	10 300	189 000
Internal Surface m^2	18,2				
Volume m^3	240				

Corrosion data used for VVER reactors / 4, 5, 6, 7/ for austenitic stainless steel type OCH18N10T are summarized in picture 2.

Our corrosion measurements together with VVER's data are in picture 3. (Experiment 1 is standard water chemistry, experiment 2 high pH chemistry and experiment 3 hydrazine chemistry.)

The steam generator tubes with different surface treatment were exposed during experiments with different coolant chemistry. Tube samples were placed in hot measuring circuit of the RVS-3 loop. The tubes with standard blasted surface and the tubes which have electropolished surface were exposed. The results of corrosion layer measurement and parameters of roughness are summarized in Table 9. Corrosion layer was distinguished in outer and inner oxide layer by procedure which consists of two dissolution steps: first step is dissolution with EDTA and the second step is dissolution with permanganate. Content of iron, chromium and nickel in outer and inner oxide layers (Fig. 4) shows the shows the differences between these layers. It was found that the outer oxide layer is Fe-rich and the inner oxide layer is Cr-rich. The differences between mass of the outer layers (see Table 9) on blasted and electropolished tubes can be explained by the fact that electropolished surfaces is less susceptible to crystallite deposition.

Table 6. Water chemistry parameters in the loop during activity build-up experiments

Parameter	Experiment		
	Standard	Higher pH	Hydrazine
H_3BO_3 $g.kg^{-1}$	6.4 ± 0.4	6.1 ± 0.2	6.1 ± 0.3
KOH $mg.kg^{-1}$	17.7 ± 3.8	72.3 ± 3.0	16.5 ± 2.7
NH_3 $mg.kg^{-1}$	15.0 ± 2.0	15.0 ± 2.3	0 - 120
N_2H_4 $ug.kg^{-1}$	-	-	30 - 100
pH 25°C	6.6 ± 0.3	7.3 ± 0.1	7.1 ± 0.4
pH 270°C (MESMER)	6.65	7.20	6.65
pH 300°C (MESMER)	6.80	7.40	6.80
H_2 Nml/kg	0.2 - 0.4	0.2 - 0.4	23 ± 4

Table 7. Corrosion rate of metal samples during experiments

	Corrosion rate $[kg.m^{-2}.s^{-1}]$			
Experiment	Blank samples		Preoxidized samples	
	Comparative channel	Measuring circuit	Comparative channel	Measuring circuit
Standard	6.9 E-10	9.4 E-10	4.5 E-10	4.5 E-10
High pH	1.5 E-9	1.2 E-9	3.9 E-10	4.4 E-10
Hydrazine	1.2 E-9	8.9 E-10	3.5 E-10	4.4 E-10
Remark: Corrosion rate during preoxidizing step was 9.2 E-10				

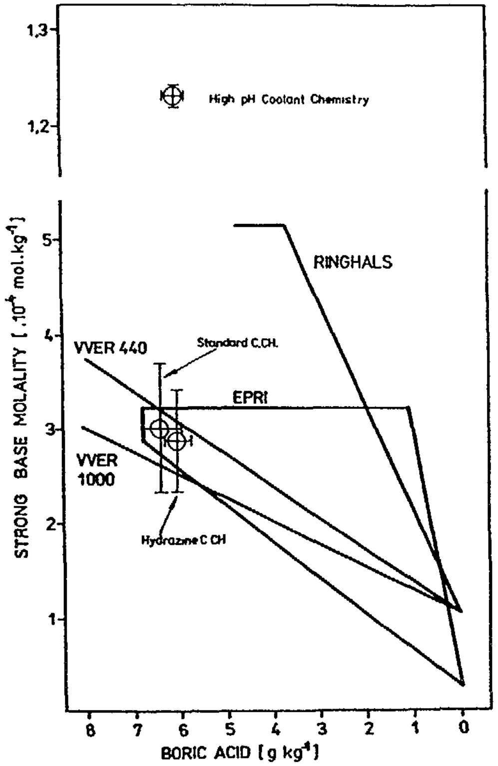

Fig. 1. Coolant Chemistry during Experiments versus recommendations for VVER 440, VVER 1000, EPRI and Ringhals

Results of deposition of activated corrosion products is summarized in Table 10. For all experiments with different coolant chemistry is typical the smaller deposition at electropolished tubes. The activity of electrópolished samples is about 48 - 62% activity of standard blasted samples.

Relative contents of iron, chromium and nikel is dependant on water chemistry and surface treatment (see Table 11). Relative content of iron in corrosion layer is higher at blasted surface and content of chromium is higher at electropolished surface. Higher content of Cr in corrosion layer and in spinel structure of mixed ferrites explains also the lower corrosion rate of electropolished surface (see Table 9).

Table 8. Corrosion rate of the loop surface calculated from decontamination data

Parameter	Standard	Higher pH$^+$			Hydrazine
Gained metals g		I.	II.	I.+II.	
Fe	58.08	63.25	29.25	92.50	35.02
Cr	2.40	8.63	4.18	12.81	4.37
Ni	5.86	6.63	2.09	8.72	2.49
Σmetals	66.34	78.51	35.52	114.03	41.88
Corrosion rate kg.m^{-2}.s^{-1}	1.56 E-9	1.72 E-9	7.78E-10	2.5 E-9	9.88 E-10
Remarks: I. - first decontamination II.- second decontamination					

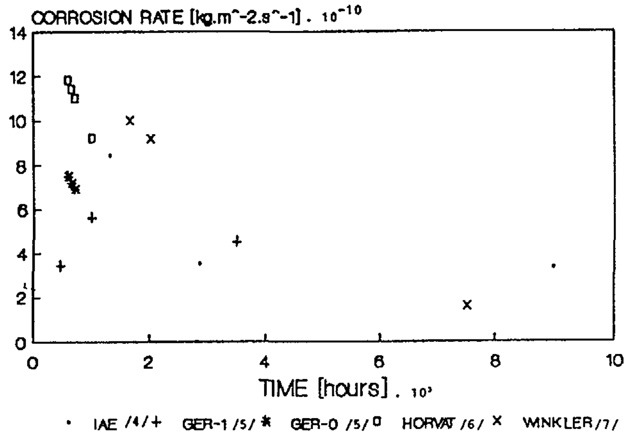

Fig. 2 Corrosion data used for stainless steel OCH18N10T

3.2 Corrosion fatique tests of tubes

Load has been induced with equipment of the RVS-3 reactor water loop in Nuclear Research Institute, dimensioned for operational parameters 15.7 MPa and 335°C with forced circulation of medium. Test section of steam generator tubes is shown in Fig. 5. This section consists of two four-meters tubes (with over-limit technological defects) interconnected by a horizontal pipe coupling. The section is equiped with measuring instrumentation indicating temperature and pressure and is joined to hot measuring circuit of the loop through closing valves.

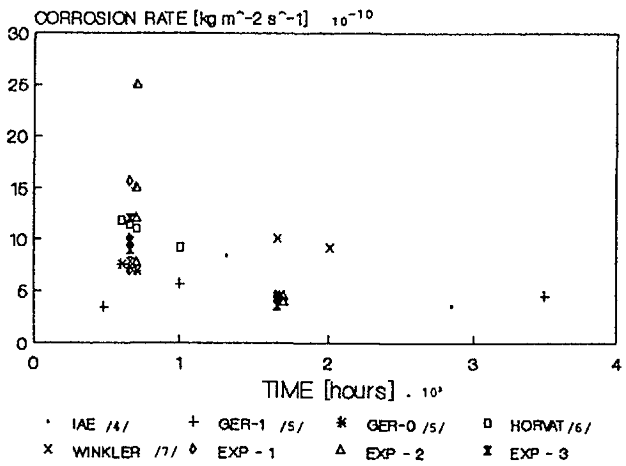

Fig. 3 Corrosion measurement (Exp. 1 - standard, Exp. 2 - high pH, Exp. 3 - hydrazine) together with VVER's data (Fig. 2)

Régime of the experiment followed from the requirement of more stringent modelling of working load of tubes by pressure, temperature, and corrosion loads.

Table 9. Oxide layer on steam generator tubes

EXPERIMENT	Mass of layer mg/cm²			
	blasted surface		electropolished surface	
	outer layer	inner layer	outer layer	inner layer
Standard	0.32	0.08	0.13	0.04
High pH	0.52	0.07	0.04	0.01
Hydrazine	0.01	0.13	0.01	0.11
Roughness, R_a	0.34		0.086	

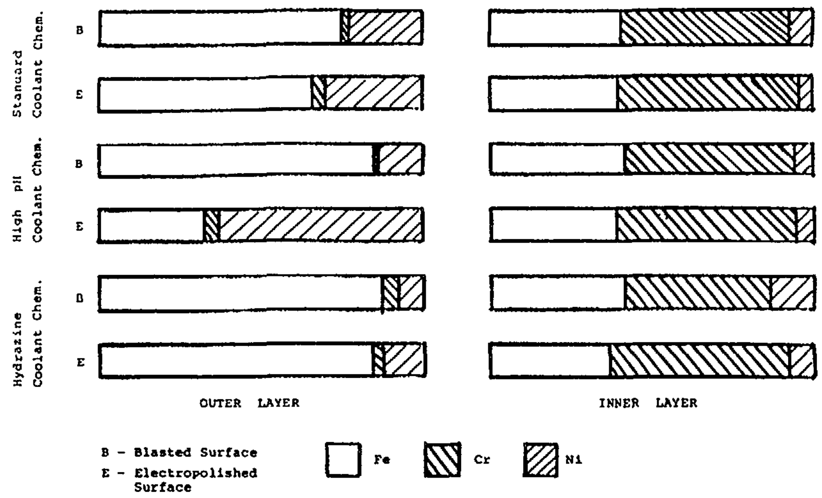

Fig.4 Relative Content of Iron, Chromium and Nickel in Oxide Layers

Tab. 10 Deposition of radioactive corrosion products on surface of tubes

Experiment	Surface	Radioactivity (Bq)		
		^{58}Co	^{60}Co	^{54}Mn
Standard	Blasted	6817	2206	7734
	El.polished	3765	1363	4538
High pH	Blasted	10854	4151	8951
	El.polished	5286	1980	4923
Hydrazine	Blasted	11870	4589	7856
	El.polished	5898	2478	4367

Tab. 11 Relative content of Fe, Cr and Ni in corrosion layer of tubes

Experiment	Relative content (%)					
	Blasted			El.polished		
	Fe	Cr	Ni	Fe	Cr	Ni
Standard	62.0	20.8	17.2	51.5	31.2	17.3
High pH	74.3	13.9	11.8	35.4	26.7	37.9
Hydrazine	67.7	22.7	9.6	58.5	31.9	9.6

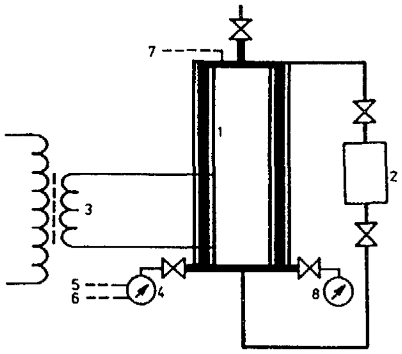

(1 - steam generator tubes, 2 - hot circuit of RVS-3, 3 - power transformer,
4 - pressure gauge with transmitter,
5 - crash pressure-regulation,
6 - regulation of pressure pulsation,
7 - crash temperature-regulation

Fig. 5. The tubes testing section

For establishment of the régime of pressure cycling (by inner overpressure) of the tubes tested, the arrangement with pressure and temperature generation in the medium by electrical heating in direct connection of part of one of the tubes tested into the circuit of the low-tension winding of transformer has been selected /8/.

The experiment has been scheduled for eight weeks. During one week, the experiment has been modified so that pressure test (20 ± 0.5 MPa) has been carried out before the temperature exposition itself. Similar test has been carried out by the end of the week. The daily régime of the experiment consisted of a continuous block of pressure cycles 14 → 11 → 14 MPa, and 12.5 → 6 → 12.5 MPa at temperature of 275 - 315°C and water environment in the loop. Between these exposure blocks, the exchange of the medium in the section (at least once during 12 hours) by the water from the loop with duration of two hours was carried out. Water chemistry in the loop corresponded to that of the VVER reactors with increased concentration of oxygen and chlorides.

Total results of corrosion fatique loading of the tubes are summarized in Table 12. After loading, the tubes have been subjected to a number of tests, mainly from the point of view of evaluation of changes on the inner surface. Corrosion layer formed on the inner surface on the tubes reached maximum thickness ~ 1 μm. The layer was composed mainly of magnetite (Fe_3O_4), partly hematite (α-Fe_2O_3). Average mass of oxidic layer reached the value of 3.9 $g.m^{-2}$. On the basis of difference between optical measurement on the layer thickness and calculation of this thickness from the mass of the layer (for ρ Fe_3O_4 = 5.19 kg dm^{-3}), it is possible to calculate the porosity of the layer, which is 25%. For the study of corrosion layers, the optical and scanning microscopy

Tab. 12 Fatique loading of the tubes

Pressure cyclus	
11 → 14 MPa	28 600 cycl., frequency 0.03 Hz
6 → 12 MPa	3 200 cycl., frequency 0.005 Hz
0 → 20 MPa	10 cycl.
Temperature	275 - 315 °C
Heating 20 → 300°C	100 cycl.
Thermal flux density	3×10^{3} W x m^{-2}
Linear flow rate	0.45 m x s^{-1}
Time exposition at 300°C	800 hours

chemical removal of the oxidic layer, and Mössbauer and infrared spectroscopy have been used.

From the point of view of technological defects on the inner surface, the increase of size of these defects, present in the tube before the experiment, has been evaluated, i.e.presence of propagation of the defects caused by simultaneous mechanical load and corrosive environment at increased content of O_2 and Cl^- has been searched. There is a caustic dependence between concentrations of oxygen and chloride and presence of corrosion cracking. According to the relation presented by Gerasimov /5/, the average time interval of appearence of cracks is lower by two orders at increased content of these components (in our case, $O_2 \leq 0.5$ mg dm^{-3}, $Cl^- \leq 0.7$ mg dm^{-3}) than in the case of standard water chemistry ($O_2 \leq 0.01$ mg dm^{-3}, $Cl^- \leq 0.1$ mg dm^{-3}). Despite of a pronounced increase of stringency of the tests, no increase of size of the defects has been observed, and no initiation of formation of cracks has occurred.

The effects of oxygen and chloride on SCC of austenitic stainless steels in high temperature water /9/ with the results of our measurement is in figure 6.

4. Conclusions

- In plant corrosion experience of steam shows no attack from the side of primary coolant. Corrosion layer is formed by magnetite spinels substitute with nickel $Fe_{3-x}Ni_xO_4$ where x = 0.25. Layer is 4 - 17 µm thick, covered with single crystals.

- Corrosion rate measurement of metal samples shows no difference between the standard, high pH and hydrazine water chemistry. Corrosion rates from decontamination of the loop surfaces increase as follows: hydrazine < standard water chemistry < high pH.

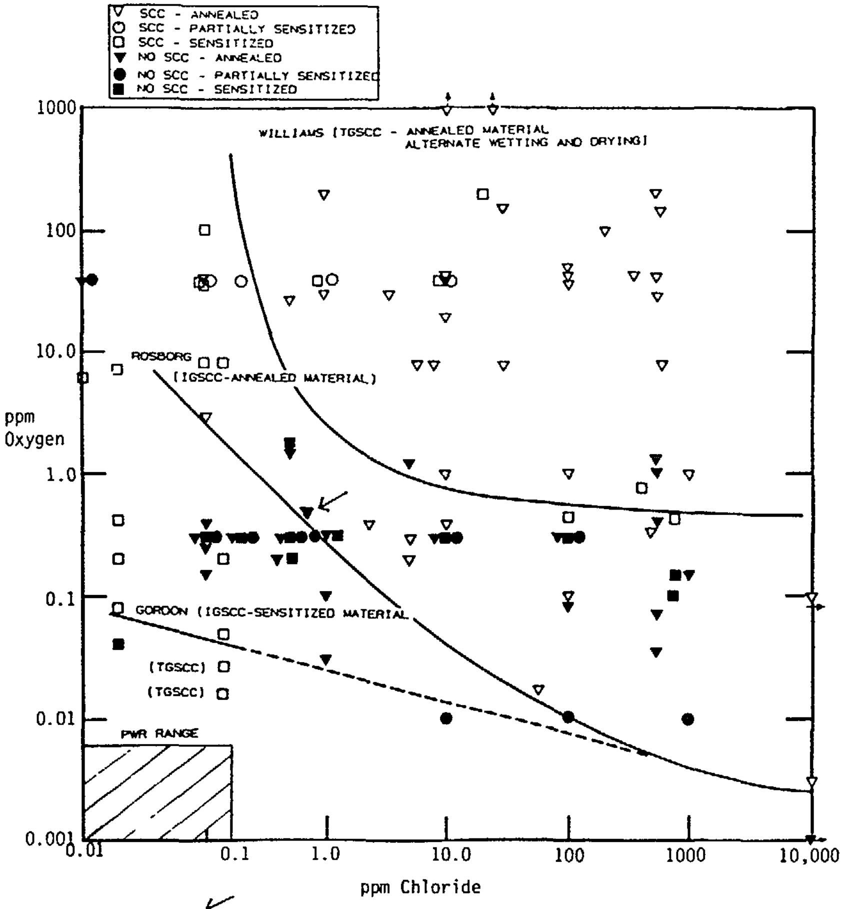

▼↙ Results of our measurements /8/

Figure 6 . The Effects of Oxygen and Chloride on the SCC of Austenitic Stainless Steels in High Temperature Water /9/

- Surface treatment of metal by electropolishing reduce corrosion and radioactive corrosion product deposition.

- No initiation of cracks was observed during corrosion fatigue tests of steam generator tubes with higher content of oxygen (0.5 p.p.m.) and chlorides (0.7 p.p.m.).

5. Recommendations

For next period we recommend:

- in-plant demonstration of corrosion measurement with high pH and hydrazine chemistry and electropolishing samples

- continuation of laboratory tests of corrosion measurements and investigation of double layer structure of corrosion layer during hot-functional tests and steady state operation.

References

/1/ Burda, J., Šplíchal, K.: Study of corrosion behaviour of 18Cr10NiTi steel, Conference on Reliability of steam generators in PWRs, Ostrava, May 1989, Czechoslovakia

/2/ Kysela, J. et al.: In-pile Loop Experiments in Water Chemistry and Corrosion, NRI Report 7750-T (1986)

/3/ Herold, C. et al.: IAEA-TECDOC-248 (1981), p.70.

/4/ Ermakov, V.A., Malova, T.I., Palkina, E.I., Černorotov,E.S.: Water Chemistry of Nuclear Power Plant, Conference of CMEN, Neubrandenburg 1978, GDR

/5/ Gerasimov, V.V.: Corrosion of reactor materials, Moskva 1980, Atomizdat

/6/ Horvath, L.G.: Radtran Code, VEIKI report 93.93-028-2

/7/ Winkler, R.: Doctor thesis TU Dresden, 1970

/8/ Zajíc, V., Kysela, J.: Report NRI 7037/T, 1984, Řež

/9/ Gordon, B.M.: Materials Performance 19, (4), 24 (1980)

IRRADIATION ASSISTED STRESS CORROSION CRACKING OF AUSTENITIC STAINLESS STEELS

I. AHO-MANTILA
Metals Laboratory,
Technical Research Centre of Finland,
Espoo, Finland

Abstract

The in-reactor components made of austenitic stainless steels have recently failed in light water reactor (LWR) environments. The failures have occured by intergranular stress corrosion cracking, which has been enhanced by irradiation. Irradiation assisted stress corrosion cracking (IASCC) seems to be time-dependent and therefore may become more important when the plants are ageing.

Typical features connected to the IASCC are that the failed components have been stressed and located in reactor cores, where the high fluence levels have prevailed. Additionally, the material has not been sensitized. In this paper, the metallurgical condition of the austenitic stainless steel and the necessary environment for the IASCC to occur, are reviewed. The composition of grain boundaries of stainless steels has been examined more closely, because the irradiation enhanced grain boundary segregation of impurities is generally thought to be involved in IASCC.

1. INTRODUCTION

In recent years austenitic stainless steels have suffered failures in the cores of both boiling and pressurized water reactors. Intergranular stress corrosion cracking of stainless steel components in in-core structures is related to the high fluence levels of the cores and called as irradiation assisted stress corrosion cracking (IASCC). The failed components have been stressed and there seems to be a certain fluence level (about $5*10^{20}$ n/cm^2, E >1MeV) after which the IASCC happens (1). The examinations of the failed components have not indicated the sensitization of the material. Shorter times to failure have been observed in BWRs, but the IASCC may affect the component degradation in both kind of ageing LWR nuclear power plants.

The first field IASCC failures were noted in fuel rod cladding in BWRs and incidents were reported also in PWRs when austenitic stainless steels were being investigated as candidates for cladding materials (1). The use of zirconium alloys for LWR fuel cladding has eliminated the concern for fuel, but IASCC has appeared in other components such as the upper guide structure, control blade tubes, and fuel assembly handle in BWRs and bolts and control rod tubes in PWRs (2).

Radiation enhanced corrosion, creep (REC), and segregation (RES) have been implicated in IASCC (2). The factors known to affect IASCC have been separated into two categories, the first a time-dependent one, the second, time-independent. The time-dependent factors are a result of irradiation and include loss of ductility, grain boundary segregation, and change of stress. Factors that are constant with time are electrochemical potential (ECP) in reactor core and strain rate (1).

The occurence of IASCC has introduced the establishment of the International Cooperative Group on Irradiation Assisted Stress Corrosion Cracking, which serves a forum for the technical interchange. This group will encourage the research related to the effects of irradiation on materials properties and subsequent SCC susceptibility and the effects of irradiation on environment and subsequent SCC susceptibility. Several research programmes concerning the IASCC have been started around the world.

In this paper the material and environment related phenomena caused by irradiation on the austenitic stainless steels of the in-core structures are reviewed. Finally measurements of the electrochemical responses of real intergranular fracture surfaces of sensitized austenitic stainless steels are reported. The aim of those measurements was to determine the differences in electrochemical behavior of AISI 304 steel caused by compositional changes of grain boundaries.

2. ENVIRONMENTAL EFFECTS IN IASCC

Radiolysis in an LWR core leads to an increase in electrochemical potential (ECP), which is estimated to be in the order of hundreds of millivolts (1). In the low temperature sensitized piping materials, the critical potential under which intergranular stress corrosion cracking does not occur, has been found and measured to be about -250 mV_{SHE} (3). In the case of in-core structures, the radiolysis could thus increase the electrochemical potential to the region, where the stress corrosion cracking susceptibility of irradiated material increases. However, the critical potential to mitigate SCC of irradiated materials has not yet been established.

Laboratory investigations of the effects of irradiation on the electrochemical potential of stainless steel in BWR-like environments has shown a significant increase in the corrosion potential (4). The corrosion potential of the type 304 SS increased about 200 mV at low oxygen levels, but the effect decreased as the oxygen level increased (Fig. 1). The platinum electrode did not respond in a similar manner, which suggests, that the ECP of type 304 stainless steel may be determined by redox reactions that involve cations with multiple oxidation states (e.g., Fe^{2+}/Fe^{3+}), which are not possible with platinum (5).

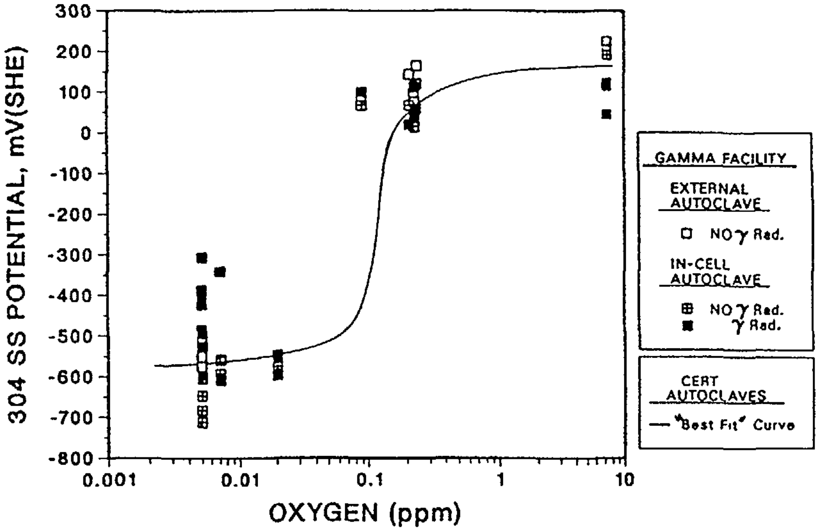

Fig.1 Steady-state ECP of type 304 SS in 289°C water from measurements on identical electrodes located outside the gamma facility and within the facility, with the gamma source on or off. Solid line represents analogous data obtained during CERT experiments without gamma radiation under similar water chemistry conditions (4).

Although the changes in potential at low oxygen levels are fairly large, the actual values of the potential during irradiation (-350 mV_{SHE}) are still quite low compared to those associated with dissolved oxygen levels in normal BWR water. In the test the flux levels from the gamma source were much lower than those in the reactor. The potential measurements performed in in-reactor at Nine Mile Point show, however, comparable results to the laboratory results (4).

The interaction of gamma radiation with aqueous environments produces a host of transient radicals, ions, and stable molecular species including $H\bullet$, $\bullet OH$, e^-_{aq}, H_3O^+, OH^-, H_2, H_2O_2, O_2, O_2^- and HO_2. Some species act as reducing agents, while others, such as H_2O_2, $\bullet OH$, O_2, O_2^- and HO_2, can act as oxidizing agents.

Whether the increase in potential under irradiation results from stable oxidizing species in the solution, permanent changes in the oxide film on the metal, or both, have been tested in ground water (6,7). The corrosion potential of AISI 316L stainless steel shifted immediately in the negative direction when the test solution was replaced by non-irradiated ground water. This, in conjunction with the rapid rise of the potential upon initiation of irradiation appears to indicate that the positive potential shifts observed are due in large part to radiolytically generated stable oxidizing species (Fig. 2).

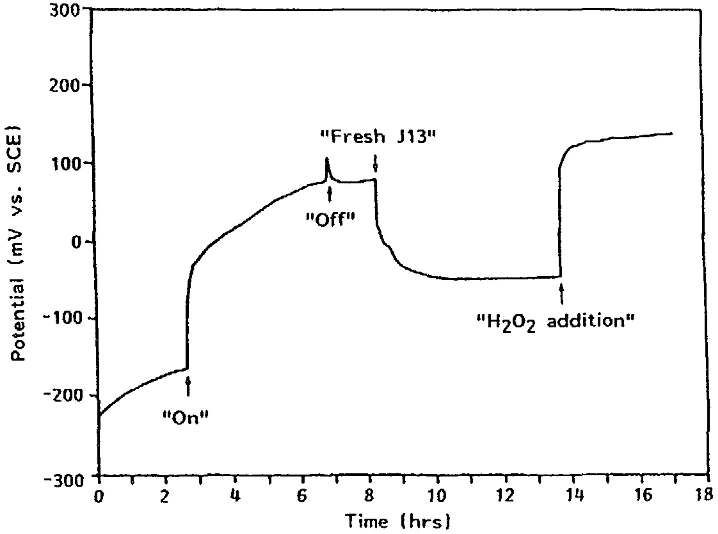

Fig.2 Corrosion potential behavior for AISI 316L stainless steel in gamma-irradiated well water (J-13). Following the "off" half-cycle the irradiated solution was decanted and replaced by a fresh, unirradiated solution. Following this, H_2O_2 was added to solution at a concentration of 0.4 mM (7).

H_2O_2 was added to the fresh ground water, producing a concentration of about 0.4 mM, in order to see whether H_2O_2 alone can produce the potential shifts of the magnitude observed under irradiation. H_2O_2 is the most concentrated radiolytic species present in an irradiated, aerated solution and seems to account for the observed positive corrosion potential shifts for stainless steels (7).

However, it is also evident that some long-term changes in the oxide film are produced since the corrosion potential does not return to the pre-radiolysis value when the fresh solution is introduced. The similar long-term corrosion potential increase has been noticed in the case of stainless steel piping materials, when the plants have aged and dose rates increased (8).

Furuya et al. (9) have studied stress corrosion cracking (SCC) of sensitized austenitic stainless steels in boiling deionized water with gamma-ray irradiation using double U-bend specimens. Gamma-ray irradiation accelerated extremely intergranular SCC in type 304 and type 304L stainless steels (Fig. 3), while type 304 ELC (C 0.015, P 0.034, S 0.003) did not crack even if irradiated with gamma-ray. The polarization curves of sensitized type 304 stainless steel in boiling deionized water with and without irradiation are shown in Fig. 4. With irradiation the corrosion potential is more noble than without irradiation and the active peak and clear passive region is not observed. This could mean that the surface of the type 304 stainless steel is passivated under irradiation because of oxidizing species.

The use of hydrogen water chemistry as a mitigating technique against IASCC is based on its ability to reduce the dissolved oxygen content and to decrease the electrochemical potential to a lower level (1).

3. IRRADIATION ENHANCED GRAIN BOUNDARY SEGREGATION

High voltage electron microscopic observations, performed at elevated temperatures, have shown that grain boundary migration happens during electron irradiation. The grain boundary migration occurs only, when difference in dislocation density between the two adjacent grains arises in an early stage of the irradiation and the grain boundary migrates toward the grain with lower dislocation density (10). The solution distribution in the vicinity of the migrated grain boundary in the high purity Fe-Cr-Ni alloy and in the 316L steel irradiated to 40 dpa at elevated temperatures are shown in Fig. 5.

Chromium segregation away from the grain boundary causes the enrichment of the chromium in front of the migrating grain boundary in the Fe-Cr-Ni ternary alloy, and massive $M_{23}C_6$ type carbide precipitation in the 316 steels containing 0.03-0.05 wt% carbon. The formation of void row along the original grain boundary in the 316L steel appears to be attributable to impurities segregated along the grain boundary during solution-annealing (10).

Grain boundary migration begins after electron-irradiation to about 3 dpa at temperatures above 673 K in Fe-Cr-Ni alloy and in 316 steel (10). Undersized nickel, silicon

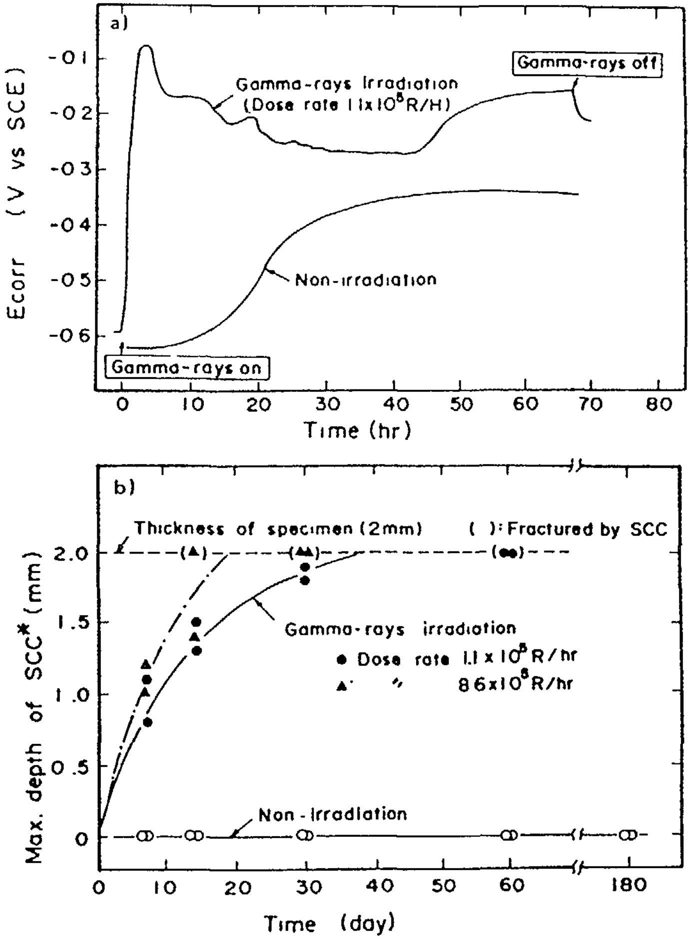

Fig.3 Effects of gamma-ray irradiation on (a) corrosion potential and (b) SCC failures of sensitized type 304 SS immersed in boiling deionized water (9). (* Inner specimen of double U-bend specimens)

and phosphorous segregate toward the grain boundary, and oversized chromium and molydnenum segregate away from the grain boundary during irradiation at 623 to 873 K (Table I). Enrichment of silicon and phosphorous along the grain boundary occurs even after the irradiation at room temperature (11). The segregation increases with irradiation temperature, and the concentration of silicon and phosphorous exhibits maximum at 773 K (Fig. 6).

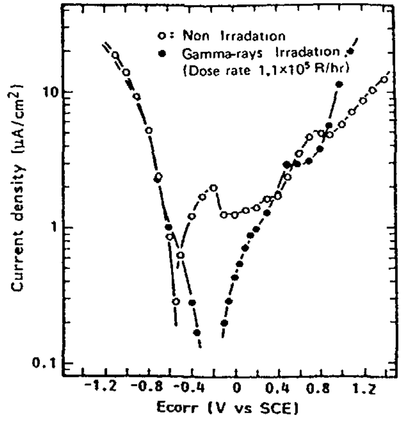

Fig.4 Polarization curves of sensitized 304 stainless steel in boiling deionized water with and without gamma-ray irradiation (9).

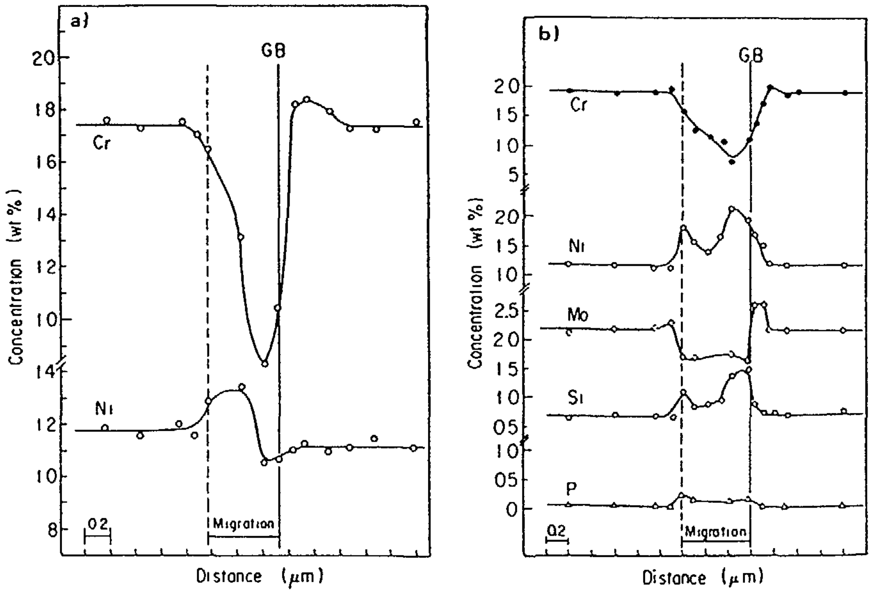

Fig.5 The solute distribution in the vicinity of the migrated grain boundary in (a) the high purity Fe-Cr-Ni alloy and (b) the type 316L steel irradiated up to 39.3 dpa at 773 K and up to 40 dpa at 873 K, respectively. Dotted and solid lines denote the positions of the grain boundary before and after the irradiation (10).

Table I. The effect of the solute atom radius to the segregation toward and away from grain boundary (11).

Solute Atoms	Atomic Radii (nm)	Ω_{sf} (%)[1]	Segregation at G B
P	0.109	-13.16[2]	↗
Si	0.117	-5.81[3]	↗
Ni	0.125	-3.2	↗
Cr	0.125	+4.8	↘
Mo	0.136	+35.9	↘

1) Ω_{sf} : Volume size factor
2) in Fe 3) in Ni

According to Fukuya et al. (13) the grain boundary migration in 304 steel is not observed in the dose range up to 13 dpa at 573 K, which is more close to the reactor temperatures. The lower limit temperature for the radiation-induced $M_{23}C_6$ formation in commercial pure 304 seems to be 773 K.

The temperature dependence of segregation and depletion of solute elements at grain boundary in c.p. 304 is shown in Fig. 7. The degree of the segregation and the depletion becomes smaller with decreasing the irradiation temperature. Phosphorous and silicon segregates at grain boundary at 573 K, while nickel segregation and chromium depletion becomes quite small at 573 K. The temperature regime of radiation induced segregation for silicon and phosphorous extends to lower temperature as compared to that of void formation.

The surface segregation of phosphorous has been analyzed in austenitic 316 stainless steel and in ferritic materials (14,2). All the alloys were irradiated with 5 MeV Ni^{++} ions to dose levels ranging from 0.01 to 12 dpa and at temperatures from 675 to 875 K. Much greater radiation induced segregation of phosphorous was observed in 316 stainless steel than in ferritic alloys (Fig. 8). The surface segregation of phosphorous decreased markedly at high dose levels in all alloys and was attributed to removal of the surface layer by ion sputtering.

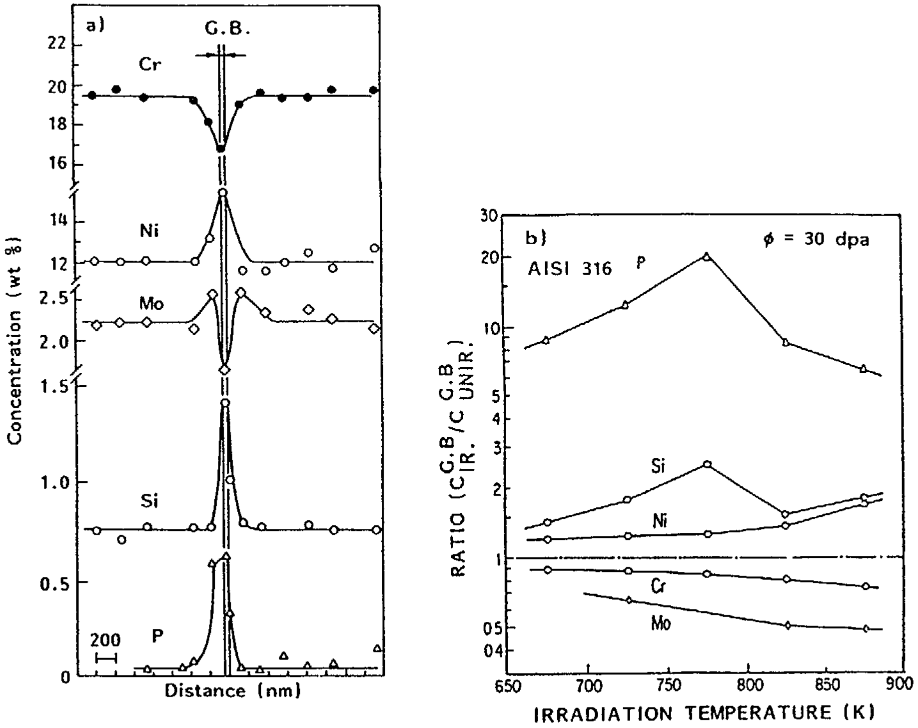

Fig.6 (a) the solute distribution in the vicinity of the grain boundary in the 316L steel irradiated to 30 dpa at 723 K (11) and (b) the temperature dependence of the grain boundary segregation in 316L steel under irradiation (12).

The use of high purity alloys in in-core structures has been one mitigating technique against IASCC and has been based on low impurity contents.

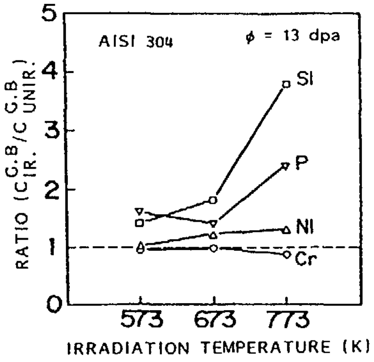

Fig.7 Temperature dependence of grain boundary segregation in C.P. 304 under electron irradiation (13).

4. OTHER IRRADIATION INDUCED CHANGES IN THE PROPERTIES OF AUSTENITIC STAINLESS STEELS

Irradiation can promote the transformation from metastable phases to more stable phases, of which austenite-to-martensite transformation is an example (1). Irradiation induces also changes in dislocation structure and mobility and can create crystal defects, and subsequent strenthening of the material (1,2,15).

Stresses at crack tips generally equal or exceed the yield strength of the material. Therefore, the effect of radiation enhanced creep is not expected to be significant in cracks of sufficient length or with sufficient stress to have a plastic zone at the crack tip, while the thermally activated creep is expected to dominate then. Radiation enhanced creep could play a significant role in components at low stresses and in crack initiation and early stages of crack growth (2).

Hydrogen buildup has been found in 304 stainless steel irradiated to a range of fast (E >1MeV) neutron fluences ($1.9*10^{18}$ to $9*10^{21}$ n/cm^2) in several different boiling water reactors (16). The irradiated materials contained >3 times as much hydrogen as unirradiated material. Hydrogen in the metal can provide necessary stress state at the crack tip for IASCC to occur or it can facilitate the phase transformations. Hydrogen sources in the metal can be (n,p) reactions and in the environment, the radiolysis of the water and formation of hydrogen radicals or the corrosion processes.

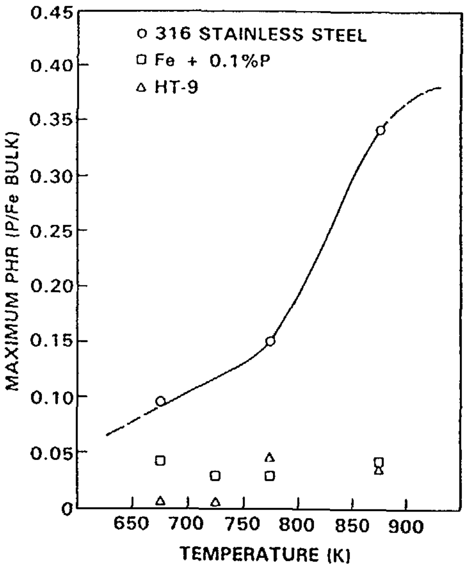

Fig.8 Temperature dependence of the maximum observed PHR of phosphorous in several alloys, ion irradiated to 0.8 dpa (14).

5. STRESS CORROSION CRACKING TESTS OF NON-SENSITIZED AUSTENITIC STAINLESS STEELS

Stress corrosion cracking tests for irradiated material have been performed in General Electric (17, 18, 19). The results of constant extension rate testing (CERT) of annealed and irradiated type 304 stainless steel material reveal an irradiation effect on SCC resistance. A sample irradiated to $3*10^{21}$ n/cm^2 (E >1 MeV) and then CERT tested in 288°C water with 32-36 ppm dissolved oxygen failed entirely by IGSCC. A specimen irradiated to $1*10^{18}$ n/cm^2 and tested identically to the above failed in a ductile mode (Table II). The low-fluence plate sample with a radiation source attached, failed in a ductile way when tested in a manner which produces IASCC in high-fluence material (18). It seems necessary, a susceptible microstructure to be produced by irradiation effects, for IASCC to occur.

The extent of IASCC in irradiated material appears greater in gamma field environment than in similar tests performed in an oxidizing environment (32 ppm dissolved oxygen)

Table II. Room temperature tensile properties and CERT results for annealed and irradiated type 304 plate material (288°C water with 32-36 mg/l O_2) (18).

Fluence	Yield Strength (MPa/Ksi)	Ultimate Tensile Strength (MPa/Ksi)	Elongation (%)
3×10^{21} n/cm^2	820/118	859/125	18
1×10^{18} n/cm^2	195/28	505/73	75

Test No.	Sample Fluence (n/cm^2, E>1 MeV)	Strain Rate (min^{-1})	Test Time (h)	Max. Stress (MPa/Ksi)	Fracture Mode (SEM)
HC-1	3×10^{21}	4×10^{-6}	191	710/103	IGSCC (100%)
HC-2	1×10^{18}	4×10^{-6}	408	372/54	Ductile
HC-3	3×10^{21}	1×10^{-4}	25	717/104	IGSCC (40%)
HC-4[a]	1×10^{18}	4×10^{-6}	382	382/52	Ductile

[a] High radiation source (1/2 of high-fluence sample) attached to test sample.

without the gamma field (19). The fluence level of the studied material was $3*10^{21}$ n/cm^2. The IASCC was mitigated in a gamma field test conducted in a hydrogen water chemistry environment (2 to 5 ppb O_2 and about 75 ppb H_2) (Table III).

Briant and Andresen (20) have been studied the grain boundary segregation and intergranular stress corrosion cracking in low carbon, non-sensitized austenitic stainless steels. They observed that intergranular stress corrosion cracking in 288°C water at a pH of 2.5 and electrochemical potential of 0 V_{SHE} can occur in these steels even in the absence of chromium depletion if sulfur is present on the grain boundaries.

The non-sensitized 316L stainless steel has been tested in 288°C water with side grooved, compact type specimen, in order to determine its susceptibility to intergranular environmentally assisted cracking and the subsequent crack growth rate (21). The measured crack propagation rate at constant stress intensity of 28 MPa$\sqrt{m}$ was $4.2*10^{-9}$ cm/s, about a factor of 8 lower than the typical crack growth rate for sensitized type 304 stainless steel under similar test conditions.

Table III. CERT test results for irradiated type 304 stainless steel in 288°C water under gamma radiation (strain rate $1*10^{-7}$/s) (19).

TEST NO	MAXIMUM BREAKING STRESS (MPa/ksi)	TIME TO FRACTURE (h)	STRAIN AT FRACTURE (%)	IASCC[a] (%)	WATER CHEMISTRY[b] OXYGEN (ppb)	WATER CHEMISTRY[b] HYDROGEN (ppb)	WATER CHEMISTRY[b] CONDUCTIVITY μS/cm AT 25°C	ELECTROCHEMICAL POTENTIAL RANGE (mV$_{SHE}$) 304SS	ELECTROCHEMICAL POTENTIAL RANGE (mV$_{SHE}$) Pt
1	602/87 4	188	8 0	85	250–570	2–9	0 1–0 15	+200/+670	−200/+635
2	870/126 2	254	14 8	0	2 5–5 3	26–75	0 2–0 29	−300/−603	−685/−590

[a] DETERMINED BY SEM

[b] MINIMUM MAXIMUM VALUES OBSERVED OVER TEST AT AUTOCLAVE INLET SAMPLE POINT

6. ELECTROCHEMICAL METHODS TO ESTIMATE IASCC SUSCEPTIBILITY OF STAINLESS STEELS

Several intergranular corrosion test methods have been utilized to the irradiated materials, but satisfactory correlation between intergranular test results and IASCC susceptibility has not been found.

The electrochemical behaviours of intergranular fracture surfaces of sensitized austenitic stainless steels have been measured in order to determine the possible differences caused by compositional changes (22). According to Auger electron spectroscopy results the impurities, such as P and S, segregate to the grain boundaries during sensitization heat treatments.

In the polarization measurements clear difference between the intergranular fracture surface and the reference specimen of sensitized stainless steel was noticed at the corrosion potential (Fig. 9). The corrosion potential of the intergranular fracture surface is lower than the corrosion potential of the reference specimen in deaerated sulphuric acid solution at room temperature. The difference was more pronounced in steels containing more phosphorous. This corrosion potential difference caused intergranular corrosion in immersion test and intergranular fracture in slow strain rate tests (Fig. 10).

Polarization measurements of the austenitic stainless steel specimens in different solutions containing impurities showed that the potential shift to a lower value is produced by adding Na_2S into 1 N H_2SO_4 solution (Fig. 11). Phosphorous in the electrolyte increases the hydrogen overpotential, but the phosphorous in the solid solution of the steel seems to decrease the hydrogen overpotential.

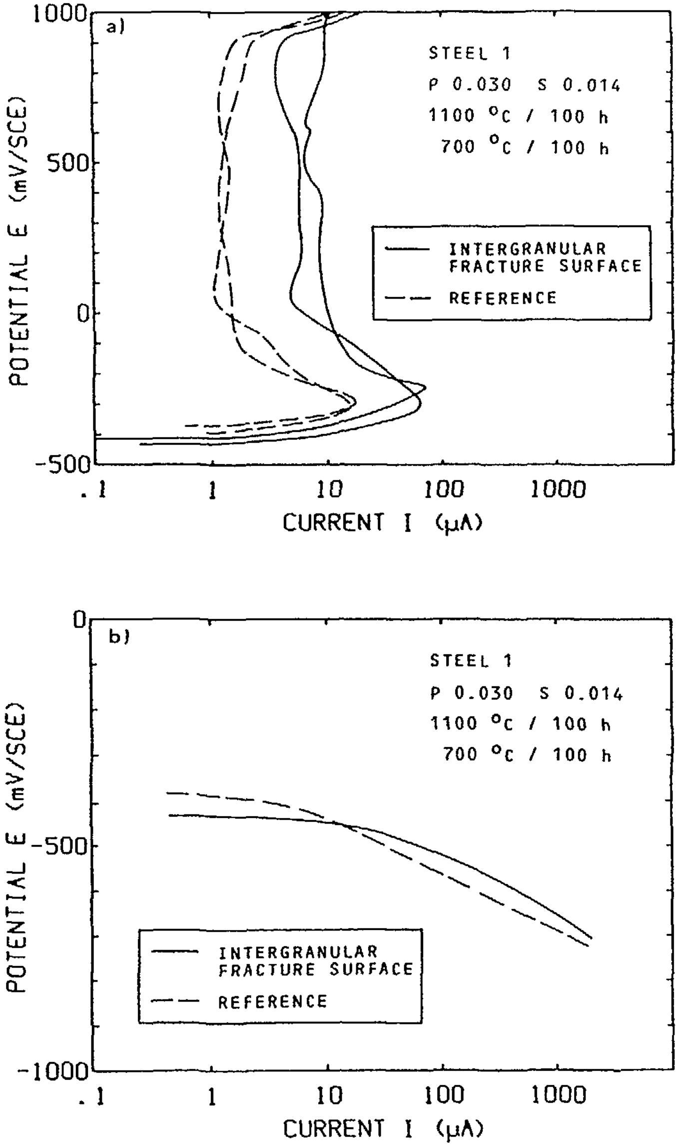

Fig.9 (a) anodic and (b) cathodic polarization curves of type 304 stainless steel.

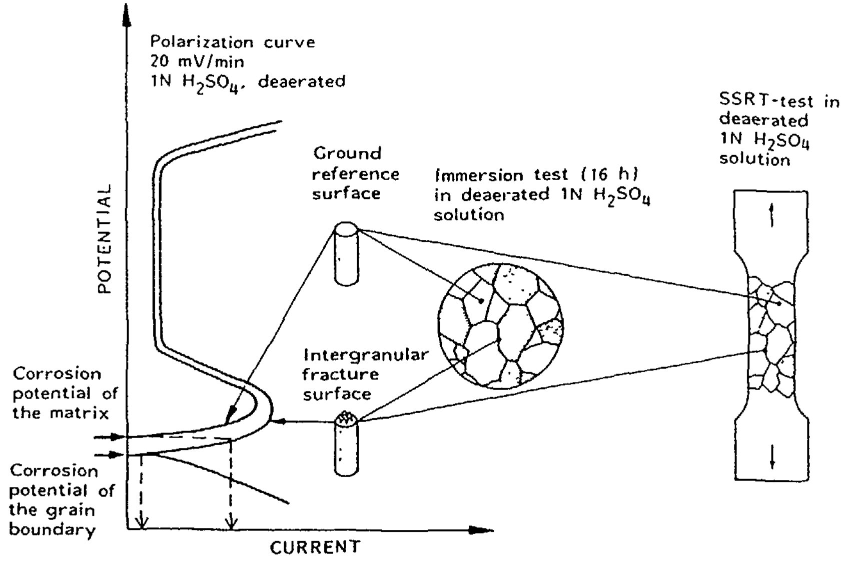

Fig.10 Schematic corrosion potential difference between matrix and grain boundary and its effect on the corrosion attack in the immersion test and in the slow strain test.

In order to electrochemically reveal SCC causing segregation in austenitic stainless steels, more work with non-sensitized austenitic stainless steels is needed.

7. CONCLUSIONS

The occurence of irradiation assisted stress corrosion cracking has been increased as an intergranular failure mode of austenitic stainless steel structures in light water reactor cores. IASCC is a time-dependent phenomenon which may become more frequent with the ageing of the plants.

Corrosion potential increase because of oxidizing conditions in the reactor cores and several possible irradiation induced changes in metallurgical structure of austenitic stainless steels, as well as in mechanical conditions, have been suggested for the reason of IASCC.

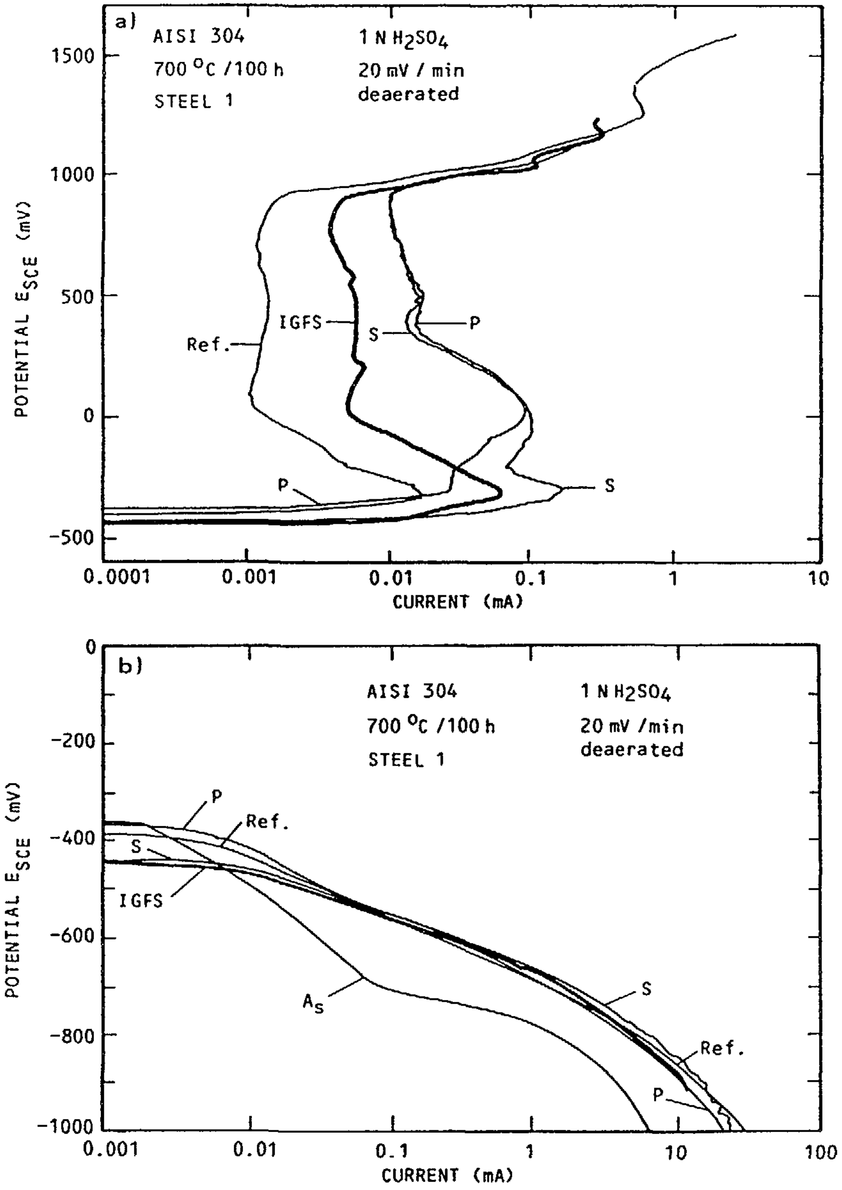

Fig.11 (a) anodic and (b) cathodic polarization measurements of intergranular fracture surface of type 304 stainless steel. The polarization curves of the matrix have been measured in different solutions containing impurities.

ACKNOWLEDGMENT

This paper is a part of the Structural Materials in Nuclear Power Plants Programme funded by the Ministry of Trade and Industry in Finland and the Technical Research Centre of Finland.

REFERENCES

(1) Jacobs, A. J. & Wozadlo, G. P., "Irradiation-Assisted Stress Corrosion Cracking as a Factor in Nuclear Power Plant Aging", Proc., International Conference on Nuclear Power Plant Aging, Availability Factor and Reliability Analysis, pp. 173-180, Ed. V. S. Goel, ASM, 1985.

(2) Jones, R. H., "Some Radiation Damage - Stress Corrosion Synergisms in Austenitic Stainless Steel", Proc., Second International symposium on Environmental Degradation of Materials in Nuclear Power Systems - Water Reactors, pp. 173-180, ANS, 1986.

(3) Aaltonen, P., "Electrochemical Measurements in Simulated Light Water Reactor Environments", VTT-MET B-106, 13 p., Technical Research Centre of Finland, 1986.

(4) Shack, W. J. et al., "Environmentally Assisted Cracking in Light Water Reactors", in Compilation of Contract Research for the Materials Branch, Division of Engineering Safety, NUREG-0975, Vol. 5, R5, pp. 229-253, NRC, 1987.

(5) Ruther, W. E. et al., "Influence of Gamma Radiation on the ECP of Type 304 SS, Ti, and Pt in 289°C Water", 15 p., ANL, 1987.

(6) Glass, R. S., "Corrosion Processes of Austenitic Stainless Steels and Copper-Based Materials in Gamma-Irradiated Aqueous Environments", Corrosion 86, Paper number 258, 12 p., NACE, 1986.

(7) Glass, R. S. et al., "Gamma Radiation Effects on Corrosion: I Electrochemical Mechanisms for the Aqueous Corrosion Processes of Austenitic Stainless Steels Relevant to Nuclear Waste Disposal in Tuff", Corr. Sci., Vol. 26, No. 8, pp. 577-590, 1986.

(8) Leibowitz, J. et al., "In Plant Measurements on Electrochemical Potentials in BWR Water", EPRI NP-3521, 88 p., EPRI, 1984.

(9) Furuya, T. et al., "Influence of Gamma-Ray Irradiation on Stress Corrosion Cracking of Austenitic Stainless Steels", Proc., Int. Top. Meet. Fuel Reprocess, Waste Manage, pp. 493-502, ANS, 1984.

(10) Nakata, K. et al., " Grain Boundary Migration during Electron Irradiation in Austenitic Stainless Steels", Journal of Nuclear Materials, Vol. 133&134, pp.575-579, 1985.

(11) Nakata, K. et al., "Solute Segregation along Non-Migrated and Migrated Grain Boundaries during Electron-Irradiation in Austenitic Stainless Steels", Journal of Nuclear Materials, to be published.

(12) Nakata, K. et al., "Radiation Induced Segregation of P, Si and Cr at Grain Boundary in Type 316 Stainless Steel", Annual Meeting of Japan Institute of Metals, 12 p., 1983.

(13) Fukuya, K. et al., "Microstructural Evolution and Microchemical Segregation in 304 Stainless Steels during Electron Irradiation at 573 K- 773 K", Scripta Met., Vol. 19, No. 8, pp. 959-962, 1985.

(14) Brimhall, J. L., "Radiation Induced Phosphorus Segregation in Austenitic and Ferritic Alloys", Journal of Nuclear Materials, Vol. 122&123, pp. 196-200, 1984.

(15) Ehrlich, K., "Deformation Behaviour of Austenitic Stainless Steels after and during Neutron Irradiation", Journal of Nuclear Materials, Vol. 133&134, pp. 119-126, 1985.

(16) Jacobs, A. J., "Hydrogen Buildup in Irradiated Type 304 Stainless Steel", Symp. on Effects of Radiation on Materials, Seattle, 15 p., 1986.

(17) Clarke, W. L. & Jacobs, A. J., " Stress Corrosion Test Facility for Studying Irradiated Materials", Materials in Nuclear Energy, pp. 153-160, ASM, 1983.

(18) Clarke, W. L. & Jacobs, A. J., "Effect of Radiation Environment on SCC of Austenitic Materials", Proc. International Symposium on Environmental Degradation of Materials in Nuclear Power Systems - Water Reactors, pp.451-461, NACE, 1984.

(19) Clarke, W. L. et al., "Effect of Gamma Radiation on SCC Testing of Irradiated Stainless Steel in High Temperature Water", Proc., Second International Symposium on Environmental Degradation of Materials in Nuclear Power Systems- Water Reactors, pp. 442-447, ANS, 1986.

(20) Briant, C. L. & Andresen, P. L., " Grain Boundary Segregation in Austenitic Stainless Steels and Its Effect on Intergranular Corrosion and Stress Corrosion Cracking", Metallurgical Transactions, to be published.

(21) Andresen, P. L., "Environmentally Assisted Growth Rate Response of Non-Sensitized 316 Grade Stainless Steels in High Temperature Water", Corrosion 87, Paper number 85, 15 p., NACE, 1987.

(22) Aho-Mantila, I. & Hänninen, H., " Electrochemical Methods to Estimate IASCC Susceptibility of Stainless Steels", International Conference on Materials for Nuclear Reactor Core Applications, Bristol, England, 8 p., BNES, 1987.

INFLUENCE OF PRIMARY COOLANT pH VALUE AND LITHIUM CONCENTRATION ON RESISTANCE OF ALLOY 600 MA STEAM GENERATOR TUBING TO PRIMARY WATER STRESS CORROSION CRACKING

R. KILIAN, N. WIELING
Siemens AG,
Unternehmensbereich KWU,
Erlangen, Germany

Abstract

To reduce the dose rate build up on PWR out-of-core surfaces the operating experience with some PWRs shows that an increase of the pH-level of the primary coolant is sucessful.

On the other hand an adjustment of a pH which is optimized regarding dose rate reduction could cause an increase of PWSCC susceptibility. Therefore the influence of pH and lithium concentration on the PWSCC behaviour of Alloy 600 MA was investigated.

Alloy 600 MA RUB's were exposed to high and standard lithium/boron coordinated primary coolant chemistry treatment at T = 330°C for max. 5000 h. The adjusted pH-values calculated for T = 330°C were 6.8, 7.1 and 7.4.

The results show that there is no influence of lithium concentation, but a minimum of PWSCC susceptibility can be observed at a pH-value of 7.1.

1.Introduction

Considerable efforts are being made worldwide to reduce the dose rate build up on PWR out-of-core surfaces. The operating experience with some PWRs shows that an increase in the pH level of the primary coolant by increasing lithium reduces the out-of-core dose rates significantly.

Alloy 600 is a commonly used material for the heat exchanger tubing of PWR steam generators. However, the experience with this alloy shows that it is not immune to Primary Water Stress Corrosion Cracking (PWSCC). Some literature data indicate that the SCC-resistance may be reduced by an increased pH-level and/or an increased Lithium concentration.

Adjustment to a pH which is optimum with respect to a dose rate reduction might therefore cause an increase in the susceptibility of the SG tubing. The objective of this program is to investigate the influence of pH and lithium concentration on the susceptibility of Alloy 600 in order to optimize primary coolant water chemistry.

Alloy 600 SCC test specimens were thus exposed in autoclaves to representative PWR primary coolant conditions with high and standard lithium/boron coordinated chemistry treatment. Because of the long incubation time for occurrence of PWSCC, test durations of at least two years were envisaged, together with more severe test conditions. These can be achieved, e.g., by increasing the test temperature to approximately 365°C and by using highly deformed test specimens. The test specimens were inspected visually at certain intervals and, depending on the inspection results, examined metallographically.

As with the well-known hot-steam test, split tube reversed U-bend (RUB) specimens were used. In order to compare the results obtained with those from other laboratory investigations, the test temperature was limited to 330°C. Literature data [1] show that this temperature is sufficient to cause PWSCC in Alloy 600 MA RUB's.

2.Experimental

The test program is described in the following sections:

2.1. Test specimens

Split tube reverse U-bend specimens (RUB) were used (Figure 1). To ensure representative and reproducible stress conditions a special bending procedure and bending tool are necessary. Therefore, a bending tool was developed to produce this kind of SCC-test specimens.

2.2. Test specimen materials

Alloy 600 MA tubes with high SCC susceptibility (representative for some W-SG's) were used as the main test material. The chemical composition and the mechanical properties are shown in Tables 1a and 1b. The material was supplied by Sandvik and given a special additional heat treatment to ensure high susceptibility to PWSCC. The minimum cracking time for RUB's made of this material in the hot steam test (400°C, 1.1 bar hydrogen partial pressure) is 7 days.

In addition to the original scope of work, RUB's made of Alloy 690 TT were also tested. The chemical composition and the mechanical properties are also shown in Tables 1a and 1b.

Fig. 1: Split tube reversed U-bend specimen (RUB)

48 RUB's made of Alloy 600 have been produced. 12 specimens and 2 additional Alloy 690 TT specimens were exposed per test environment.

2.3. Test environment conditions

The coolant chemistry conditions were chosen under consideration of results from a C.N. Almaraz dose rate build-up study (Fig. 2). So that the test results give sufficient information about the influence of Li and pH on PWSCC. In order to obtain test results as rapidly as possible several test runs were performed simultaneously.

The water chemistry conditions used in this program are given in Table 2.

2.4. Test facilities

To investigate only the influence of Li and B contents on the susceptibility to PWSCC the other test parameters had to be kept as uniform as possible, especially the temperature of the four test autoclaves.

TABLE 1a. CHEMICAL COMPOSITION (in wt%)

	C	Si	Mn	P	S	Cr	Ni	Co	Ti	Cu	Al	Fe	N	B
Alloy 600 MA (19,05x1,09mm)	.027	.29	.80	.008	.003	16.55	72.7	.011	.29	.010	.14	9.19		
Alloy 690 TT (22,23x1,27mm)	.019	.38	.29	.010	.002	29.9	59.2	.013	.31	.010	.035	9.79	.028	.0010

TABLE 1b. MECHANICAL PROPERTIES

	Yield Strength [N/mm²]	Tensile Strength [N/mm²]	Elongation in % of 2"
Alloy 600 MA	399	715	42
Alloy 690 TT	338	729	48

A prerequisite for constant test temperatures in the four test autoclaves was that their characteristics, such as

- construction
- material
- volume
- heat capacity and
- temperature adjustment

are identical.

Because four identical autoclaves with suitable dimensions were not available, new equipment (see Figs. 3 and 4) had to be fabricated.

Figure 4 shows the four vertical autoclaves, which are installed together in a heater.

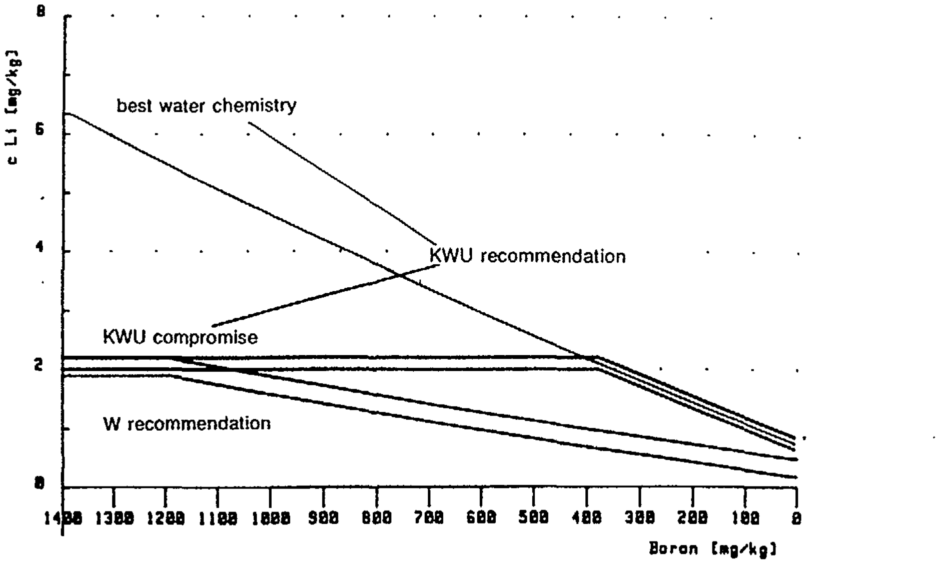

Fig. 2: N.N.Almaraz: Different recommendations for coordinated B/Li-treatment

TABLE 2. WATER CHEMISTRY CONDITIONS

Test No. / Content	1.Test	2.Test	3.Test	4.Test
Li	6.5ppm	2ppm	3.5ppm	3.5ppm
B	1400ppm	1400ppm	1400ppm	700ppm
pH	7.4	6.8	7.1	7.4
H_2	3ppm	3ppm	3ppm	3ppm

The temperature adjustment of the heater and the temperature measurement of the individual autoclaves was carried out by a special control unit (see Fig. 5). The safety equipment of the autoclaves, the arrangement for dosing of Ar and H_2 gas and for measurement of H_2 gas can be seen in the photo and the block diagram (see Figs. 6 and 7).

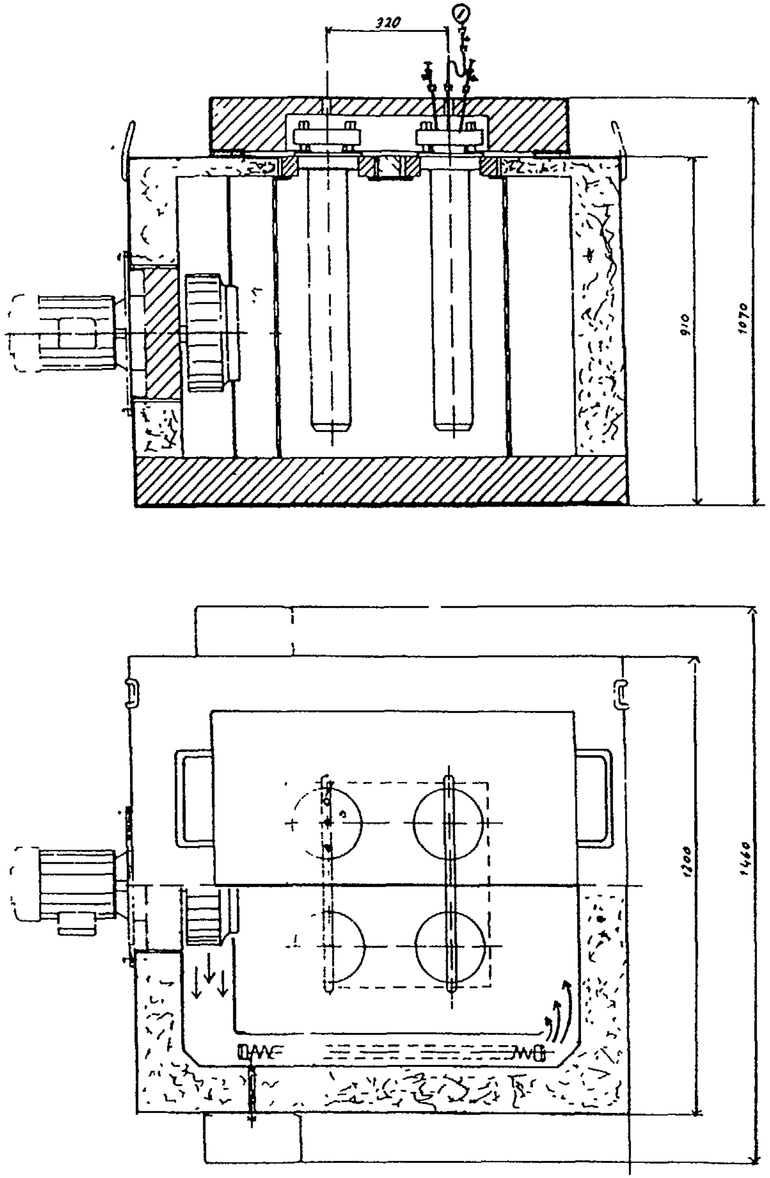

Fig. 3: Heating unit for 4 autoclaves (sectional drawing)

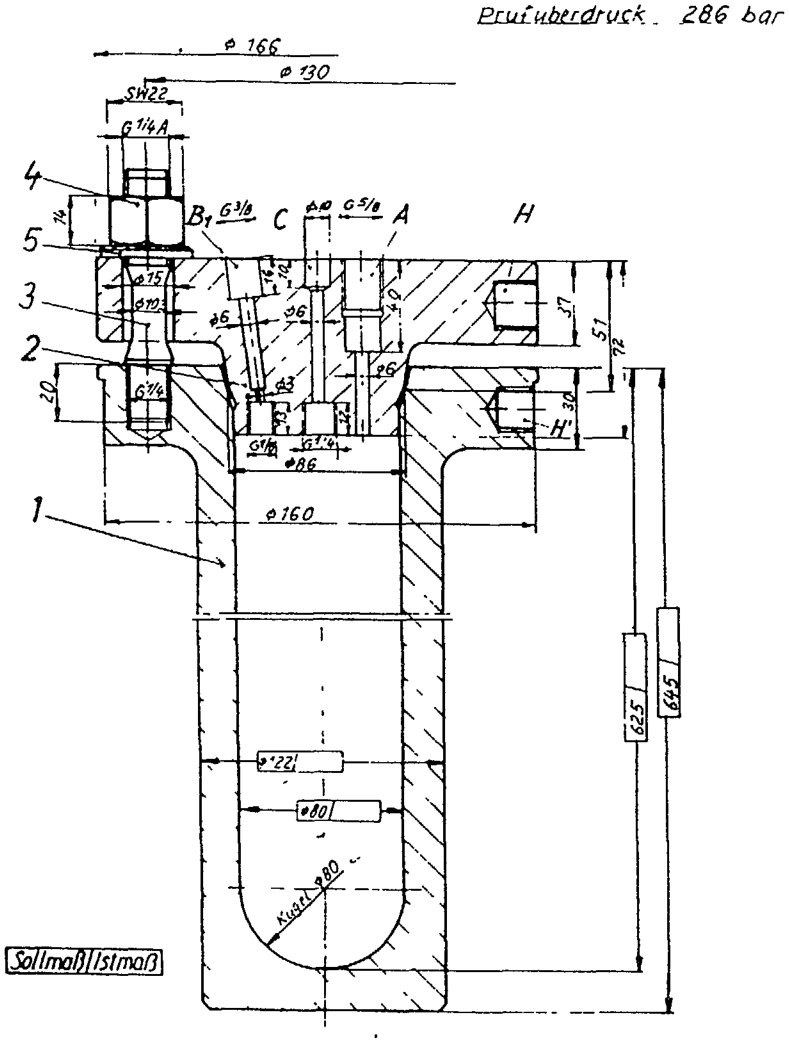

Fabr Nr	å.ϕ	Li.ϕ	Länge innen	Länge außen
88.12.266/1	122,6	80,0	623,5	645,5
88.12 266/2	122,4	79,9	624,7	645,5
88.12 266/3	122,3	80,0	623,9	645,6
88.12 266/4	122,6	79,9	624,5	645,3

Fig. 4: Autoclave for PWSCC-tests

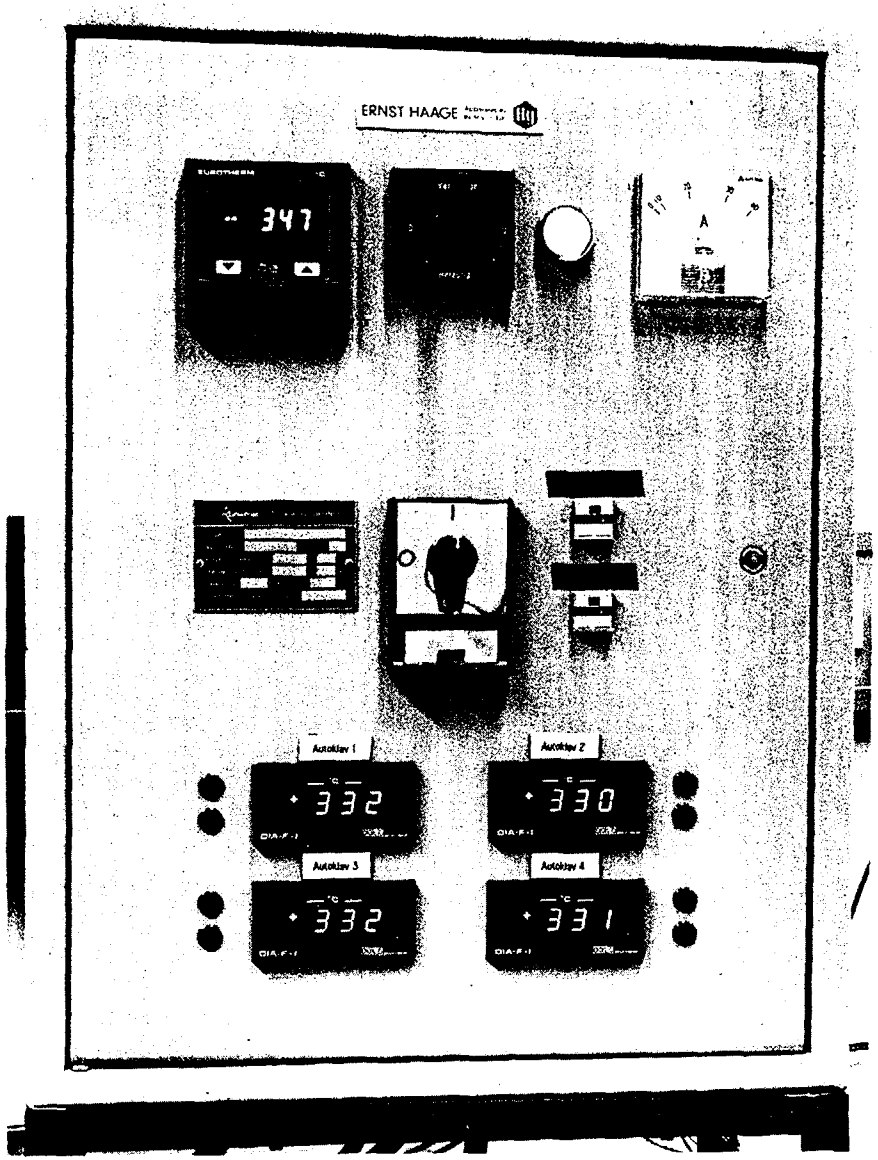

Fig. 5: Switch box with temperature control and temperature gauges

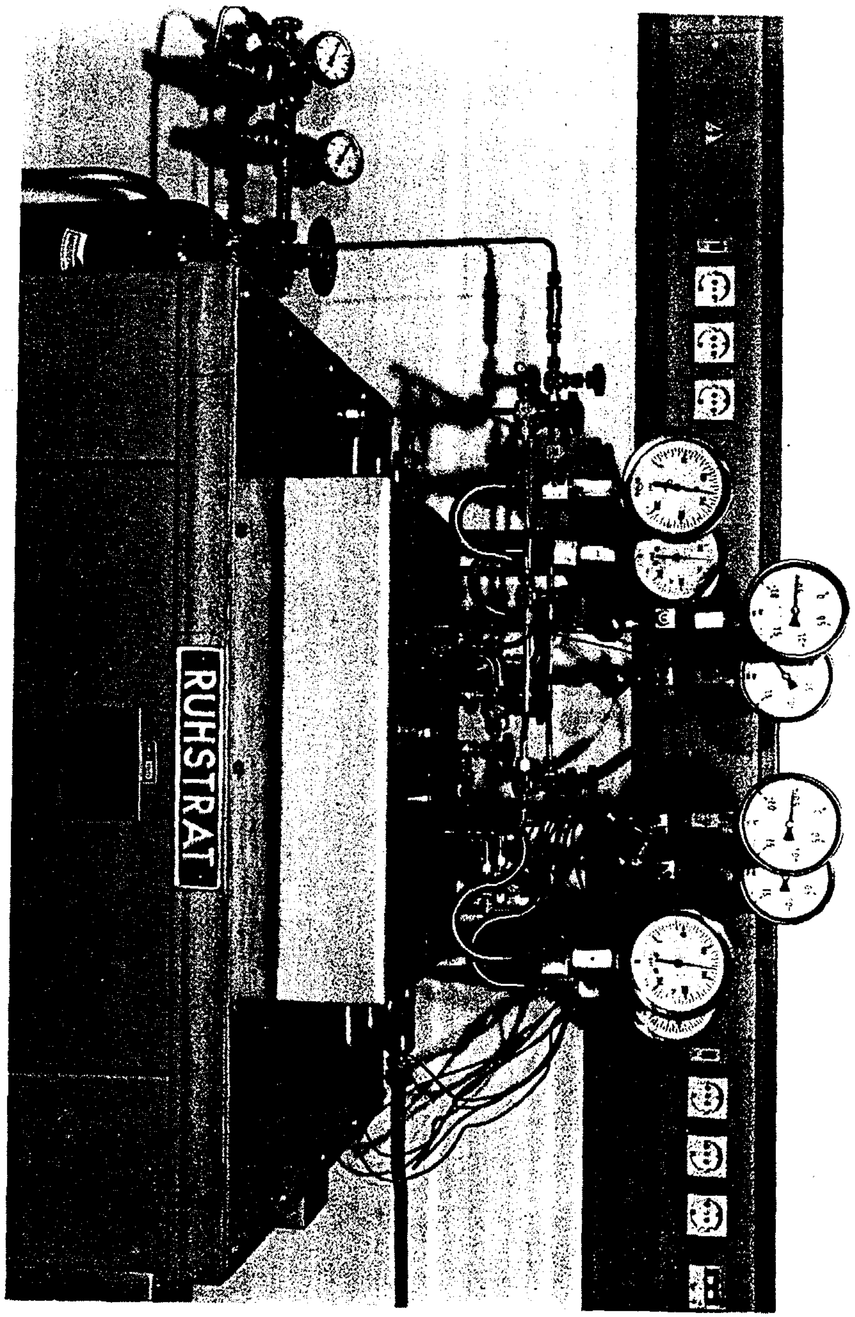

Fig. 6: Heating unit with 4 autoclaves in operating

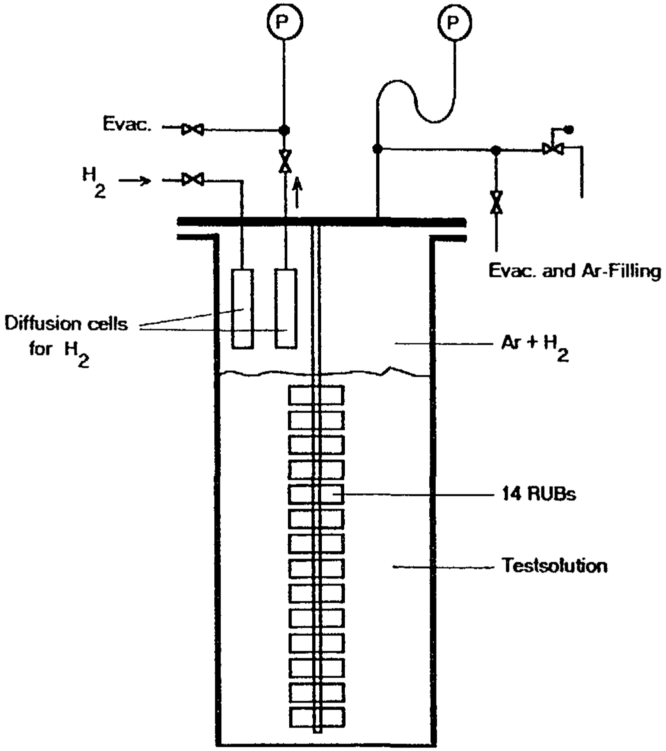

Fig. 7: Static autoclave for PWSCC-tests at T = 330°C

2.5 Test Performance

The stressed and cleaned specimens were installed in the autoclave.
Each autoclave was filled with 1500 ml of water with composition as mentioned above.
After closing the autoclaves, the heat insulation was fixed in place. Lastly the burst membrane, the two different gases Ar and H_2, and the vacuum pump were connected (see Fig. 6).
Before heating, the autoclaves were simultaneously evacuated until the water vapour pressure at room temperature was reached. Then the autoclaves were purged with Argon. This procedure was twice repeated. Then the heater was switched on and the temperature of T = 330°C was reached after about eight hours. At the same time, H_2 was allowed to flow through the diffusion cells into the autoclaves with a pressure of about 0.3 bar.

The necessary hydrogen-pressure inside the autoclaves was calculated according to Henry's law and Himmelblau as 0.25 bar in order to reach a hydrogen content of 3 ppm in the water.

After each planned test period, the heater and the gas supply were switched off and the autoclaves allowed to cool down to room temperature before the specimens were removed. The specimens were examined visually for cracks at 10 - 20 times magnification and the colours of the surface-oxide were recorded.
At the end of the test, one RUB from each autoclave was examined metallographically.

2.6 Test Duration

After a pretest of about 118 d the main test was carried out. The specimens were inspected after 336, 648, 1200, 2500, 3340, 4180 and 5000 hours of exposure. These inspection intervals were chosen under consideration of the known literature data about PWSCC rates of Alloy 600 and with regard to the intermediate results obtained.
The test was stopped after reaching 5000 h of exposure, because most of the tested Alloy 600 MA RUB specimens had cracked.

3. Results

The findings of the inspections are listed in table 3. No cracks were observed during the first 1200 hours of exposure. Several cracked specimens could be detected after 2500 hours. With increasing exposure time, the number of cracked specimens of Alloy 600 MA increases.
No cracks could be found in Alloy 690 TT up to the end of the test.
The results of the metallographic examinations are shown in Figures 8 - 11. As expected the cracks are intergranular.

To evaluate the results regarding pH, the findings were compared to the calculated pH value at 300°C. Figure 12 shows the resulting diagram. A minimum number of cracked specimens is observed at a pH value of 7.1. This value corresponds to the 3rd. test (see Table 2).

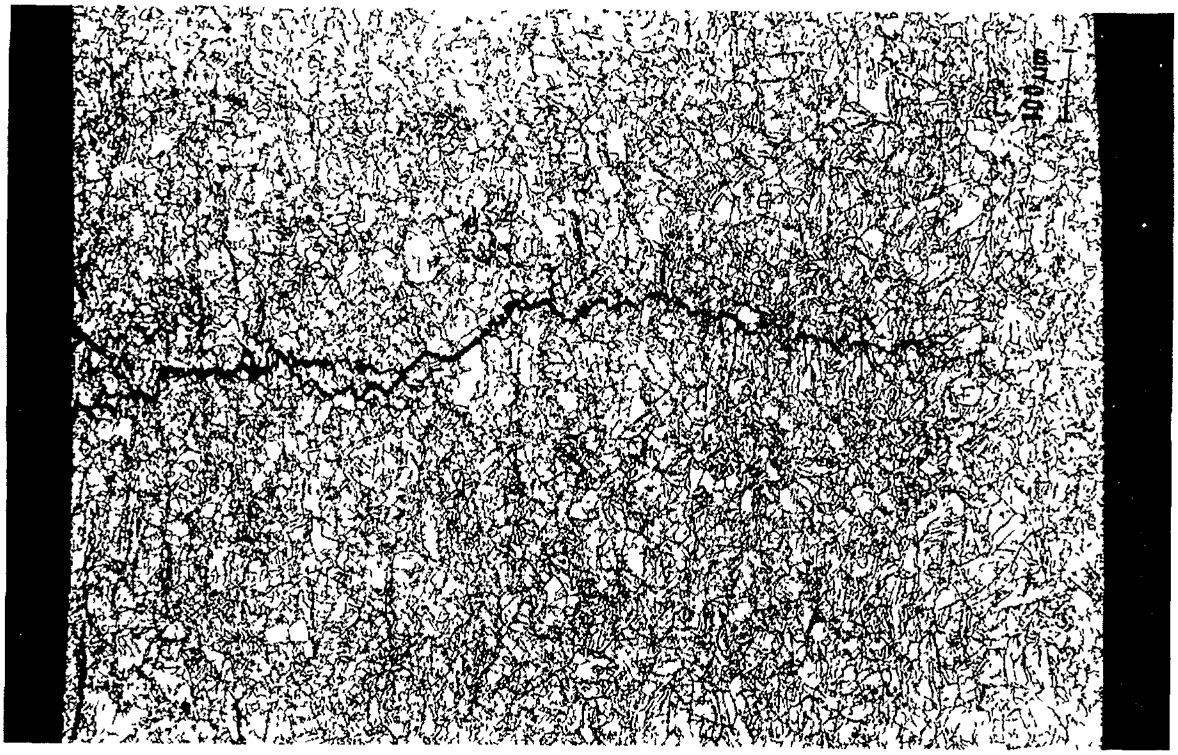

Fig. 8: Cross section of Alloy 600 MA RUB exposed for 5000h in primary water with 1400 ppm B, 6.5 ppm Li and 3 ppm hydrogen at T = 330°C

TABLE 3. INFLUENCE OF pH AND LITHIUM CONCENTRATION ON THE SUSCEPTIBILITY TO PWSCC OF STEAM GENERATOR TUBES (3 ppm hydrogen, T = 330°C)

water chemistry B/Li[ppm]	pH1)	material	cracking results after the following test durations				
			14/27/50d	104d	139d	174d	208d
1400/2.0	6.8	A600 MA A690 TT	0/12 0/2	5/12 0/2	8/12 0/2	10/12 0/2	11/12 0/2
1400/3.5	7.1	A600 MA A690 TT	0/12 0/2	1/12 0/2	2/12 0/2	3/12 0/2	4/12 0/2
1400/6.5	7.4	A600 MA A690 TT	0/12 0/2	4/12 0/2	5/12 0/2	8/12 0/2	10/12 0/2
700/3.5	7.4	A600 MA A690 TT	0/12 0/2	4/12 0/2	7/12 0/2	9/12 0/2	12/12 0/2

1): pH-values calculated for 300°C

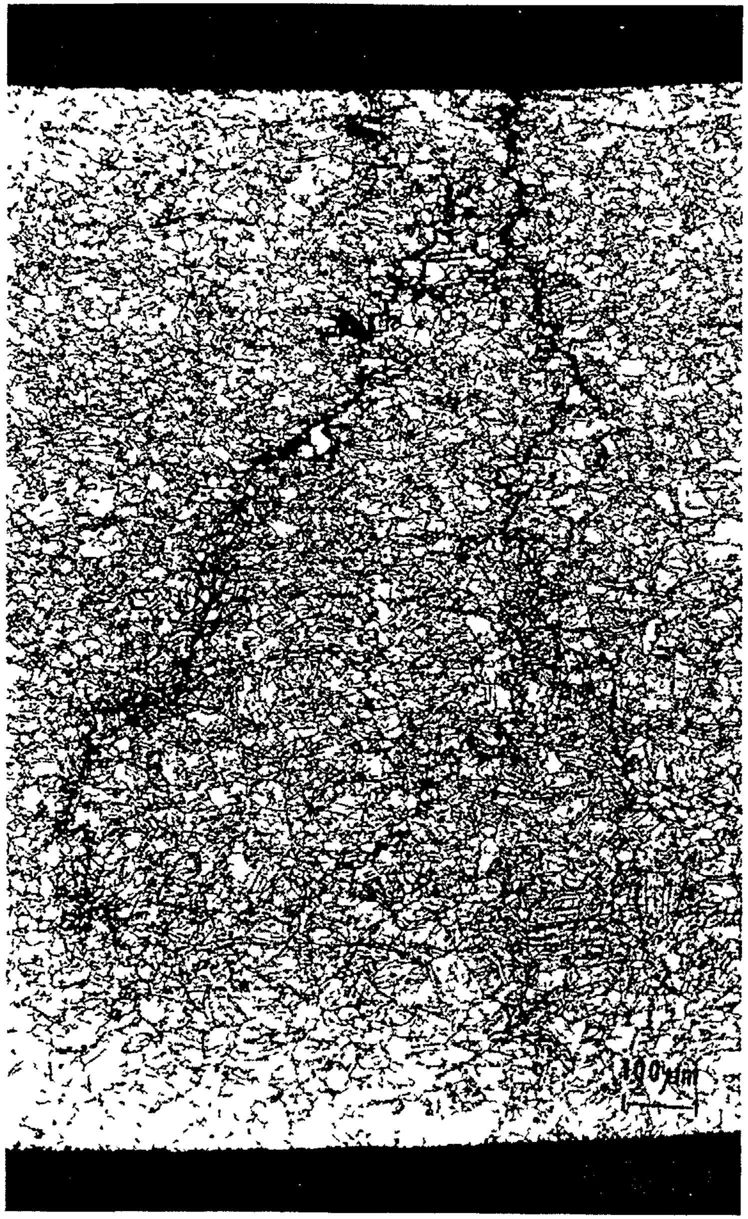

Fig. 9. Cross section of Alloy 600 MA RUB exposed for 5000h in primary water with 1400 ppm B, 2 ppm Li and 3 ppm hydrogen at T = 330°C

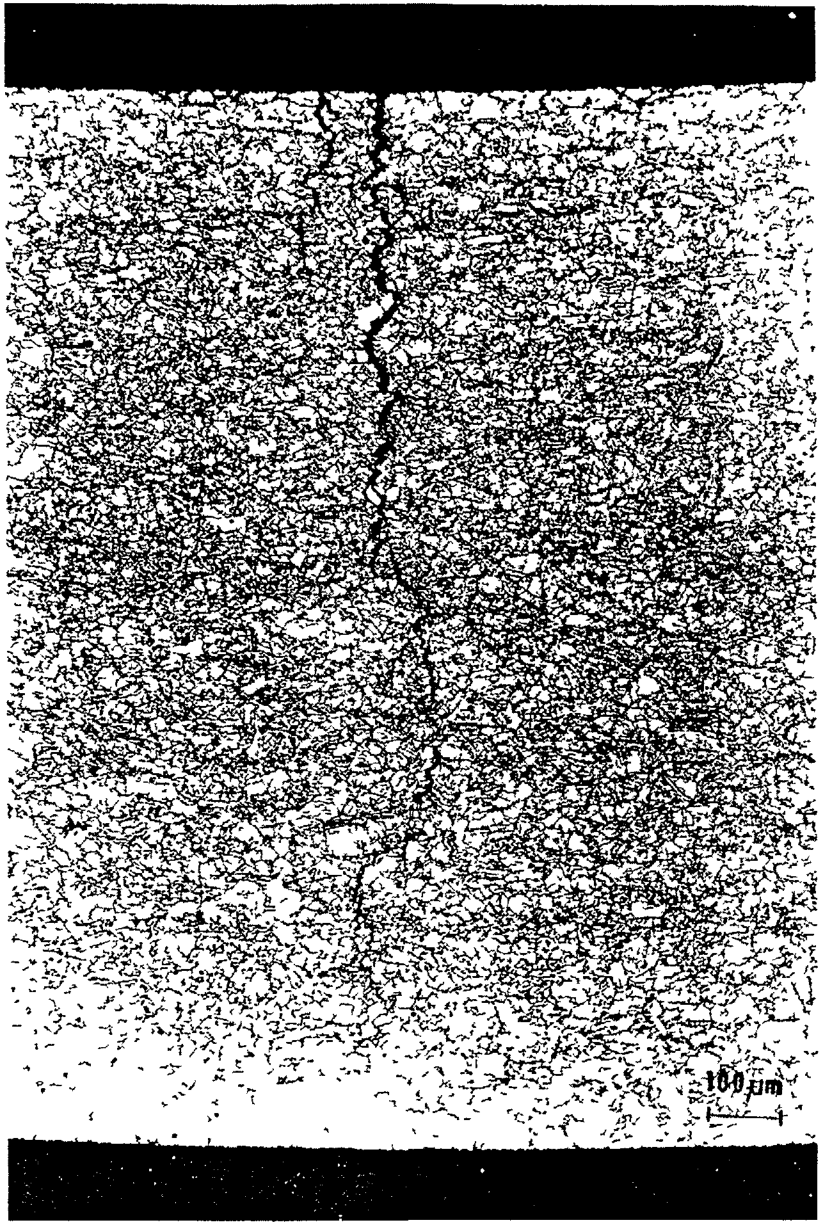

Fig. 10. Cross section of Alloy 600 MA RUB exposed for 5000h in primary water with 1400 ppm B, 3.5 ppm Li and 3 ppm hydrogen at T = 330°C

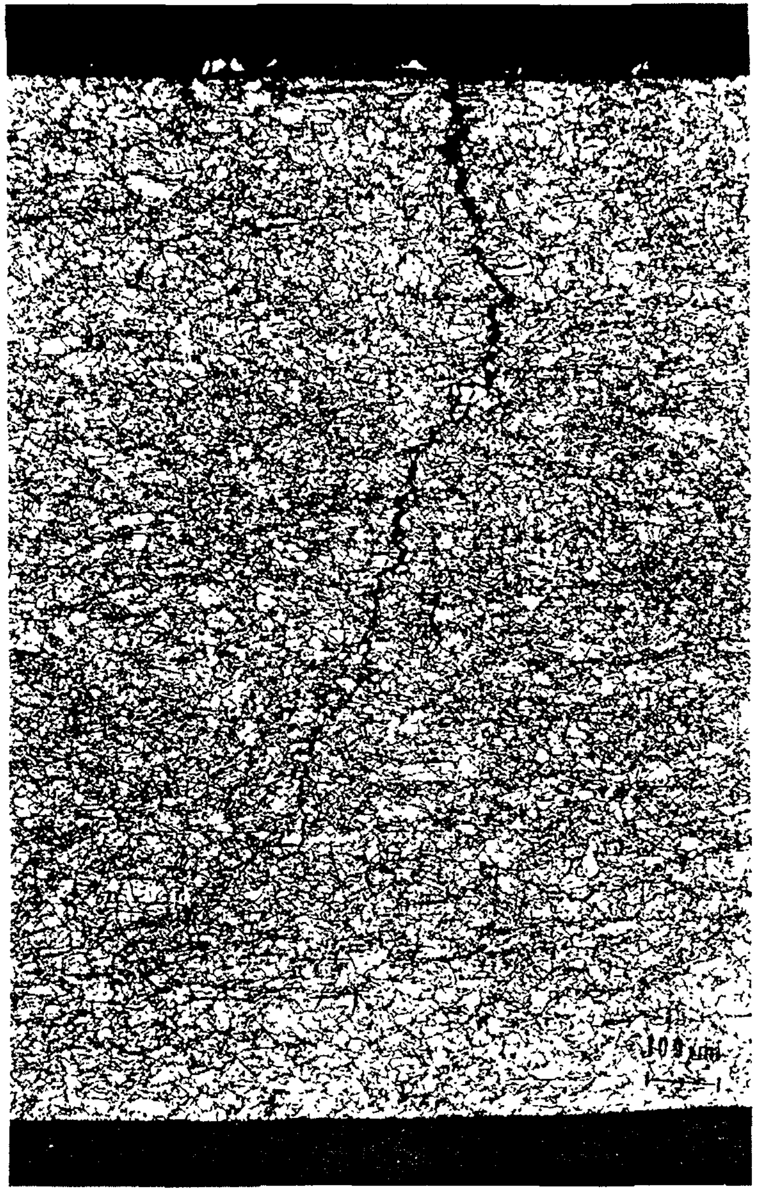

Fig. 11: Cross section of Alloy 600 MA RUB exposed for 5000h in primary water with 700 ppm B, 3.5 ppm Li and 3 ppm hydrogen at T = 330°C

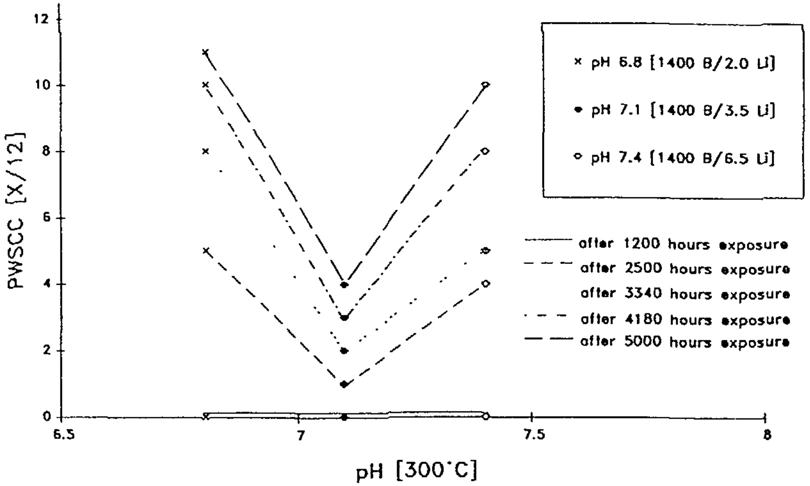

Fig. 12: Influence of pH and lithium concentration on the susceptibility to PWSCC of steam genarator tubes (I 600 MA) [3 ppm hydrogen, T = 330°C]

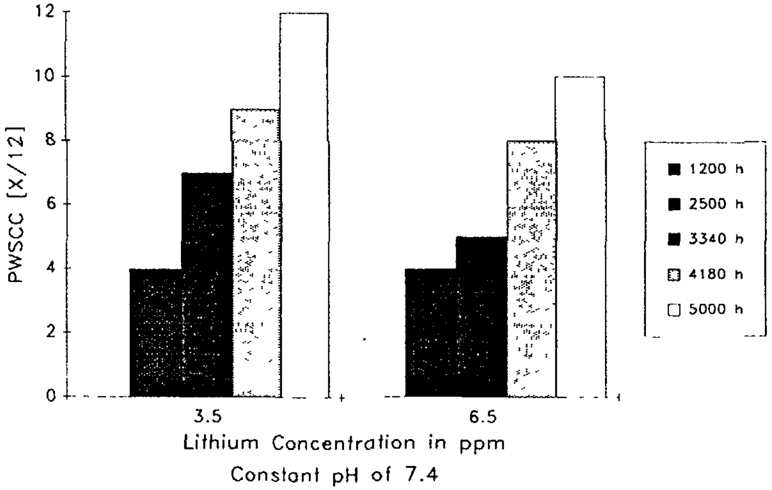

Fig. 13: Influence of lithium concentration on the susceptibility to PWSCC of Alloy 600 MA at T = 330°C

No clear influence of the lithium concentration can be observed, as shown by the results in Figure 13.

4. Discussion

The results obtained show an increase in PWSCC resistance of Alloy 600 MA at a pH value of 7.1. A check of the test conditions of the test run with pH 7.1 gives no considerable deviations compared to the other test runs.

Therefore a dependence of PWSCC susceptibility of Alloy 600 MA on pH can be assumed.

Other investigators [2] observed the best PWSCC resistance at the highest pH 7.4 tested. This is not in accord with the results reported here. On the other hand, a comprehensive consideration of the influence of different factors on PWSCC indicated, that the role of pH was not yet clear [3].

References

[1] G. Economy, F.W. Pement
Temperature Effects on Alloy 600 PWSCC from 310 to 330°C
Corrosion 89, No. 493

[2] R.J. Jacko, C.J. Wood
Lithium and Boron Effects on PWSCC of Alloy 600
Fontevraud2, Chinin, France, Sept. 1990, pp.250

[3] Z. Szklarska - Smialowska
Factors Influencing IGSCC of Alloy 600 in Primary and Secondary Waters of PWR Steam Generators
Proc. 4th Int. Sym. Environmental Degradation of Materials in Nuclear Power Systems - Water Reactors, Jekill Island 1989, Ed. D. Cubicciotti, Nace 1990, pp. 6-1

MATERIAL CHARACTERISTICS OF PRIMARY HEAT TRANSPORT SYSTEMS — MATERIAL INTEGRITY DURING OPERATION OF PHWRs

K.S. VENKATESWARLU, P.K. MATHUR,
S.V. NARASIMHAN, G. VENKATESWARAN
Water Chemistry Division,
Bhabha Atomic Research Centre,
Trombay, Bombay,
India

Abstract

Important characteristics of various materials used in the primary heat transport systems of PHWRs have been described and various factors affecting their integrity during plant operation are discussed. It has been pointed that maintaining an optimum water chemistry control helps in keeping corrosion of constructional materials to the minimum.

1. Introduction

The successful operation of a nuclear power plant depends among other things on the optimum water chemistry control which keeps the corrosion of constructional materials to the minimum. This optimisation requires an intimate knowledge of the various interactions occurring among system constructional materials and their environment under operating parametric conditions such as water chemistry, temperature, pressure, radiation effects etc.

2. Primary Heat Transport System

Several materials of construction (Table-1) are employed in the Primary Heat Transport System of PHWRs. In addition to the important criterion of corrosion resistance for each material, some other considerations also dictate the choice of various materials, for example, the neutron economy for the use of zircaloys for pressure tubes and fuel cladding, high tensile strength and adequate hardness in the rolled joint areas determine the use of 400 series steels for coolant channel end fittings and so on.

Zircaloys are protected against corrosion by a thin protective oxide film. The oxide growth which follows cubic rate law undergoes transition to a linear rate only under exceptional circumstances. On the otherhand, local boiling of primary coolant and concomitant oxidising conditions along with concentratation of lithium at bubble nucleation sites will increase the zircaloy corrosion by disrupting the protective film. High concentrations of dissolved deuterium (hydrogen) cause Zirconium deuteride (hydride) precipitation and the deuterium can migrate depending on the stress and temperature graidents. In this connection pressure tube integrity is of primary concern than the integrity of fuel clad because of the longer residence time of pressure tube as compared to residence time of the fuel clad.

Table I

Materials of Construction in PHT Systems of PHWRs

Material	Location	Nominal compositions	Desirable low cobalt levels
Zircaloy-2	In core (fuel-clad, coolant tubes)	Zr, Sn 1.5% Fe 0.07%, Ni 0.05%, Cr 0.05%	--
Zircaloy-4		Zr, Sn 1.5%, Fe 0.18% Ni 0.007%, Cr 0.07%	
Zirc-Niobium alloy		Zr, Nb 2.5%	
Carbon steel	System piping, headers and feeders	Fe, C 0.2%, Si 0.15%, Mn 0.6%, S 0.05%, P 0.4%	0.006% (max)
Stainless/ High alloy steels	Pumps	Fe, Cr 5-20%, Ni 0-10% C 0.03-0.1%, Si 0.3-0.8%, Mn 0-15%, S 0-0.02%, P 0-0.2%	--
SS 400 series	End fittings	Fe, Cr 4-18%, Ni 2.5% (max), C 0.15-0.2%	--
Monel-400	Steam generator tubes	Fe 2.5%, Ni 63-70%, Cu (bal)	0.005% (max)
Inconel-600		Fe 6-10%, Ni 72%, Cr 14-17%	
Incoloy-800		Fe (bal), Ni 30-35%, Cr 19-23%	
Stellites	Valve seats	Co 50-60%, Cr 20-33%, W 5-20%, Ni 0-13%, Mo 0-6%, C 0-2.5%	being replaced by non cobalt based alloys

In addition to the corrosion and corrosion products release rates both under normal and transient water chemistry conditions which are of primary importance, factors like mechanical and heat transfer properties, cost and availability decide the selection of steam generator tube material. High nickel alloys (Monel-400, Inconel-600 and Incoloy-800) have been used as the steam generator tube materials as well as the tube materials of some other heat exchangers. Despite their low release rates, the basic cause of the activity transport problem is due to the very large surface areas of these materials exposed in the Steam Generators.

The use of carbon steel for feeders, headers, system piping and vessel shells is an inherent feature of PHWRs. The general corrosion rates of carbon steel and rates of release of corrosion products are kept under control by maintaining optimum high pH (in the range 10.2 to 10.8 at 298 K) and low dissolved oxygen concentration in the primary coolant. Proper hotconditioning of the PHT system surfaces prior to reactor operation, optimum water chemistry control during operation, reduced cobalt content in the system constructional materials and improved system design have been the main contributors towards the achievement of the efficient radiation field control. In the designs of advanced PHWRs the maximum cobalt content in the carbon steel feeder piping and high nickel alloy steam generator tubings has been brought down to about 0.005%. Moreover, almost all high cobalt containing wear-resistant alloys, such as stellites have been eliminated except for a few critical valves in bleed lines and fuelling machine drive mechanisms. As a result of these improvements, low boiler cabinet radiation fields are being encountered. Similarly the radiation fields on the outside of the feeder insulation cabinets in the recent PHWRs have generally been lower by about a factor of ten than those at plants ten years older.

3. Steam Generator System

It is worthwhile to discuss a little more on the corrosion characteristics of steam generator materials because their integrity is very important for the efficient operation of the plant. Monel-400 has been used in several operating PHWRs. It is felt to be generally free from stress corrosion cracking. However, it can corrode significantly under oxygenating conditions or under localised boiling conditions permitted in the recent designs of PHWR core, where it is more difficult to suppress the radiolytically produced dissolved oxygen. The service performance of Monel-400 in commercial PHWRs has been excellent. Inconel-600 was chosen as SG tube material, primarily because of its excellent resistance to chloride induced transgranular stress corrosion cracking and because it has low corrosion rates even in oxygenated water. However, Inconel-600 with its high Ni content is susceptible to intergranular stress corrosion cracking. Incoloy-800 has been chosen as SG tube material in the later and advanced PHWRs mainly becuase of the following reasons: (a) better resistance to stress corrosion cracking in high purity water, (b) better resistance to corrosion caused by pH excursions on the acidic side during regular operation or acidic chemical cleaning solutions, (c) less contribution to radiation fields and (d) resistance to localised corrosion in concentrated caustic or phosphate solutions as good as that of Inconel-600. Experience with Incoloy-800 steam generator tube material has been generally very good. However, there is a slight disadvantage in using Incoly-800. Its thermal conductivity is lower than that of Inconel-600.

Tubesheets are either carbon steel or low alloy steel overlaid with a nickel alloy on the primary side. Tube supports in the operating steam generators are all made of carbon steel for fresh water cooled stations and type 410 stainless steel and Inconel-600 for sea water cooled stations. Carbon steel is used for the shell and head of all PHWR steam generators.

FUEL CLADDING INTEGRITY IN PHWRs

K.S. VENKATESWARLU, P.K. MATHUR,
S.V. NARASIMHAN, G. VENKATESWARAN
Water Chemistry Division,
Bhabha Atomic Research Centre,
Trombay, Bombay,
India

Abstract

Fuel performance in PHWRs has generally been satisfactory in terms of statistics. However, there is a need to further reduce the already low fuel failure rates keeping in view the current stringent restrictions on person - sievert budgetting for nuclear power plants operation. Hence the effect of various factors controlling fuel clad integrity, viz, quality of clad tubes, mode of reactor operation, damage due to debris in the coolant, coolant water chemistry control, sheath fretting, sheath overstraining and power ramp defects caused by refuelling, etc. are discussed and the methods for failed fuel detection and location are described.

1. Introduction

Pressurised Heavy Water Reactors (PHWRs) employ natural UO_2 as the fuel. The UO_2 is clad in a collapsible zircaloy-2 or zircaloy-4 sheath and fuelling is done on-power. Fission products are normally contained within the fuel pellet and pellet-clad gap. When the clad develops a defect which may be a slow release or fast release defect, the fission products get released to the coolant in Primary Heat Transport (PHT) system and their behaviour will be governed by their chemical nature in the coolant medium.

Fuel performance in PHWRs has been generally good with failure percentages mostly around 0.1.(1-4) Though in terms of statistics this is an highly satisfactory fuel performance behaviour, still from the current stringent restrictions on person-sievert budgetting for operation of nuclear power plants, a need is felt to further reduce these low fuel failure rates.

2. Factors controlling fuel clad integrity

Fuel clad integrity is controlled by

(i) quality of the clad tubes employed and quality control checks adopted for the manufacture of fuel bundles - lot to lot variation in chemical composition, impurity levels, alloying elements and mechanical properties are to be avoided. These will have an effect on the corrosion behaviour of the clad and hence on its integrity.

(ii) mode of reactor operation - the causes of fuel failure associated with reactor operations could be classified as:

1. damage due to debris in the coolant

2. water chemistry control of the coolant - zircaloy corrosion, hydrogen absorption, crud deposition in core and thereby clad overheating are the parameters to be considered.

3. sheath fretting

4. overstraining of sheath due to high bundle power.

5. power ramp defects caused by refuelling and too frequent start-ups and shutdowns.

The formation of an adherent, less porous protective ZrO_{2-n} ($n < 0.05$) layer on the surface of zircaloy-2/4 in high temperature water lends resistance to corrosion for these alloys. The kinetics exhibits a cubic rate law in the pre-transition period and a linear law in the post-transition period. Under normal PHWR water chemistry conditions of the coolant, the cubic to linear rate law transition occurs beyond the design discharge burnups of the fuel and hence clad integrity is not hampered by corrosion. Since the impurities such as Al and N in zircaloy have been fixed at conservatively low levels (5), adherence to clad quality specifications keeps enhanced corrosion due to such impurities within acceptable limits.

In the manufacture of fuel bundles, individual fuel elements are Helium leak tested and seen to conform to He leak rate specifications, but when these individual elements are assembled into a bundle with wire wrap/split spacer attachments and end/tie plate weldments, it would be desirable to test the finished bundle for He leaks so that these weld locations referred here do not form new sources of leak on the fuel sheath. In this connection hot He leak test can also be carried out on selected bundles and the results compared with those from cold He leak test. Further a non-destructive test method for examining the end plug welds on fuel pencils will be useful.

In PHWRs hydrogen is injected into the primary coolant to suppress the radiolysis and thereby control the dissolved oxygen level in the coolant which is very important for minimising the corrosion of different structural materials employed in the PHT system. The dissolved hydrogen should not exceed the specified amount of 3-10 cc/Kg of D_2O. Excess of dissolved hydrogen in the coolant can result in increased hydrogen absorption by the cladding and pressure tubes. Formation of radially oriented zirconium hydride platelets can severely affect the mechanical integrity of the clad from the coolant side. Though zircaloy-4 and Zr-2.5% Nb alloys show reduced hydrogen pick-up as compared to zircaloy-2, it is a good practice to adhere to the specified dissolved hydrogen levels in the coolant.

The problem of hydriding of the internal surfaces of the clad from the fuel side, showing up as early life (low burn-up) failures in early Light Water Reactors (LWRs) has been overcome by careful control of moisture levels in the UO_2 pellets, so much so for PHWRs this problem has been eliminated.

In the temperature range 523-588 K and pH$_{298K}$ region 10.3-10.7, the solubility of magnetite shows a positive temperature coefficient. Hence magnetite solubility increases in the coolant channel from inlet to the outlet of the core, thus reducing the residence time of crud in the core (6). Hence pH control over a narrow range of 10.3-10.7 instead of earlier followed wide range viz., 9.5-10.5 can minimise the specific activity of the crud by lowering its deposition on the fuel. However, pH > 10.7 regime is to be avoided since high concentration of LiOH have been observed to increase the corrosion rate of zircaloy dramatically(7), which can result in growth of thick oxide films, lithium hide-out and possible radiolysis occurring within the pores of such films causing a locally altered chemistry regime as compared to the bulk chemistry regime.(8)

Out of pile tests of wire wrap fuel bundles at simulated conditions of pressure, temperature, flow and residence time has shown that fretting is minimum. Post-irrradition examination on fuel till date has not revealed any fretting damage on fuel sheaths(2).

An analysis of the supposed problem of overstraining of fuel sheaths due to high bundle power, made by correlating the number of failed fuel bundles with the bundle power in the coolant channel containing the defective bundle (failed channel) has shown that fuel bundles have failed well below the maximum bundle powers generally observed in the core. The power at which fuel bundles fail cover a wide range. Thus if the bundle power is held within design limits, the available data indicates that failure cannot be correlated to the bundle power.(2)

One of the major causes of fuel failure identified for LWRs is pellet-cladding interaction (PCI) and associated stress corrosion cracking mechanism due to power ramping. This normally occurs at high burn-ups (~20000 MWD/T U in earlier LWrs to ~40000 MWD/T U in current LWRs) which the fuel has to withstand in these reactors. As against this, the PHWR fuel which by design is very different from LWR fuel, has to withstant burn-ups ≤ 10000 MWD/T U and as such PCI type of failures is of a less probable nature in these reactors. Nevertheless, to avoid pellet cracking due to thermal shocks which results in a sort of acceleration of the PCI process, it is a standard practice in PHWRs to increase the reactor power after start-up in a controlled manner. While global power ramping due to frequent start-ups and shut downs can be controlled, there can be local power ramping during refuelling. But here again to date no correlation exists between fuel failure and power ramp due to refuelling.(2)

3. Failed fuel detection and location

Unlike the vessel type of reactors like PWRs and BWRs wherein only occurrence of fuel failures can be dected but locating these has to wait for a refuelling shut down, since the PHWRs employ individual pressure tubes which contain the fuel, detecting the occurrence of fuel defect, detecting the coolant channel containing the defective fuel and removing the defective fuel when the reactor is on power are possible in these reactors. This enables removal of defective bundles in time so as to minimise their residence time in the core thereby maintaining a relatively clean PHT system.

In PHWRs failed fuel detection is done by radioiodine and/or fission gas monitoring in the gross coolant.(9,10) Either on-line monitoring of gross coolant or grab sample method or in some cases both the methods are used for failed fuel detection. Fission gas monitoring appears to be a better method for failed fuel detection than radioiodine monitoring because iodines are subjected to removal by the purification system whose operation can be varied. Altering the purification system flow alters the radioiodine activities to different extents depending on their half-lives so much so even the iodine activity ratios, say $^{133}I/^{131}I$, $^{135}I/^{131}I$ are subjected to variation with clean-up flow.

The channel containing the failed fuel is identified (failed fuel location) by monitoring each coolant channel feeder sample for delayed neutrons and/or r-activities. Delayed neutron monitoring appears to be useful for detecting recoil and fast release type of defects. Channel r-monitoring for fission gases seems to be useful for identifying slow release defects by using their burst release characteristics. Even in the slow release defect case, fission gas monitoring appears to be helpful when not more than 5-10 channels develop fuel defects simultaneously.(11)

4. Conclusion

Though balancing the burn-up losses associated with premature refuelling against the risk of contaminating the PHT system was the governing criterion earlier in the operation of PHWRs, of late the balance is tilted more in favour of reduction in person-sievert for occupational personnel. This can be achieved at the expense of increased quality control checks in the manufacture of fuel bundles, slight restriction in operation, improvement in failed fuel detection and its removal.

REFERENCES

1. R.S.Rustagi and M.Das, "Experience with modelling and behaviour of defected fuel in RAPS-1". Proc. of the IAEA Tech. Comm. Specialists' meeting on the 'Behaviour of defected Zirconium alloy clad ceramic fuel in Water Cooled Reactors', pp 45-47, Sep. 1979, Chalk River, Canada.

2. Report of the Committee formed by DAE Safety Review Committee regarding Failed fuel in Indian PHWrs - Private Communication (1988)

3. P.T.Truant, "CANDU Fuel Performance - Power Reactor Experience", IAEA/CNEA, International Seminar on 'Heavy Water Fuel Technology', San Carlos de Bariloche, 1983 (AECL - MISC 250-2).

4. A.J.Hains, R.L.daSilva and P.T.Truant, "Ontario Hydro Fuel Performance Experience and Development Program", International Conf. on 'CANDU Fuel', Chalk River, Canada (1986).

5. M.Das, "Effect of impurity elements on corrosion behaviour of Zircaloy in high temperature steam". Proc. of a Tech. Comm. Meeting organised by IAEA on 'External Cladding Corrosion in Water Power Reactors', Cadarache, France. pp 94-98 (Oct. 1985), IAEA, Vienna (1986).

6. V.F.Urbanic, R.Gray and D.H.Lister, "Review of in-reactor Zircaloy corrosion and crud deposition experience at AECL", EPRI NP-1254 (1979).

7. S.G.McDonald, G.P.Sabol and K.D.Sheppard, "Zirconium in Nuclear Industry", ASTM STP 824, p 519 (1982).

8. A.B.Johnson, Jr., "Oxide thickness effects on Zircaloy oxidation and hydriding under irradiation", BNWL Rept. BN-SA-1921 (1984).

9. A.M.Manzer, "In-core assessment of defective fuel in CANDU-600 reactors". Proc. of a Specialists' meeting on 'Post irradiation examination and experience' organised by IAEA and held in Tokyo, pp 263-275 (Nov. 1984).

10. A.M.Manzer and N.Macici. "Fuel defect detection by radioiodine monitoring", 8th Annual Conf. of the Canadian Nuclear Society, pp 272-279 (1987).

11. G.Venkateswaran and K.S.Venkateswarlu, "Theoretical assessment of channel fission gas monitoring vis-a-vis channel DN monitoring for PHWRs". Ann. Nucl. Energy (1988 - in press).

ASSESSMENT OF IRRADIATION EFFECTS ON CORROSION OF REACTOR ALLOYS

K. ISHIGURE
Department of Nuclear Engineering,
Faculty of Engineering,
University of Tokyo,
Tokyo

K. FUKUYA
Nuclear Engineering Laboratory,
Toshiba Corporation,
Yokohama

Japan

Abstract

This paper reviews examples of the radiation effects on corrosion that was observed in laboratory experiments and operating nuclear power plants.Experimental results on Inter-granular stress corrosion cracking and Irradiation assisted stress corrosion cracking are examined.The effect of neutron fluence,stress intensity,water chemistry and material variation on SCC susceptibility of irradiated stainless steel have been investigated.

1. INTRODUCTION

Corrosions of structural materials have caused various types of problems related to the reliability and safety of nuclear power plants in the past operational history of LWR. The examples of such corrosions problems are the stress corrosion crackings of BWR piping, the steam generator corrosion troubles, the corrosions of Zircaloy fuel claddings, and the increase in the occupational radiation exposures caused by activated corrosion products. Most of these problems were settled or improved by various countermeasures not only in the material side but also in the water chemistry control. On the basis of these operational experiences it has been currently recognized that more and more rigorous control of water chemistry is essential for attaining the high reliability and low radiation levels of nuclear power plants.

In these situations a wide attention has recently been paid on the effect of radiation on corrosion of materials, especially, which are used under the intense radiation in the core of nuclear reactors.

The investigations on the effect of radiation on corrosions have been extensively carried out with Zirconium alloys for the past decades, and the considerable amounts of the data have been accumlated regarding the radiation effect on the Zircaloy corrosions, which will be reviewed elsewhere and not included in this article.

A current major concern is concentrated on another type of the corrosion called IASCC (irradiation assisted stress corrosion cracking). IASCC is a type of IGSCC (intergranular stress corrosion cracking) enhanced by radiation, and observed mainly with unsensitized austenitic stainless steels and nickel-based alloys such as inconel used in the core of not only BWR but also PWR. The IASCC of the core internals has a possibility to be critical to the life extension of BWR, and the systematic investigations on this type of corrosions have started a few years ago. The data obtained so far show that IASCC is a rather complicated phenomenon including radiation damages to the materials and also chemical changes of environment by radiation, and it may be necessary for the elucidation of its mechamism fully to understand all the aspects of the radiation effects on corrosion environment as well as on metalic materials.

Hydrogen water chemistry (HWC) is a current topics in water chemistry control in BWR, and aims mainly at the suppression of intergranular stress corrosion cracking (IGSCC) of stainless steel piping in recirculation lines. However, there has been increasing interest in the feasibility of HWC for suppressing IASCC of core internals.

General corrosions of core components in nuclear reactors are another concern in relation to the radiation build-up of primary circuits. The recent strict control of water chemistry has markedly reduced the input of the corrosion products into the core of reactors which give the sources of radionuclides causing the radiation fields on the piping outside the core. Consequently, the relative importance increased in the release of the radioactive and non-radioactive elements as corrosion products from the core components, and the measures for the control of this release process have been seeked for.

This review is written with the main emphasis on the radiation effect on the corrosion processes under nuclear power reactor condition. However, the radiation effect on corrosion has drawn attention in relation to other aspects of nuclear technology. Among others is the corrosion of metal canisters or overpacks of high level radioactive wastes disposed in the repositories inside geological formations. The canisters or overpacks corrode in contact with underground water under irradiation by radioactive solid wastes. The quantitative estimation of the corrosion rates in the radiation field is required for the safe isolation of the radioactive nuclides. Significant research activities have currently arised in this field, and have focused on the radiation effects on the corrosions of canister materials.

Corrosion process is a phenomenon at the interface between metal and environment. If radiation is present in the corroding system, it has a possibility to give influences on the both sides of the metal and the environment. Gamma radiation has no significant effect on metal itself in relation to the corrosion, but high energy particles such as neutrons and heavy ions produce point deffects like interstitials and vacancies which lead to cluster formation, segregation or deposition of some components and so on. These radiation demages may affect the corrosion process.

Radiation induces chemical changes in the water environment of the corrosion systems, producing oxidising and reducing chemical species which, without doubt, participate the corrosion reactions. Thus, information on water radiolysis is essential to understand the radiation effect on corrosion

When water in the close vicinity of metal surface is exposed to radiation, the radiolysis of water at the interface is somewhat different from that in bulk, being affected by the metal surface.

Corroding metal surfaces are usually covered with thin metal oxide layers of which the physico-chemical properties control the corrosion processes. The some propoerties of the metal oxide layers are changed by radiation, and this effect may be in some cases reflected in the corrosion processes.

In this review are shown, first of all, some examples of the radiation effects on corrosions that were observed in laboratory experiments and operating nuclear power plants. Then, the various aspects of the radiation effect on corrosions mentioned above are described in more detail, and finally future works required are indicated.

2. EXPERIMENTAL AND FIELD OBSERVATIONS OF RADIATION CORROSIONS

There are a large number of examples reported in which the effects of radiation on corrosion processes were observed with many types of metals under various conditions in laboratory experiments or in operations of nuclear power plants. The examples described here are confined to the corrosions of iron-and nickel-based alloys under the conditions relevant to nuclear power technology.

2.1 General Corrosions

Byalobzheskii(1) studied the effect of gamma-radiation on the corrosion of iron steel in aqueous solutions at room temperature. Long term (1000 hr) corrosion experiments showed that the gamma irradiation at dose rate of 4.0 X 10^{15} eV/cm^3·sec increased the corrosion rates of iron steel in distilled water, 0.5 N NaCl solution and 0.01 N H_2SO_4 solution at 25° C by a factor of 1.6 to 4.0 relative to those in the absence of radiation, and the highest rate was observed with the iron steel in 0.01 N H_2SO_4 solution under the irradiation. They also carried out the corrosion experiments with armco iron specimens in aqueous solutions under the irradiation of 1 MeV electrons at a dose rate of 6.6 X 10^{18} eV/cm^3·sec, and observed the high enhancement factors of 2.9 to 12.7 in the corrosion rates under the irradiation compared with those without radiation.

Marsh and Taylor (2) investigated the influence of gamma-radiatio on the corrosion of carbon steel coupons immersed in argon purged synthetic seawater at 90° C. As shown in Fig. 2·1·1 the overall corrosion rate in the synthetic sea water increased with radiation dose rate, and the local corrosions were observed with the specimens corroded under the irradiation, while no local attack was detected with the specimens corroded without radiation. On the other hand, the corrosion rate increased by a factor of 30 in the presence of radiation with carbon steel specimens immersed in argon purged synthetic grnanitic water, of which major gradients are 244 ppm HCO_3, 106 ppm Na^+, 35.5 ppm Cl^-, 24 ppm SO_4^{2-} and 20 ppm Ca^{2+}, and no local attack was observed with either of the specimens with nor without radiation.

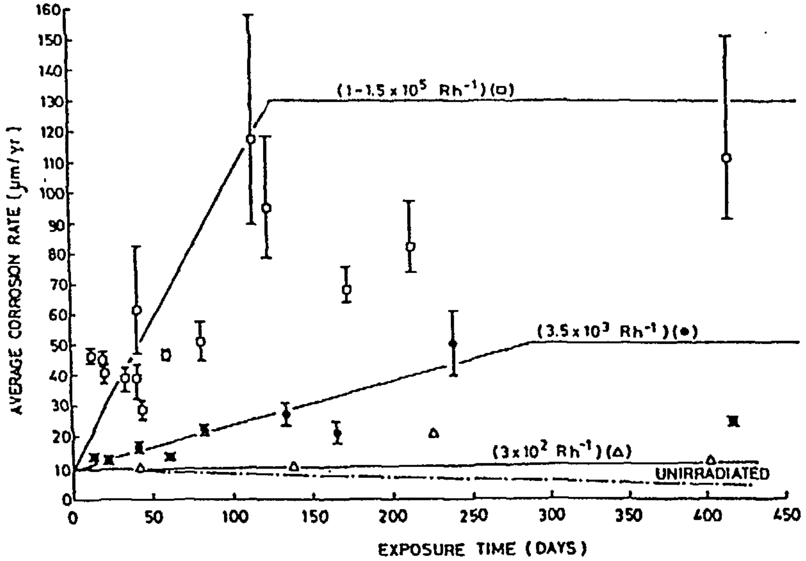

FIG. 2.1.1. Average general corrosion rates of forged 0.2%C steel in de-aerated substitute seawater at 90°C with and without γ radiation.

On contrary to carbon steel, corrosion behavior of stainless steel under irradiation is rather complex. In some cases corrosion of stainless steel is suppressed by radiation owing to the anodic passivation. One of the Russian groups found that the corrosion rate of stainless steel in 1.0 N H_2SO_4 at ambient temperature was reduced by two orders of magnitude by gamma-irradiation of 1.5 X 10^{15} eV/cm^3·sec, and another group observed the inhibition of crevice corrosion of 1kh13 steel in 3% NaCl solution by gamma-irradiation1).

There are other cases where radiation increases the corrosion of stainless steel under certain condition.

Byolobzheskii also carried out a long term corrosion experiment of stainless steel in 1.0 N H_2SO_4 at 25° C under gamma-irradiation at a dose rate of 4.0 X 10^{15} eV/cm^3·sec, and found that the corrosion was accelerated under the irradiation within the first 500 hours but afterwards the corrosion rate without radiation was the same as that with radiation1).

Burns et al.(3) measured the amount of the hydrogen evolved from gamma-irradiated stainless steel vessels containing air-saturated pure water at 30 ~ 50° C, and observed the amount of the excess hydrogen

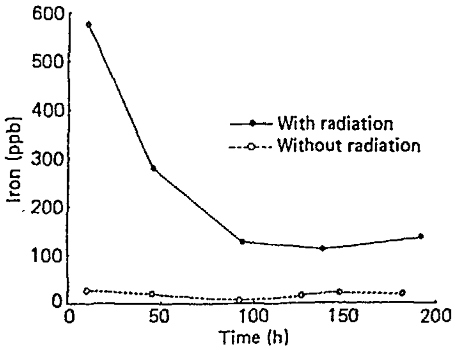

FIG. 2.1.2a. The release levels of crud iron from carbon steel at 250°C in the presence of 20 ppb O_2.

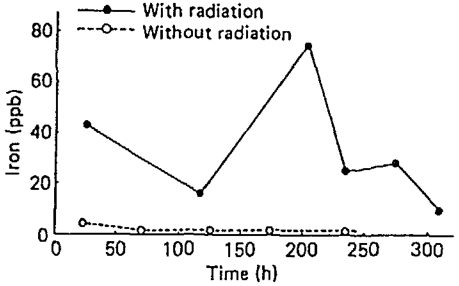

FIG. 2.1.2b. The release levels of crud iron from type 304 stainless steel at 250°C in the presence of 20 ppb O_2.

generated from the corrosion process of the stainless containers increased by a factor of 20 in the presence of radiation at a dose rate of 2M rad h^{-1}. They also compared similarly the amount of the excess hydrogen in the presence of mild steel with surface area one tenth of the stainless steel containers, and obtained the enhancement factor of 2.8 and 2.0 at 2 Mradh^{-1} and 0.2 Mradh^{-1}, respectively, and tried to explain these experimental results on the basis of the involvement of transient radiolysis products in the surface reactions.

Ishigure et al [4] measured the release rates of corrosion products from mild steel and type 304 stainless steel in deoxygenated pure water under gamma-irradiation at 250° C using a once-through type experimental loop. They found that radiation markedly increases the release rates of insoluble corrosion products, metal oxide particulates, as shown in Fig.2·1·2, while the release rates of soluble corrosion products are not significantly influenced by the gamma-irradiation. The increase in the insoluble corrosion product release rates was considered to arise from the oxidation of ferrous ions released to ferric ions by the radiolysis products followed by hydrolysis of ferric ions and precepitation of hydroxides.

Morikawa et al. measured [5] the release rates of corrosion products and oxide growth rates of Inconel X 750 under simulated BWR core condition where 200 ppb of hydrogen peroxide was injected at 270° C to pure water containing 400 ppb O_2 and 60 ppb H_2 under gamma-irradiation of at a dose rate of 3 × 10^5 R/hr, and found that the release rates of Cr, Ni and Fe ions and also the oxide growth rates were increased under the simulated BWR core condition in comparrison with the reference state without radiation and H_2O_2 injection. This enhancement of the corrosion rates in the simulated BWR core environment was attributed predominantly to the presence of H_2O_2.

REFERENCES

1) A. V. Byalobzheskii, Radiation Corrosion (English Translation), p.128 (Keter Press), 1970.
2) G. M. Marsh, K. J. Taylor, Corrosion Sci., 28, 289 (1988).
3) W. G. Burns, W. R. Marsh, W. S. Walters, Radiat. Phys. Chem., 21, 259 (1983).
4) K. Ishigure, N. Fujita. T. Tamura, K. Oshima, Nucl. Tech., 50, 169 (1980).
5) Y. Morikawa, T. Baba, H. Nagao, K. Shimizu, S. Yoshikawa, N. Ichikawa, N. Saito, Y. Hemmi, Proceedings of JAIF Int. Conf. on Water Chemistry of Nuclear Power Plants, Tokyo, 2, p.373 (1988).

2.2 Intergranular Stress Corrosion cracking (IGSCC)

Fujita et al. 1) carried out constant elongation rate tests (CERT) of sensitized 304 stainless steel speciments at 250° C in pure water containing initially different amounts of oxygen under gamma-ray irradiation. They found that the effect of radiation largely depends on the initial concentration of oxygen as shown in Fig. 2·2·1. It is seen in this figure that radiation rather suppresses the IGSCC of stainless steel when the concentration of the initial oxygen is lower than 500 ppb, while it accelerates the IGSCC in the presence of oxygen of the initial concentration higher than 500 ppb.

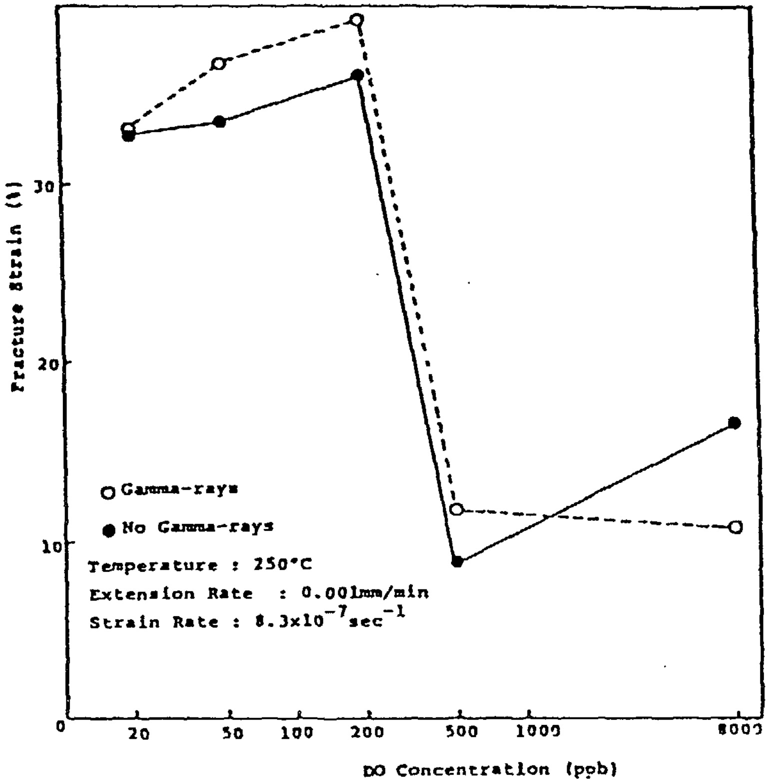

FIG. 2.2.1. Variation of the fracture strain of sensitized type 304 stainless steel with DO concentration at 250°C.

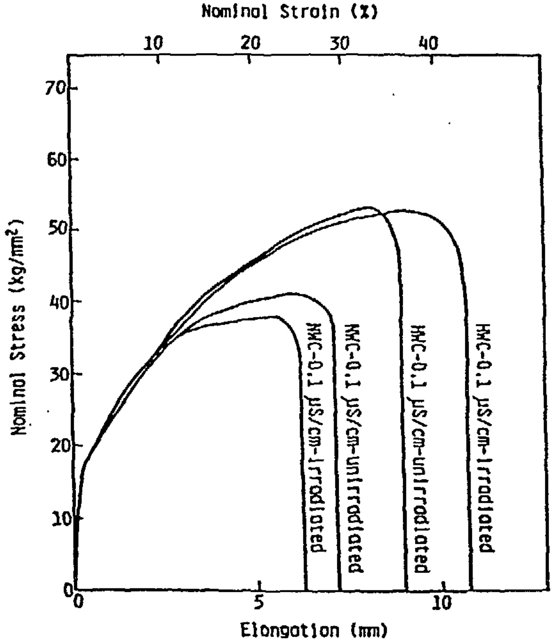

FIG. 2.2.2. Stress strain curves of SSRTs in NWC and HWC conditions.

Sudo et al. 2) carried out CERT tests of sensitised type 304 stainless steel specimens with and without gamma-radiation using a circulation loop at 270° C under simulated normal and hydrogen water chemistry conditions of BWR. The electrochemical potentials of stainless steel electrodes were monitored during the CERT tests. As shown in Fig. 2·2·2, the time of fracture is elongated by the irradiation under the hydrogen water chemistry condition, though the fracture mode was ductile both with and without radiation. On the other hand, the gamma-irradiation reduced the time to fracture under the normal water chemistry condition. The fracture mode of the specimens was observed to be IGSCC in both the cases, and the IGSCC ratio in the fracture surface was increased from 26% to 37% by the irradiation. The electrochemical potential monitored significantly increased by radiation under the normal water chemistry condition, while it decreased by radiation under the hydrogen water chemistry. It was considered that the enhancement of IGSCC by radiation well corresponds to the positive shift of the electrochemical potentials of the stainless steel.

Another IGSCC test was carried out with constant strain type specimens of sensitized type 304 stainless steel. 3) In this tests the specimens were irradiated with γ-rays at dose rates of 116 rad/h and 63.5 k rad/h in boiling 12% NaCl solutions buffered at pH3 and in pure water at 230° C, respectively. In both the cases the sucsceptibility of the stainless steel to IGSCC is enhanced by the gamma-irradiation. This enhancement of IGSCC was attributed to the presence of Fe^{3+} ions produced by the oxidation of Fe^{2+} ions by the radiolysis products in the boiling 12% NaCl solutions, but in the latter case the oxidising species produced by radiolysis was considered to be responsible for the enhancement.

REFERENCES

1) N. Fujita, M. Akiyama, T. Tamura, Corrosion, 37, 335 (1981).
2) A. Sudo, M. Itow, T. Okada, N. Saito, N. Ichikawa, Y. Hemmi, Proceedings of JAIF Int. Conf. on Water Chemistry of Nuclear Power Plants, Tokyo, 2, p.723 (1988).
3) M. Kuribayashi, N. Morishige, M. Murai, H. Okabayashi, IHI Engineering Review, 17, (No.2), 4 (1984).

2.3 IASCC

Irradiation-assisted stress corrosion cracking(IASCC) is a form of intergranular stress corrosion cracking of materials exposed to radiation. The first observation of IGSCC in irradiated stainless steels was a cracking incident of fuel claddings. Recent cracking incidents on power reactor core components indicate that IASCC is a common phenomenon on stainless steels used in high radiation field. Thus, experiments intended to simulate or reproduce the IASCC have been performed with post-irradiation laboratory tests and in-pile tests. At the same time, to get better understanding of the IASCC mechanism, microstructual change and segregation have also been evaluated with using new analyzing facilities.

2.3.1 Field observations

(1) SCC in fuel claddings[1][2]

In 1960's, failures of type 304 stainless steel fuel claddings were reported in some US BWRs and PWRs. The morphology of cracking was intergranular and the cracks initiated from the cladding outer surface. The cracks were observed both in annealed and cold-worked material. Strauss test showed that the materials were unsensitized. In Valecitos BWR the peak fuel-rod burnup was 6000-8000 MWd/tU at the time of cracking. The failure rate was higher under higher surface heat flux and higher stress condition. Type 348 stainless steel fuel claddings in Yankee Reactor were not cracked up to 17000MWd/Mt. At that time, the cracking of fuel claddings was considered to be IGSCC, and the presence of impurities, phosphorus and silicon, at grain boundary increased the susceptibility of intergranular corrosion based on the fact that irradiation enhanced intergranular attack in boiling HNO_3+Cr^{6+} solution.

(2) Control rod absorber tube in BWR[3]

The failure of control rod absorber tubes was reported in a BWR(KRB-I). The tube was made by a type 304 stainless steel, in which the B_4C powder was compacted. The longitudinal cracks were observed in high local ^{10}B burnup (30-35%) regions and the metallographycal examination showed that the cracks were typically intergranular with many brachings. Strauss test revealed that the materials were not sensitized. Swelling of solidified B_4C exerted increasing circumferetial stress in the absorber tubes, leading to longitudinal stress corrosion cracking in reactor coolant water.

(3) Control assemblies in PWR[4]

Cracking was reported in the cladding of rod cluster control assemblies in US PWRs. The longitudinal cracks were observed in high-fluence region of the rods. At the Point Beach PWR, cracked rods were found after 11 cycles of operation, the fluence of which may be above $5x10^{21}n/cm^2$. The cracking mechanism was considered to be related to stresses produced by absorber/cladding mechanical interactions and radiation damage of the claddings.

(4) Fuel element in UK SGHWR[5]

Failure was reported in stainless steel fuel element of the Winfrith SGHWR. The cracks were observed in the 20%Cr/25%Ni/Nb stabilized stainless steel intermidiate grid assemblies. The grid is located in the structure with A286 precipitation hardened alloy rivets through the ferrules which fasten them to Zry-2 water sparge tubes. The morphology of cracks was intergranular with intergranular attack on the inside surfaces. The severe cracking occured in high neutron flux region along the axial direction and in the center ferrules. The neutron fluence was about 2.5x10^{21} n/cm^2(E>0.15MeV). The sensitization of the material was negative by Strauss test both before and after irradiation. This cracking was considered to be a irradiation and crevice enhanced SCC in a high temperature water.

(5) Other SCC on reactor core internal materials

Field crackings which were considered to be IASCC were reported on neutron source holder, in-core monitor dry tube, control blade sheath and various volts and springs. Recent reviews have suggested the followings[6][7].

- Dymanic strain of high stresses produced IASCC in most early cases but, from recent results, the stress threshold for IASCC may be lower than initially believed.
- The fluence threshold for IASCC is about 5x10^{20}n/cm^2 (E>1MeV).
- The cracked materials were not sensitized when conventional material tests such as Strauss test were applied. No grain boundary carbides were osberved.

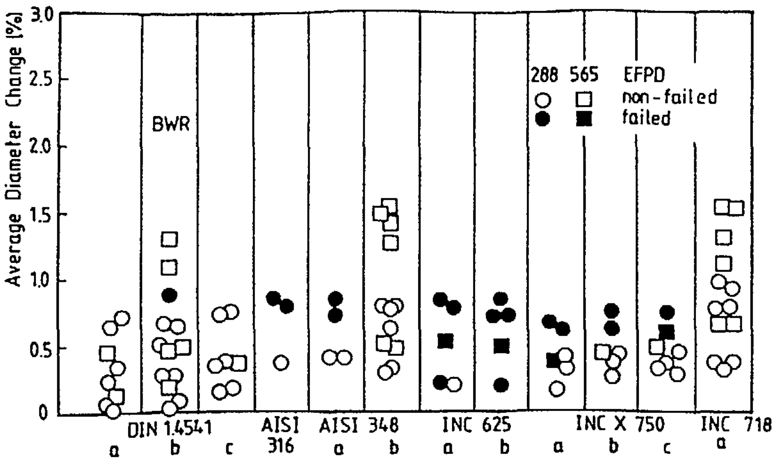

Strain to failure of various alloys in the core of a BWR

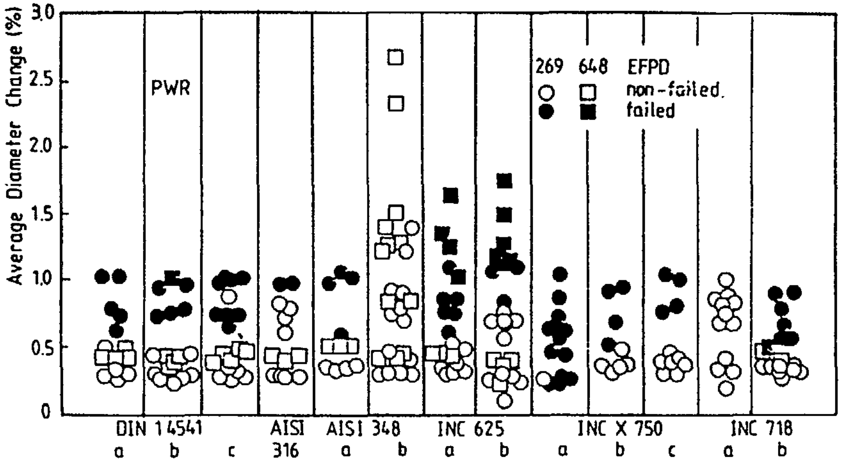

Strain to failure of various alloys in the core of a PWR

FIG. 2.3.1.

2.3.2 In-pile SCC test

KWU has performed in-pile SCC test using swelling tube for two cycle irradiation in a BWR and a PWR[8][9]. The swelling tube was consisted by a specimen tube filled with Al_2O_3 or Al_2O_3/B_4C pellet which swells under neutron irradiation and exerts the stress to the tube. The test materials were various austenitic stainless steels and Ni-based alloys with various impurity content and heat treatment(Table 2.3.1). Most materials suffered intergranular cracking in high fluence region

TABLE 2.3.1. CHEMICAL ANALYSIS (%) OF THE TEST MATERIALS

Element	DIN 1.4541ª		AISI 316	AISI 348		Inconel 625		Inconel X750	Inconel 718
	a,d	b,c		a	b	a	b	a,b,c	a,b
C	0.057	0.052	0.044	0.074	0.041	0.02	0.01	0.04 -	0.03
Fe	Bal.	Bal.	Bal.	Bal.	Bal.	2.5	3.2	8.1	18.4
Ni	10.5	10.1	11.3	11.5	11.0	Bal.	61.2	72.1	53.4
Cr	18.1	17.9	16.9	17.4	17.7	22.2	22.6	14.9	18.0
Mn	1.70	1.44	1.51	1.56	1.65	0.03	0.19	0.22	0.10
Mo			2.3	0.20		9.0	8.5		2.95
Nb + Ta				0.81	0.70	3.5	3.64	1.01	5.36
Ti	0.39	0.39				0.24	0.32	2.50	0.99
Al						0.19	0.12	0.65	0.53
Si	0.64	0.33	0.50	0.59	0.01	0.2	0.15	0.28	0.13
	(0.36)	(0.15)	(0.40)	(0.34)	(0.02)	(0.42)	(0.12)	(0.14)	(0.10)
S	0.010	0.009	0.010	0.012	0.008	0.007	0.009	0.001	0.003
	(0.009)	(0.008)	(0.009)	(0.009)	(0.007)	(0.003)	(0.002)	(0.002)	(0.003)
P	0.019	0.015	0.039	0.017	0.008	0.005	0.006	0.007	0.010
	(0.014)	(0.016)	(0.026)	(0.009)	(0.002)	(0.004)	(0.009)	(0.011)	(0.008)
				(0.004)					
N			0.031	0.032					
	(0.012)	(0.012)	(0.027)	(0.042)	(0.008)	(0.045)	(0.030)	(0.005)	(0.006)

(x) check analysis on samples from the tubes used in this program. All other data from supplier.
ª corresponding to AISI 321

($1.5x10^{21} n/cm^2$) of both BWR and PWR at high strain above 0.5%. (Fig. 2.3.1) However, Inconel 718 with proper heat treatment and high purity 348 stainless steel were not cracked even at high strain. The correlation between the diametral strain of the tube specimens and the grain boundary corrosion rate in boiling HNO_3+Cr^{6+} solution was observed.

2.3.3 Out-of-pile test of irradiated materials

The effects of neutron fluence[10]-[13], stress[13], water chemistry[11][12] and material variation[12] on SCC susceptibility of irradiated stainless steels have been investigated.

Systematic studies[10][11] with slow strain rate tests in a high temperature water have shown that there is a threshold neutron fluence in IASCC. In a type 304 stainless steel tested in 288 C water containing 32ppm dissolved oxygen(DO), at a starin rate of 10^{-7} /s, the threshold lies $5x10^{20}$-$1x10^{21}$ n/cm^2 (E>1MeV). (Table 2.3.2 and Fig. 2.3.2) This value is consistent with that of the field cracking observations, although environmental factors such as stress and water chemistry were different between

TABLE 2.3.2. CERT RESULTS FOR SAMPLES FABRICATED FROM IRRADIATED REACTOR TUBING (288°C WATER WITH 32-36 mg/L O_2)

Test No.	Sample Fluence (n/cm^2, E>1 MeV)	Strain Rate (min^{-1})	Test Time (h)	Max. Stress (MPa/Ksi)	Mode (SEM)
3-13-DL	$2.77x10^{21}$	$1x10^{-5}$	1	194/28	IGSCC (100%)
4-13-DH	$2.30x10^{21}$	$1x10^{-5}$	28	303/44	IGSCC (11%)
3-13-DG	$2.08x10^{21}$	$5x10^{-6}$	41	641/93	Ductile
3-13-DF	$2.01x10^{21}$	$1x10^{-5}$	93	572/83	IGSCC (45%)
4-13-DE	$2.01x10^{21}$	$1x10^{-6}$	329	503/73	IGSCC (55%)
3-13-CB	$1.28x10^{21}$	$5x10^{-6}$	98	406/59	IGSCC (5%)
3-13-BK	$9.50x10^{20}$	$1x10^{-5}$	85	537/78	IGSCC (5%)
4-13-BH	$5.0x10^{20}$	$1x10^{-5}$	32	462/67	IGSCC (8%)
4-13-AL	$6.0x10^{19}$	$1x10^{-5}$	56	331/48	Ductile

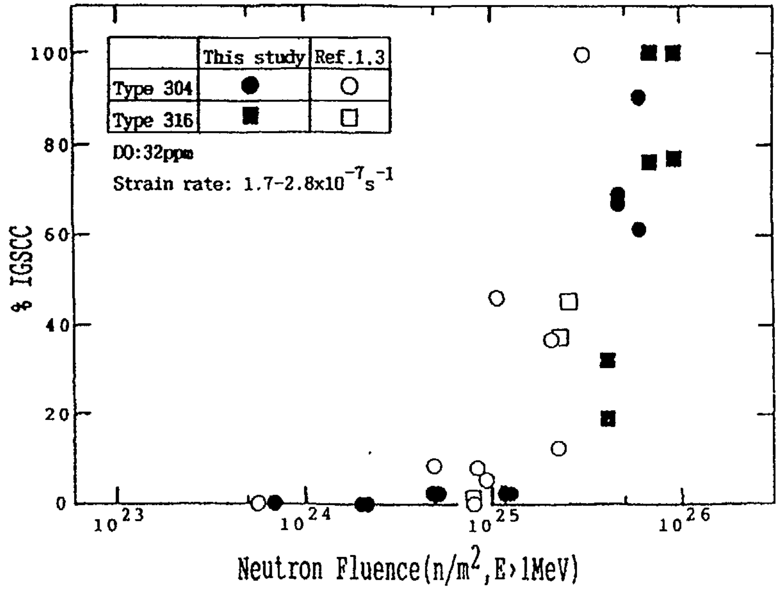

FIG. 2.3.2. Fluence dependence of %IGSCC in types 304 and 316 stainless steel (Ref. [1] data obtained from type 304 stainless steel irradiated in BWR. Ref. [3] data obtained from types 304 and 316 stainless steel irradiated in advanced test reactor (ATR)).

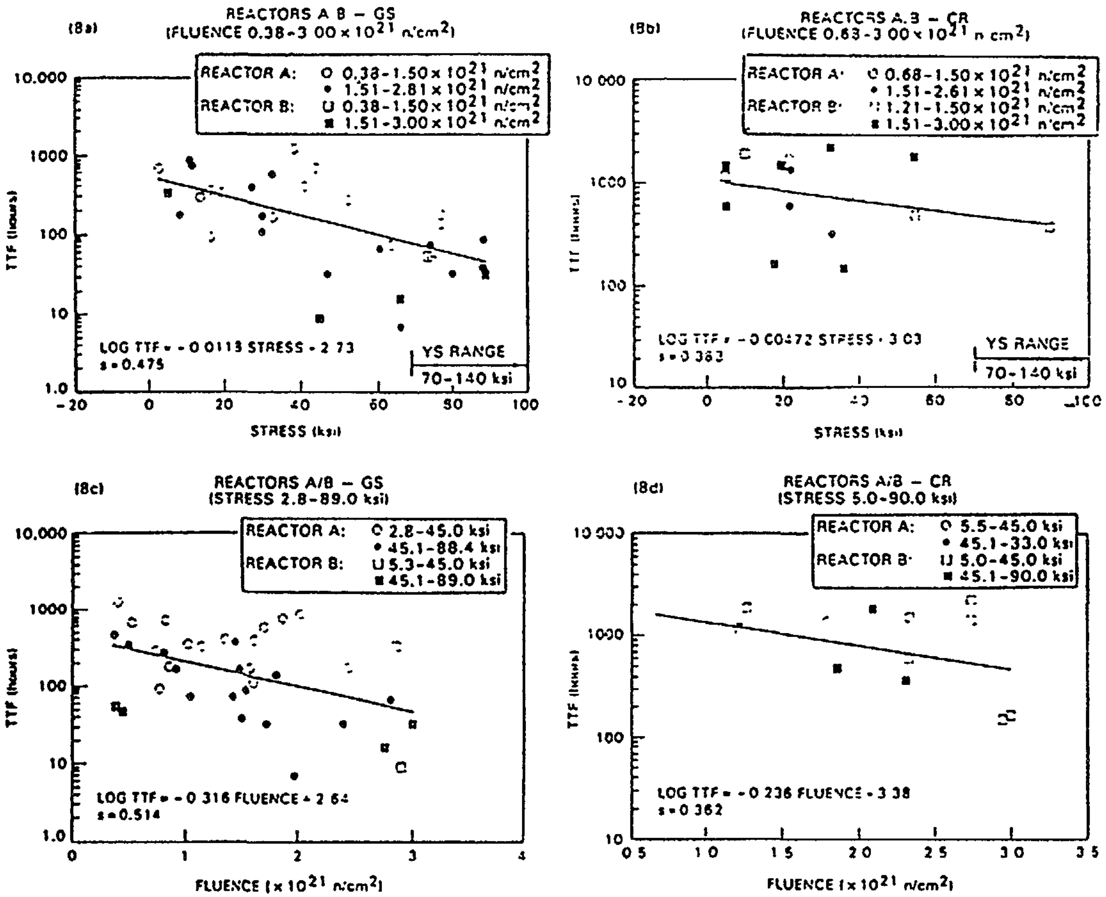

FIG. 2.3 3. Plots of time-to-failure (TTF) vs stress and fluence for gage section (GS) (left side) and crevice (CR) (right side) failures obtained in specimens from reactors A and B Stresses are net section stresses in gage section areas.

out-of-pile test and actural reactor core. Increasing strain rate[10] and decreasing DO concentration [11][12] reduce SCC susceptibility in irradiated type 304 stainless steels.

Uniaxial constant load tests in 288 C water containing 32ppm DO on irradiated BWR control rod components (type 304 stainless steel) showed that the threshold fluence was 3-$4x10^{20}n/cm^2$ but that a stress threshold was not observed[13]. Time-to-failure decreased with increasing stress and increasing fluence. (Fig. 2.3.3)

Effects of alloy composition and impurity amount in stainless steels have not been well understood. Four types of stainless steels, 304, 304L, 316L and 316NG were tested with SSRT in

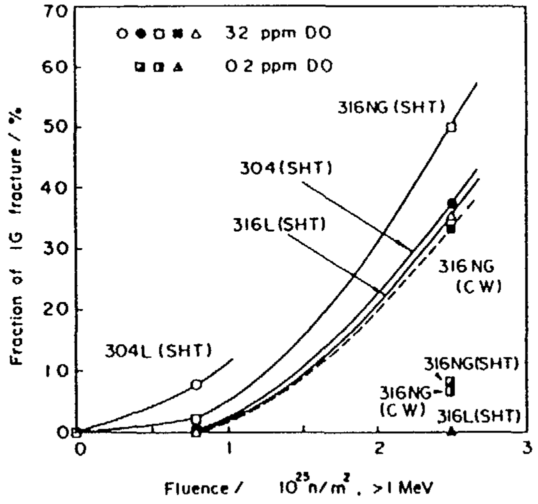

FIG. 2.3.4. Neutron dose dependent fraction of intergranular fracture after the SSRT test in water with 32 and 0.2 ppm DO at 561 K.

32ppm DO water after neutron irradiation[12]. All materials irradiated had SCC susceptibility. (Fig. 2.3.4) Impurities such as phosphorus and silicon were believed to change SCC susceptibility. In-pile type 348 stainless steel data reported by KWU indicated that the decrease of phosphorus and silicon could reduce SCC susceptibily[9]. However, recent data[14] showed that phosphorus and silicon had no effect on SCC susceptibility in irradiated type 304L.

Data of Water chemistry effect on IASCC is quite limited except for dissolved oxygen. One study of gamma irradiaiton on irradiated type 304 stainless steel showed that the extent of IGSCC in a normal BWR water chemistry appears greater with gamma irradiation than without gamma irradiation[15]. In a hydrogen water chemistry IGSCC was mitigated inspite of gamma irradiation together with the reduction of electrochemical potential (ECP). (Table 2.3.3)

TABLE 2.3.3. CERT TEST RESULTS FOR IRRADIATED TYPE 304 STAINLESS STEEL IN 288°C WATER UNDER GAMMA RADIATION ($\dot{\epsilon} = 1 \times 10^{-7}$/s)

TEST NO.	MAXIMUM BREAKING STRESS (MPa/ksi)	TIME TO FRACTURE (h)	STRAIN AT FRACTURE (%)	IASCC[a] (%)	WATER CHEMISTRY[b]			ELECTROCHEMICAL POTENTIAL RANGE (mV_{SHE})	
					OXYGEN (ppb)	HYDROGEN (ppb)	CONDUCTIVITY µS/cm AT 25°C	304SS	Pt
1	602/87.4	188	8.0	85	250–570	2–9	0.1–0.15	+200/+670	−200/+635
2	870/126.2	254	14.8	0	2.5–5.3	26–75	0.2–0.29	−300/−603	−685/−590

[a] DETERMINED BY SEM.

[b] MINIMUM-MAXIMUM VALUES OBSERVED OVER TEST AT AUTOCLAVE INLET SAMPLE POINT.

2.3.3 Microstructural studies

Recent experimental studies have been focused on microstructural and microchemical changes in irradiated materials to get better understanding of IASCC and its mechanims.

The enrichment of phosphorus, silicon and nickel and depletion of chromium due to radiation induced segregation at grain boundary has been commonly observed in irradiated stainless steels[16]-[22]. High resolution STEM and AES analyses have confirmed that the segregated width along grain boundary was only 2-5nm (Fig. 2.3.5) and that the segregation became significant at a fluence around 5-10x10^{20} n/cm^2, which corresponds to the threshold fluence of IASCC[17]. (Fig. 2.3.6) Thus, chromium depletion and/or impurity segregation due to irradiation are considered to be a potential cause of IASCC. The roll of chromium depletion in the IASCC mechanism may be similar to that in IGSCC mechanism in thermally sensitized stainless steels by reducing stability of passivation.

It was reported that hydrogen content in a BWR core component irradiated up to 9x10^{21}n/cm^2 was three times higher than in unirradiated materials[23]. The source of hydrogen was thought to be transmutation and electrochemical reaction due to corrosion. The retention of hydrogen was attributed to radiation induced traps such as defect clusters. Based on this data and the facts that both the depletion of chromium and the enrichment of

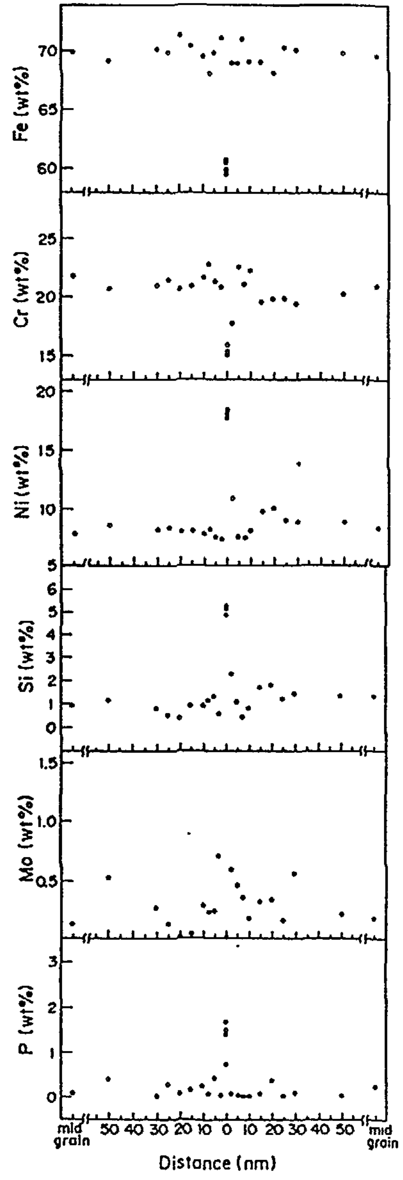

FIG. 2.3.5. Compositional profiles of a grain boundary in type 304 steel neutron irradiated to 6.0 × 10^{25} (E > 1 MeV) at 561 K.

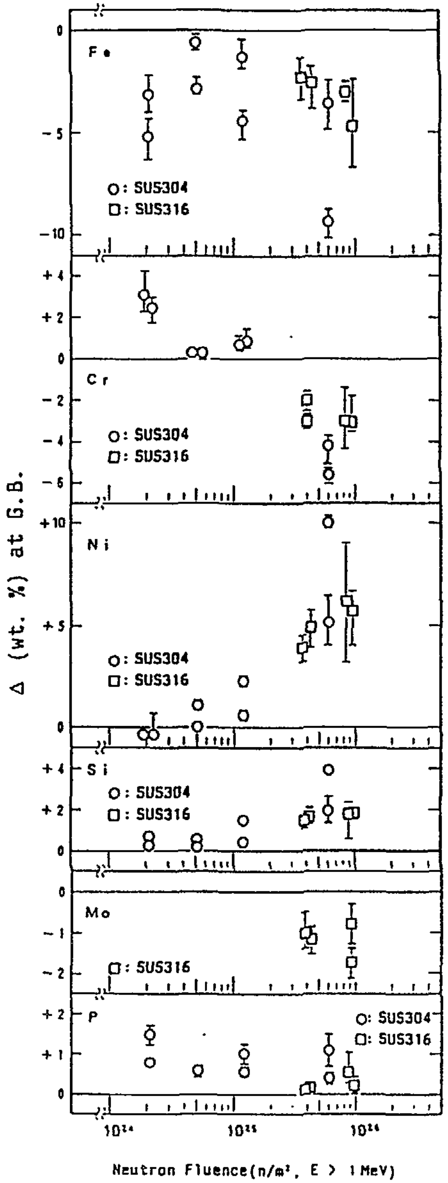

FIG. 2.3.6. Neutron fluence dependence of grain boundary contents of alloying or impurity elements. Composition differences between the value of the grain boundary and that in the mid of grain are displayed.

phophorus at grain boundary is known to enhance hydrogen induced cracking(HIC)[24]-[26]. HIC may be another potentail mechanism of IASCC.

Fig.2.3.7 is a schematical summary of possible interaction between irradiation and the material in the IASCC mechanism[27].

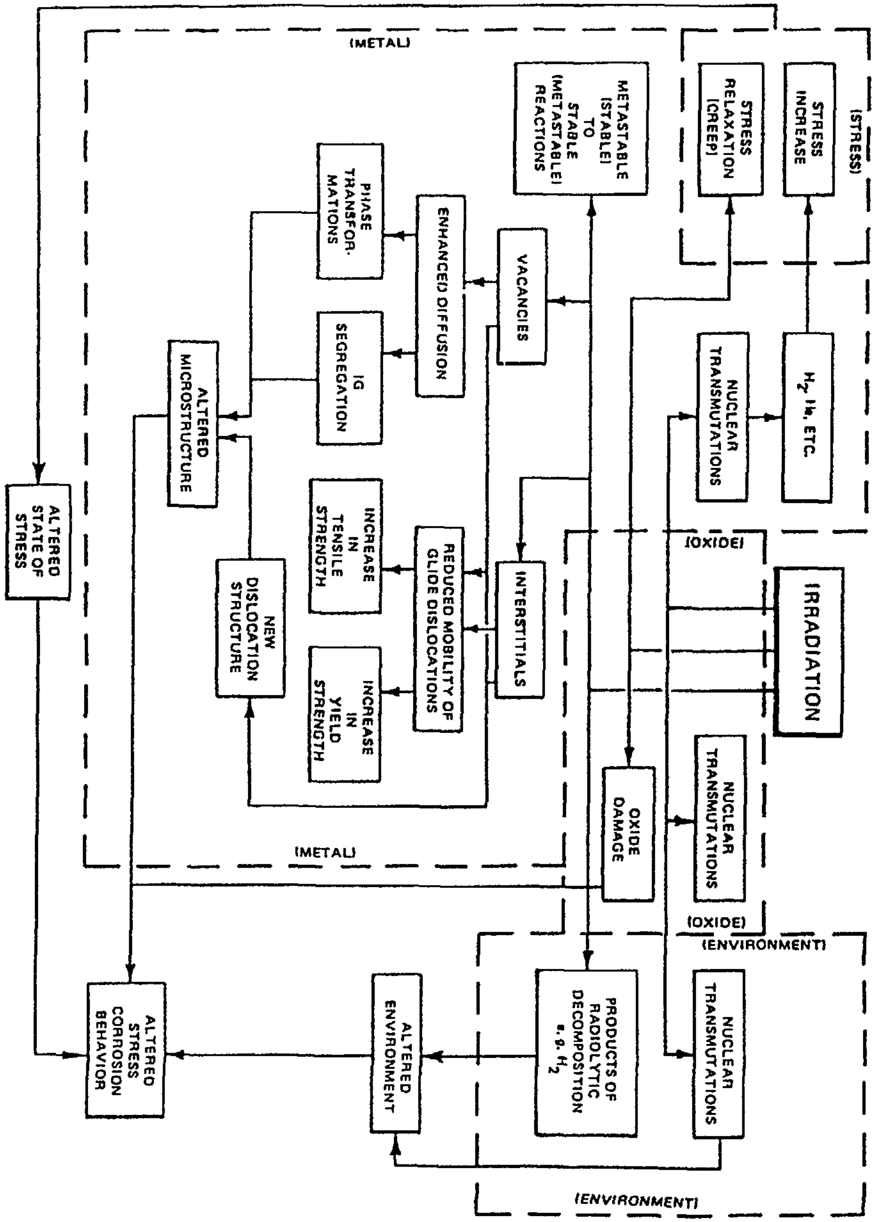

FIG. 2.3.7. Summary of possible interactions between irradiation and the material (metal/oxide) — Environment-Stress Triad.

REFERENCES

[1] Behavior of Stainless Steel in Reactor I, Materials and Technology Division Special Session, Trans. ANS 7(1964)416
[2] R.N.Duncan, Stainless Steel Failure Investigation Programme, Final Summary Report, GEAP-5530(1969)
[3] N.Eickelpasch et al, Nucl.Tech., 60(1983)362
[4] M.P.Manahan et al, Trans. Int. Conf. Structural Mechanics for Reactor Technologies, 9th, No.c, 1987, pp.75
[5] P.M.Scott et al, NEA/UNIPEDE Specialist Meeting on Life Limiting and Regulatory Aspects of Core Internals and Pressure Vessels, 1986
[6] B.M.Gordon et al, Nucl.Eng.Design, 98(1987)109
[7] P.L.Andresen et al, Proc. 4th Int. Symp. on Environmental Degradation of Materials in Nuclear Power Systems-Water Reactors, Jekyll Island, GA, NACE, 1990
[8] F.Garzarolli et al, Proc. 2nd Int. Symp. on Environmental Degradation of Materials in Nuclear Power Systems- Water Reactors, AIME, 1985, p.131
[9] F.Garzarolli et al, Proc. 3rd Int. Symp. on Environmental Degradation of Material in Nuclear Power Systems-Water Reactors, AIME, 1986, p.657
[10] W.L.Clarke et al, Proc. Int. Symp. on Environmental Degradation of Materials in Nuclear Power Systems-Water Reactors, AIME, 1983, p.451
[11] M.Kodama et al, presented in 5th Int. Sypm. on Environmental Degradation of Material in Nuclear Power Systems-Water Reactor, Monterey, NACE, 1991
[12] A.J.Jacobs et al. ibid.[9], p.673
[13] A.J.Jacobs et al, corrosion 91, Cincinnati, NACE, 1991
[14] K.Fukuya et al, Annual Meeting of Japan Institute of Metals, April 1990

[15] W.L.Clarke et al, ibid.[7], p.442
[16] K.Fukuya et al, ibid.[9], p.651
[17] K.Asano et al, ibid.[11]
[18] A.J.Jacobs et al, ibid.[7]
[19] A.J.Jacobs et al, ASTM STP 956, 1987, pp.239
[20] H.M.Chung et al, 18th Water Reactor Safety Information Meeting, Rockville, 1990
[21] K.Nakata et al, J.Nucl.Mater., 148(1988)185
[22] S.M.Bruemmer et al, Corrosion 90, Las Vegas, NACE, 1990
[23] A.J.Jacobs et al, ASTM STP 956, 1987, pp.239
[24] C.L.Briant, Met.Trans., 9A(1978)731
[25] C.L.Briant, Met.Trans., 10A(1979)181
[26] S.M.Brummer et al, *ibid.*[7]
[27] A.J.Jacobs et al, Int. Conf. on Nuclear Plant Aging, Availability Factor and Reliability Analysis, San Diego, July 1985

INFLUENCE OF FUEL CLAD SURFACE ON PERFORMANCE UNDER OPERATIONAL AND ACCIDENT CONDITIONS

S.A. ANTIPOV, V.V. DRANENKO, V.F. KON'KOV,
I.B. SOKOLOV, A.A. KHAIKOVSKIJ
A.A. Bochvar's All-Union Scientific Research
Institute of Inorganic Materials,
Moscow, Union of Soviet Socialist Republics

Abstract

In this document methods of cladding preoxidation by autoclaving or anodizing before irradiation are described . This treatment prevents or decreases the amount of corrosion product deposit on the fuel sheath during irradiation.

During a reactor operation fuel clads are subject to an intricate physical, mechanical, chemical and physico-chemical influence. In this case the conventional corrosion problem is complicated by thermal stresses and their variations on thermal cycling, high coolant rates, contamination of coolant with corrosion products, irradiation induced changes of a coolant composition (e.g., water radiolysis), compositional and structural changes of clads with burn-up etc.

Thus, to solve the problem whether a material can be used as a fuel clad one must have at one's disposal the results of many different tests and investigations into corrosion, mechanical, thermal and hydroulic properties.

The serviceability of fuels is significantly affected by the initial state of a clad surface.

In the Soviet Union prior to loading into a reactor fuel elements are autoclave tested to check their corrosion resistance and to produce an oxide film at their surfaces.

A dense oxide film protects the outer surface of elements from slight mechanical effects which is especially important during a fuel rod assembling when the available oxide film significantly reduces the friction between a fuel clad and a spacer grid.

The autoclave effected surface passivation of fuels is also beneficial.

However, it should be pointed out that the autoclave treatment is labour-consuming, power-intensive and makes the process of fuel production by a factor of 3÷5 longer, moreover, the periodicity of the process upsets the continuity of the total process cycle.

An alternative to this is electrochemical anodizing that replaces autoclaving and retains its beneficial functions, besides it permits a continuous process of fuel fabrication.

As distinct from autoclaved oxide films anodized ones mainly consist of an amorphous oxide of an almost stoichiometric composition.

Under operational conditions anodized films of any thickness change with time into conventional thermal ones. As it was shown in some investigations the structural characteristics and the main physico-chemical properties of thermal and anodized oxide films are fully identical.

There is a difference in the fluorine behaviour between anodized and thermal oxide films which should be discussed. Independent of the anodizing schedules the fluorine contained by the tube surface remains in anodized films and concentrates at the "metal-oxide" interface. Under actual operation conditions fluorine by diffusion gradually escapes to a coolant and this can have a harmful effect on fuel serviceability.

During autoclaving fluorine leaves the tube surface, therefore thermal oxide films resulting from autoclave tests have a lower fluorine content.

To prevent fluorine of anodized films from escaping to a coolant an additional operation is required , viz., an alkaline treatment of fuels that neutralizes fluoride impurities contained by fuel rod surfaces. Thus, a one minute alkaline treatment at 80°C reduces the fluorine content of the fuel rod surface by an order of magnitude. When combined with a supersonic treatment the effect of a fluorine removal is still more significant and the treatment time is reduced to a few seconds therefore this operation can be incorporated in the production line thereby ensuring the low fluorine surface content of a product.

Thus anodized oxide films formed at fuel clad surfaces are almost fully identical to autoclaved oxide films in their physicochemical, structural and protectiv properties. The alkaline surface treatment introduced into the process to neutralize fluoride impurities prevents fluorine from entering a nuclear reactor circuit.

The substitution of a labour-consuming, power-intensive and intricately instrumented autoclave treatment by anodizing makes it possible to provide a continuous production line for all process operations and reduce by a factor of 3÷5 the total technological production cycle thereby cutting the labour and power consumption per a unit of a finished product and saving working areas.

In the Soviet Union 42 assemblies containing fuels with anodized clads were reactor tested at the Kursk and Leningrad nuclear power plants. The "hot" cell examination of the assemblies did not show any significant difference between the anodized and autoclave tested fuels. The burn-up of the assemblies examined was 1664 MW.day/assembly. The clad surface had a black lustrous oxide film without any cruds. It should be noted that in some instances fuel clads with both anodized and autoclaved oxide films showed a nodular corrosion adjacent to the spacer grids; the maximum density being at the site between the 5th and 7th spacer grids. No other damages were observed.

The assemblies examined are to be reloaded into a reactor.

The initial condition of the fuel clad surface significantly affects also the fuel serviceability at nuclear plants for district heating (NPDH) where the operating temperature is 200÷230°C and the operation time is 8-10 years.

To check the effect investigations were carried out using fuel clads with differently treated surfaces:

1 - as supplied (as etched and alkaline treated)
2 - as autoclaved (300°C - 72 hours)
3 - as anodized (schedules of a producer-plant)

The tests were performed under conditions close to the water chemistry of nuclear plants for district heating:

- the temperature 230°C
- the pressure 25÷30 atmospheres

- a helium - 4% vol. molar hydrogen mixture was measured into the autoclave
- the testing time - 13000 hours.

The results of the corrosion studies are presented in the figure.

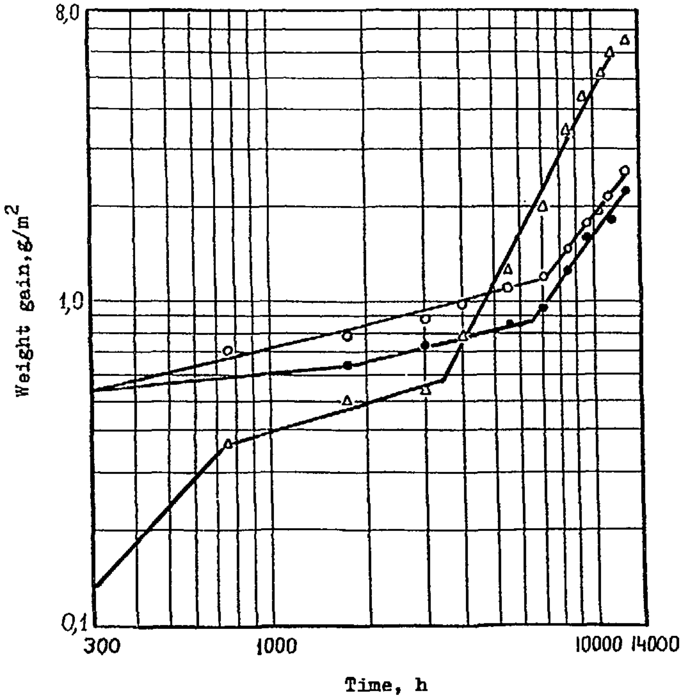

Kinetics of aqueous corrosion of 110 alloy at 230°C:
Δ as supplied
○ as autoclaved
● as anodized.

On a long-term attack the specimens as supplied are significantly inferior in their corrosion resistance to the autoclaved and anodized specimens.

For the as supplied specimens the first stage of the kinetics is controlled by the atmospheric oxygen-metal surface interaction. The process goes on at an accelerated rate until protective oxide film is formed.

The autoclaved and anodized specimens are not subject to such an accelerated corrosion due to their protective films formed during preliminary autoclaving and anodizing.

For all surface conditions the period of decelerated corrosion is controlled by the oxygen diffusion through the oxide film and proceeds until the oxide film loses its protective properties. After that the corrosion kinetics shows a sudden change and transition to an accelerated corrosion.

For the as supplied specimens this time is equal to 3500 hours while for the anodized and autoclaved ones it is 6500 and 6700 hours, respectively.

At the end of the tests the weight gain in the as supplied specimens (6.5 g/m^2) was more than a factor of 2.5 in excess of the weight gains in the autoclaved (2.5 g/m^2) and anodized (2.3 g/m^2) specimens.

Thus, one can state that from the viewpoint of corrosion the preliminary surface autoclaving and anodizing are a good practice for the successful operation under the water chemistry conditions of nuclear plants for distfict heating.

It should be pointed out that the initial state of a fuel clad surface can significantly influence the fuel condition in the computed tentative accidents including the maximum tentative accident (MTA). The USSR adopted concept of the analysis of a fuel condition in MTA contemplates primarily the design of the most unfavourable (the maximum clad temperature) event, i.e., the design of a fresh fuel rod having the maximum power density.

To analyze the influence of the initial surface condition of clads on their oxidation kinetics at high temperatures pertinent to MTA we studied the corrosion behaviour of fuel clads after autoclaving and without it. The clads were tested in steam within 700-1200°C in a continuous weighing unit.

No significant effect of pre-autoclaving was noted in the temperature range 900-1200°C

The investigations carried out within 700-850°C allow a preliminary conclusion to be drawn that in the initial oxidation period (at the interaction time up to 10^3s) the autoclave effected oxide film has protective properties. Thus, at 700°C the weight gain in non-autoclaved specimens is significantly higher and after 20 hours it exceeds by a factor of 1.73 the weight gain in the autoclaved ones.

The maximum local oxidation depth equal to 18% is reached by non-autoclaved specimens in 20 hours while the maximum value is not reached by the autoclaved ones even after 30 hours.

Thus, it can be concluded that an oxide film available at a fuel clad surface has a beneficial effect on both the assembly process and the performance under water chemistry conditions at NPPS and nuclear plants for district heating as well as at high temperatures pertinent to accident conditions.

INFLUENCE OF SOME PARAMETERS ON SENSITIVITY OF ZIRCONIUM ALLOYS TO NODULAR CORROSION

S.A. ANTIPOV, V.F. KON'KOV,
A.V. TOKMAKOV, A.A. KHAIKOVSKIJ
A.A. Bochvar's All-Union Scientific Research
Institute of Inorganic Materials,
Moscow, Union of Soviet Socialist Republics

Abstract

In this paper the results of expirements on the influence of cladding pretreatment (autoclaving or anodizing) on nodular corrosion are presented. It is concluded that autoclaving is of good practice for Zr-Nb alloys as well as for binary alloys of Zr with Fe, Ni, Cr, Sn or combined composition: Zircaloy. The corrosion behaviour of these alloys except Zr-Nb is penalized by anodizing. The propension to nodular corrosion seems correlated to the presence of fluorine.

Recently due to an increase in water-cooled reactor fuel life-time studies of zirconium alloy corrosion again attracted much attention. The longer staying of fuel in the core is related to both a higher fuel burn-up and a lower capacity factor (CF). Thus, under load-follow operation conditions CF may be significantly reduced up to 0.5-0.6 resulting in a 1.5-2 times increase of the fuel operation time.

As is known, on a long-term fuel operation nodular corrosion starts which can significantly limit the fuel performance. The danger of nodular corrosion lies in the fact that its rate is many times higher than that of uniform one. Besides, the non-uniform distribution of the neutron flux density aggravates nodular corrosion in high flux areas which can result in shape changes and even ovalization of claddings.

The propensity of zirconium alloys for nodular corrosion is significantly affected by both the alloy composition and the surface condition of fuel claddings.

To estimate the influence of the surface condition on the propensity of zirconium alloys for nodular corrosion accelerated laboratory tests were conducted in high temperature steam by a two stage method:

I stage - 410°C, 100 atm, steam, 3 hours;
II stage - 520°C, 100 atm, steam, up to 0.5 hour.

The extent of the formed oxide film non-uniformity was determined visually, with an optical microscope and gravimetrically.

For the investigation we used binary zirconium alloys with 1% alloying elements (iron, nickel, chromium and tin) as well as Zr-1% Nb alloys, zircalloy-2 and Zr+1% Nb+1% Sn+0.5% Fe alloy.

The tests were conducted using specimens as etched, with the surface contaminated with fluorine, as autoclaved, anodized as well as affected by all the factors enumerated. Specimen etching was accomplished in an aqueous mixture of hydrofluoric and nitric acids while its contamination with residual fluorine was achieved through drying the dilute etching solution applied to the specimen.

The level of residual fluorine as determined by the proton-activation method was equal to 0.3-0.5 g/cm^2 for the etched specimens and 1.0-1.5 g/cm^2 for the contaminated specimens.

The specimen anodizing was conducted in a 0.5% NaOH solution until a ~ 0.25 μm thick film resulted. The specimen autoclaving was performed in distilled water in a stainless steel vessel at 300°C and 120 atm for 72 hours.

Table 1 contains the results of the gravimetric analysis of the investigated specimens as dependent on their surface condition. For the sake of convenience all the specimens are subdivided into two groups: those etched and contaminated with residual fluorine. Besides, before corrosion testing some of the thus treated specimens were anodized and some were autoclaved.

Table 1. Results of Gravimentric Analysis as Dependent on Surface Condition of Investigated Specimens

Alloy	Surface condition		Notes
	Etching, weight gain,mg/dm^2	Contamination, weight gain,mg/dm^2	
	18	76	
Zirconium-iron	42	128	Anodized
	53	20	Autoclaved
	30	211	
Zirconium-nickel	112	140	Anodized
	38	22	Autoclaved
	41	318	
Zirconium-chromium	288	755	Anodized
	31	20	Autoclaved
	367	445	
Zirconium-tin	268	710	Anodized
	191	20	Autoclaved
	24	27	
Zirconium-niobium	15	25	Anodized
	25	26	Autoclaved
	20	42	
Zircalloy	29	45	Anodized
	24	27	Autoclaved
	19	50	
Zr-Sn-Fe-Nb	10	35	Anodized
	22	24	Autoclaved

First of all it should be pointed out that nodular corrosion was observed in all the specimens investigated for the exception of those containing niobium. The binary Zr-1% Nb alloy as well as the multicomponent Zr-Nb-Sn-Fe alloy had no traces of nodular corrosion independent of the version of the surface treatment, i.e., it can be stated that Nb alloying suppresses the propensity of zirconium for nodular corrosion.

Fig. 1 shows photographs taken from the surfaces of binary Zr-Fe (fig. 1a) and Zr-Nb (fig. 1b) alloys and giving an idea of the corrosion of the two groups of the alloys. From the results of table 1 one can easily trace the relationship between the surface condition and the propensity of the alloys for nodular corrosion.

In all the specimens studied for the exception of those containing niobium the residual fluorine contamination of their surfaces aggravated the non-uniform (nodular corrosion).

Corrosion testing of anodized specimens having pre-etched and pre-contaminated surfaces shows that in all cases the nodular corrosion was intensified. In this case too the exception was a group of niobium-containing alloys the surface of which did not show nodular corrosion.

The most interesting results were obtained for specimens as autoclaved.

First of all, it should be pointed out that the corrosion testing of as autoclaved specimens indicated a significantly improved corrosion resistance of essentially all specimens

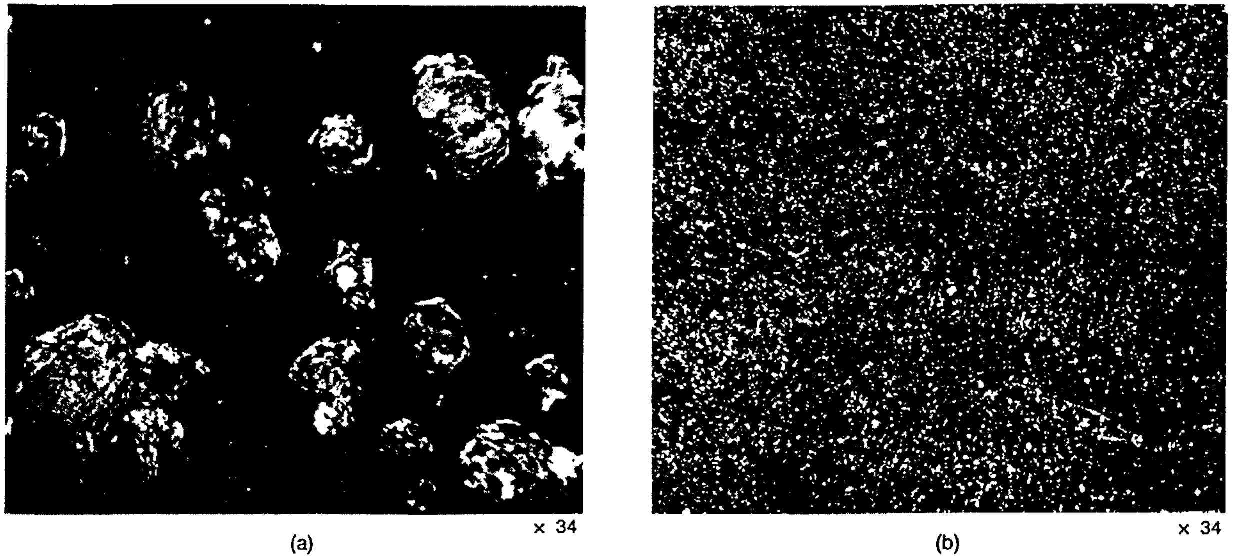

(a) (b)

FIG. 1. Structure of binary Zr-Fe (a) and Zr-Nb (b) specimen surface.

under study; even alloys having a higher propensity for nodular corrosion (Zr-Cr, Zr-Fe, Zr-Sn) practically did not show its traces.

Attention is drawn to the fact that the autoclaving of specimens pre-contaminated with fluorine significantly improved their corrosion-resistance and in some instances suppressed the nodular corrosion. The above refers to the whole group of the alloys investigated.

The experiments that studied the influence of the surface condition on the corrosion behaviour of the alloys revealed some regularities:

1. Niobium present in zirconium alloys improves their corrosion resistance and makes them insensitive to nodular corrosion independent of the pre-treatment of their surfaces.

2. Binary alloys with iron, nickel, chromium or tin as well as their combined composition (zircalloy) showed propensity for nodular corrosion.

3. In all cases the fluorine contamination up to 1.0-1.5 mkg/cm^2 of the specimen surfaces impaired their corrosion resistance.

4. The anodizing of specimen surfaces penalizes their corrosion behaviour (except for niobium containing alloys) and increases their propensity for nodular corrosion which is especially marked in contaminated specimens. This phenomenon can be explained by the fact that during anodizing the whole fluorine available at the specimen surface is concentrated in the anodic film and aggravates its negative effect on corrosion.

5. Pre-autoclaving significantly improved the corrosion resistance of the alloys investigated and in some cases suppressed the nodule formation at their surfaces. This positive effect of autoclaving on the corrosion of the alloys can be explained by the removal of fluorine from the specimen surfaces during autoclaving. According to the results of the proton-activation analysis the fluorine content of the autoclaved specimen surface decreased by 2-5 times.

It is undoubtedly interesting to investigate fuel elements having operated at NPPs with WWER-1000 type reactors.

For hot-cell post-irradiation investigations two fuel assemblies (FA) were taken:

1. FA № 1114, the Vth unit of the Novo-Voronesh nuclear power plant, the uranium-235 enrichment of 4.4 and 3.6%, the burn-up of 44.76 MW.day/kg uranium, loaded into the reactor on 25.07.84, discharged on 25.07.87, leak-tight.

2. FA № 0106, South-Ukranian nuclear power plant, the burn-up of 37.0 MW.day/kg U, unwrapped, leak-tight.

The fuel elements contained by the fuel assemblies were subjected to autoclaving at 320-340°C, the pressure of 120 atm for 36 hours.

After cooling in a pond in august 1990 the assemblies were unwrapped and in september the preliminary visual hot-cell examination of the spent fuels was conducted.

The surface of the fuels of both the assemblies was covered with a dark-grey dull closely - adherent oxide film without traces of nodular corrosion. It can be pointed out that the bottom (to the second spacer grid) fuels of the unwrapped assembly have a thin grey layer that is easily removed with a cotton wool wad. In the middle portion of some fuels contour stains were found out that were also easily removed.

Thus, it may be concluded that fuel elements subjected to preliminary autoclaving showed reliable serviceability during the three year operation of the WWER-1000 reactor (a three year cycle).

PARTICIPANTS IN THE CO-ORDINATED RESEARCH PROGRAMME

ARGENTINA

Ablesa, M.	Departamento de Química de Reactores, Comisión Nacional de Energía Atómica, Avenida del Libertador 8250, 1429 Buenos Aires
Corti, H.R.	Departamento de Química de Reactores, Comisión Nacional de Energía Atómica, Avenida del Libertador 8250, 1429 Buenos Aires
Maroto, A.J.G.	Departamento de Química de Reactores, Comisión Nacional de Energía Atómica, Avenida del Libertador 8250, 1429 Buenos Aires
Piacquadio, N.H.	Departamento de Química de Reactores, Comisión Nacional de Energía Atómica, Avenida del Libertador 8250, 1429 Buenos Aires
Regazzoni, A.	Departamento de Química de Reactores, Comisión Nacional de Energía Atómica, Avenida del Libertador 8250, 1429 Buenos Aires

BELGIUM

Blanpain, P.	Belgonucléaire SA, 25, rue du Champ de Mars, B-1050 Brussels

BULGARIA

Dobrevsky, I.	University of Chemical Technology, 8010 Bourgas
Litovska, G.	University of Chemical Technology, 8010 Bourgas
Vassilev, R.	University of Chemical Technology, 8010 Bourgas

CANADA

Lister, D.H.	Atomic Energy of Canada Ltd, Chalk River Nuclear Laboratories, Chalk River, Ontario K0J 1J0
Speranzini, R.A.	Atomic Energy of Canada Ltd, Chalk River Nuclear Laboratories, Chalk River, Ontario K0J 1J0

CHINA

Fan Junfu	Reactor Structure Materials and Water SWCR Chemistry Experiment Research Division Chengdu, Sichuan Province

CZECHOSLOVAKIA

Burclova, J.	Radiation Safety Department, Nuclear Power Plants Research Institute, Okruzná 5, CS-918 64 Trnava
Kysela, J.	Department of Radiation Experiments, Nuclear Research Institute, CS-250 68 Rez/Prague

FINLAND

Aaltonen, P.	Technical Research Centre of Finland, Vuorimiehentie 5, SF-02150 Espoo
Aho-Mantila, I.	Metals Laboratory, Technical Research Centre of Finland, SF-02150 Espoo

FRANCE

Beslu, P.	Centre d'études nucléaires de Cadarache, Commissariat à l'énergie atomique, Saint-Paul-lez-Durance

GERMANY

Hickling, J.	Siemens AG, KWU Group U9 23, Hammerbachstrasse 12/14, D-W 8520 Erlangen
Hüttner, F.	Institut für Energietechnik, Technische Universität Dresden, Mommsenstrasse 13, D-O 8027 Dresden
Riess, R.	Siemens AG, KWU Group U9 23, Hammerbachstrasse 12.14, D-W 8520 Erlangen
Winkler, R.	Institut für Energietechnik, Technische Universität Dresden, Mommsenstrasse 13, D-8027 Dresden

HUNGARY

Horvath, G.L.	Nuclear and Thermal Power Plant Division, Institute for Electrical Power Research, P.O. Box 233, H-1368 Budapest
Matus, L.	Department of Chemistry, Central Research Institute for Physics, P.O. Box 49, H-1525 Budapest 114

INDIA

Mathur, P.K.	Water Chemistry Division, *Bhabha Atomic Research Centre*, Trombay, Bombay 400 085
Narasimhan, S.V.	Water Chemistry Division, Bhabha Atomic Research Centre, Trombay, Bombay 400 085
Venkateswaran, G.	Water Chemistry Division, Bhabha Atomic Research Centre, Trombay, Bombay 400 085
Venkateswarlu, K.S.	Water Chemistry Division, Bhabha Atomic Research Centre, Trombay, Bombay 400 085

JAPAN

Ishigure, K.	Department of Nuclear Engineering, University of Tokyo, Bunkyo-ku, Tokyo

KOREA, REPUBLIC OF

Yang, Jae-Choon	Department of Physics, Chungnam National University, 220 Gungdong, Yousung, Taejon 300-31

POLAND

Ostyk-Narbutt, J.	Department of Radiochemistry, Institute of Nuclear Chemistry and Technology, U. Dorodna 16, PL-03195 Warsaw

RUSSIA

Antipov, S.A.	VNIINM, Rogov St. 5, 123060 Moscow
Khitrov, Yu.	VNIPIET, Dibunovskaja St. 55, 197228 Saint Petersburg
Pashevich, V.I.	Minatomenergoprom, Zotatomenergo, Kitajskij PZ7, Moscow K-74
Rybalchenko, I.L.	*VNIPIET*, Dibunovskaja St. 55, 197228 Saint Petersburg
Sedov, V.M.	Institute of Technology, Saint Petersburg
Versin, V.V.	VNIPIET, Dibunovskaja St. 55, 197228 Saint Petersburg

SPAIN

Martín, L.	Nuclear Safety Council, Justo Dorado 11, Madrid 28040

SWITZERLAND

Alder, H.P.	Materials Technology, Paul Scherrer Institute, CH-5303 Würenlingen

UNITED KINGDOM

Brookes, I.	Plant Chemistry Branch, CEGB Berkeley Nuclear Laboratories, Berkeley, Gloucestershire GL13 0PB
Butter, K.R.	Winfrith Atomic Energy Establishment, United Kingdom Atomic Energy Authority, Dorchester, Dorset DT2 8DH
Campion, P.	Chemistry Division, Winfrith Atomic Energy Establishment, United Kingdom Atomic Energy Authority, Dorchester, Dorset DT2 8DH

UNITED KINGDOM (cont.)

Comley, G.	Plant Chemistry Branch, CEGB Berkeley Nuclear Laboratories, Berkeley, Gloucestershire GL13 0PB
Pick, M.	Plant Chemistry Branch, CEGB Berkeley Nuclear Laboratories, Berkeley, Gloucestershire GL13 0PB
Thornton, E.W.	Plant Chemistry Branch, CEGB Berkeley Nuclear Laboratories, Berkeley, Gloucestershire GL13 0PB

INTERNATIONAL ATOMIC ENERGY AGENCY

Chantoin, P.	Division of Nuclear Fuel Cycle and Waste Management, International Atomic Energy Agency, Wagramerstrasse 5, P.O. Box 100, A-1400 Vienna

Consultants Meetings

Vienna, Austria: 23-25 November 1987, 18-20 October 1988, 6-8 November 1990

Consultants Meeting on Decontamination

Berlin, Germany: 26-27 April 1990

Research Co-ordination Meetings

Heidelberg, Germany: 31 May - 3 June 1988
Vienna, Austria: 20-23 November 1989, 6-9 May 1991